A THESIS

Microwave spectral studies on aniline and some other molecules

Submitted to the University of Glasgow in part fulfillment for the degree of Doctor of Philosophy in the Faculty of Science

by DAVID G. LISTER, B.Sc.

Chemistry Department

October, 1968.

ProQuest LLC.
789 East Eisenhower Parkway
P.O. Box 1346
Ann Arbor, MI 48106 – 1346

ACKNOWLEDGEMENT

I would like to thank my supervisor Dr. J.K. Tyler for his help and encouragement throughout this work.

Gifts of compounds from the following are gratefully acknowledged:

Professor Luttke of the University of Gottingen for aniline $-^{15}N$ and acetanilide $-4D_1$.

Dr. J. M. Hollas of the University of Reading for aniline $-D_7$.

Dr. N.M.D. Brown of the University of Glasgow for 2,1,3 - benzoxadiazole and 2,1,3 - benzothiadiazole and for many discussions about these two molecules.

My thanks are also due to my colleague Mr. J.N. Macdonald and to the research students in the departments of physical and theoretical chemistry for many helpful suggestions.

Finally, I would like to thank Professor D.W.J. Cruickshank and Professor J.M. Robertson in whose departments this work was carried out and the Science Research Council for a maintenance grant.

SUMMARY

This thesis contains an account of microwave spectral studies aniline, propiolic acid, 2,1,3 - benzoxadiazole and 2,1,3 - benzothiadiazole, and glycollonitrile. All of the spectra were observed at room temperature using a conventional Stark modulation spectrometer.

A brief description of the spectrometer, the method used to calculate rigid asymmetric top energy levels and the location of atoms in a molecule are given in Chapter 1. Chapters 2 - 5 are devoted to the spectral studies on the molecules mentioned above and Chapter 6 contains details of the preparation of a number of these compounds.

The microwave spectra of ten isotopic species of aniline have been observed and transitions due to molecules in the ground and a very low first excited vibrational state have been assigned. A low first excited vibrational state is characteristic of a pyrimidal configuration about the nitrogen atom

and an inverting amine group. The inertial defects, and substitution co-ordinates of the amino-hydrogen atoms confirm that aniline is non-planar and an r_s structure has been derived for the $C - NH_2$ group. The co-ordinates of the ring hydrogen atoms in aniline indicate that the phenyl group is somewhat narrower and elongated compared to benzene.

Three species of propiolic acid have been studied and the planar nature and cis conformation of the hydroxyl relative to the carbonyl group in this molecule are confirmed. Allowance has been made for centrifugal distortion in deriving the rotational constants, but it is impossible to derive accurate values for the centrifugal distortion constants from the measured line frequencies. The dipole moment of propiolic acid has been obtained from Stark effect measurements and lies almost parallel to the direction of the C = O bond.

The spectra of the normal isotopic species of 2,1,3 - benzoxadiazole and 2,1,3 - benzothiadiazole have been assigned and the inertial defects indicate that these molecules are planar. Structures with considerable double bond fixation in the six membered rings are proposed for these molecules.

Some preliminary conclusions about the structure of glycollonitrile are given in chapter 5. Spectra of the normal and one deuterated species ($DOCH_2CN$) have been assigned. The inertial defects of these molecules and the substitution co-ordinates of the hydroxyl hydrogen atom show that glycollonitrile exists in the gauche form.

CONTENTS

CHAPTER 1.

INTRODUCTION

A variety of interesting information about isolated molecules may be obtained by studying the microwave spectra of low pressure gases. Pure rotational transitions are usually observed and microwave spectroscopy is therefore limited to molecules with a permanent dipole moment. The analysis of such spectra leads to moments of inertia, and, provided the spectra of a number of isotopic species have been observed, accurate molecular structures may be obtained.

The Stark effect provides a convenient method of measuring electric dipole moments, and in the case of asymmetric top molecules the direction as well as the magnitude of this quantity may be derived. Fine structure due to the coupling of nuclear quadrupole moments with the angular momentum of the molecule is often observed on microwave lines. The nuclear quadrupole coupling constants are a measure of the

gradient of the electric field at the nucleus, and this information together with the electric dipole moment often indicates a particular distribution of electrons within a molecule.

Hindered internal motions such as the internal rotation of methyl groups or the inversion of amine groups lead to a splitting of lines or to a characteristic pattern of vibrational satellites and accurate values for the potential barriers to these motions may be obtained.

The quantum mechanics of the rotation of molecules is treated in reference 1. The experimental methods of microwave spectroscopy, Stark effects and nuclear quadrupole coupling are discussed in the standard text books [2,3,4].

The remainder of this chapter contains a description of the spectrometer used in this work, the method used to calculate rigid asymmetric rotor energy levels and the location of atoms in a molecule

by isotopic substitution. The following chapters deal with spectral studies on aniline, propiolic acid, 2,1,3 - benzoxadiazole and 2,1,3 -benzothiadiazole, and glycollonitrile. The final chapter contains details of the preparation of a number of these compounds when carried out by the author.

(1) The spectrometer.

All of the measurements in this work have been made on a conventional Stark modulation spectrometer operating at room temperature. A block diagram of the instrument is shown in fig 1.1.

The cell is a twelve foot length of copper X band waveguide with a flange at each end. Thin mica windows are cemented onto the flanges with wax and the cell is evacuated through a small hole bored centrally in the broad face of the waveguide.

The Stark septum is tapered acutely at each end to reduce reflections and is supported on milled teflon spacers. A 100 kc/s Industrial Components

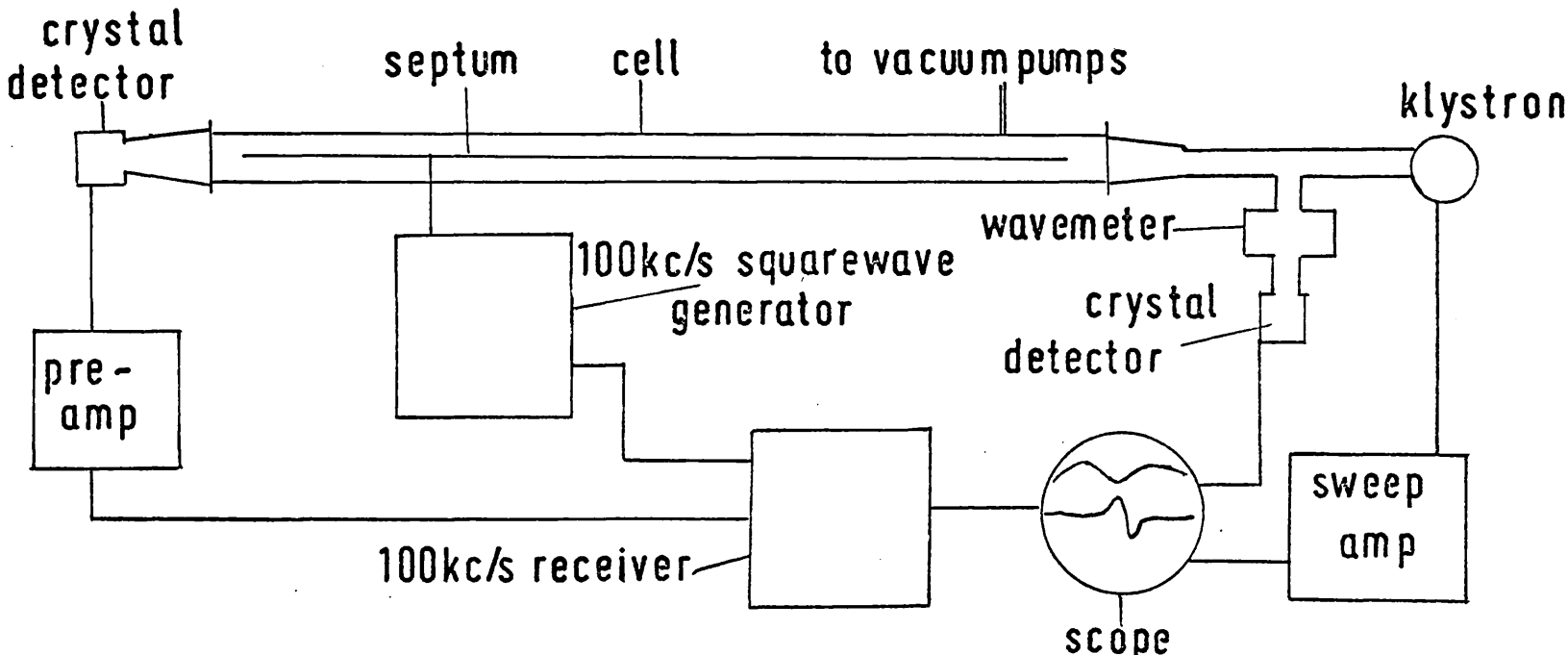
crystal
detector
septum
cell
to vacuum pumps
klystron
wavemeter
100kc/s squarewave
generator
crystal
detector
pre-
amp
sweep
amp
100kc/s receiver
scope

fig.1-1

Incorporated square wave modulation and phase sensitive detection system is used and electric fields of up to 4000 volts/cm are available for the study of molecules with low dipole moments.

A low voltage E.M.I. klystron is used to cover the frequency range 8000 - 12000 mc/s and the range 12000 - 40000 mc/s is covered by a number of high voltage E.M.I. klystrons. A significant improvement in the stability of the high voltage tubes was obtained when their heater currents were taken from accumulators.

The following types of crystal detector were used

CS9B	8000 - 12000 mc/s	X band
IN26	12000 - 18000	J band
	18000 - 26000	K band
SIM.8	26000 - 40000 mc/s	Q band

Oscilloscope presentation of spectra was usually used and a useful feature of the spectrometer is the

provision of facilities for observing lines using slow sweep rates. Under these conditions a gain in sensitivity by a factor of ten to twenty may be obtained. Permanent records of spectra were made using a Bausch and Lomb recorder.

Approximate frequency measurements, correct to $\pm$ 5 mc/s, were made using cylindrical cavity wave meters. Accurate frequency measurements were made using the system shown in fig. 1.2. The Micronow frequency multiplier chain provides harmonics of 50, 150 and 450 mc/s of a 5 mc/s variable frequency oscillator and these are fed onto the crystal normally used as a detector for the wave meter. This crystal serves both as harmonic generator and mixer. Harmonics spaced by 50 mc/s are produced in the microwave region and mixed with some of the power from the klystron. The beat frequency is taken through a radio receiver and when the frequencies of the harmonic of the Micronow and klystron differ by

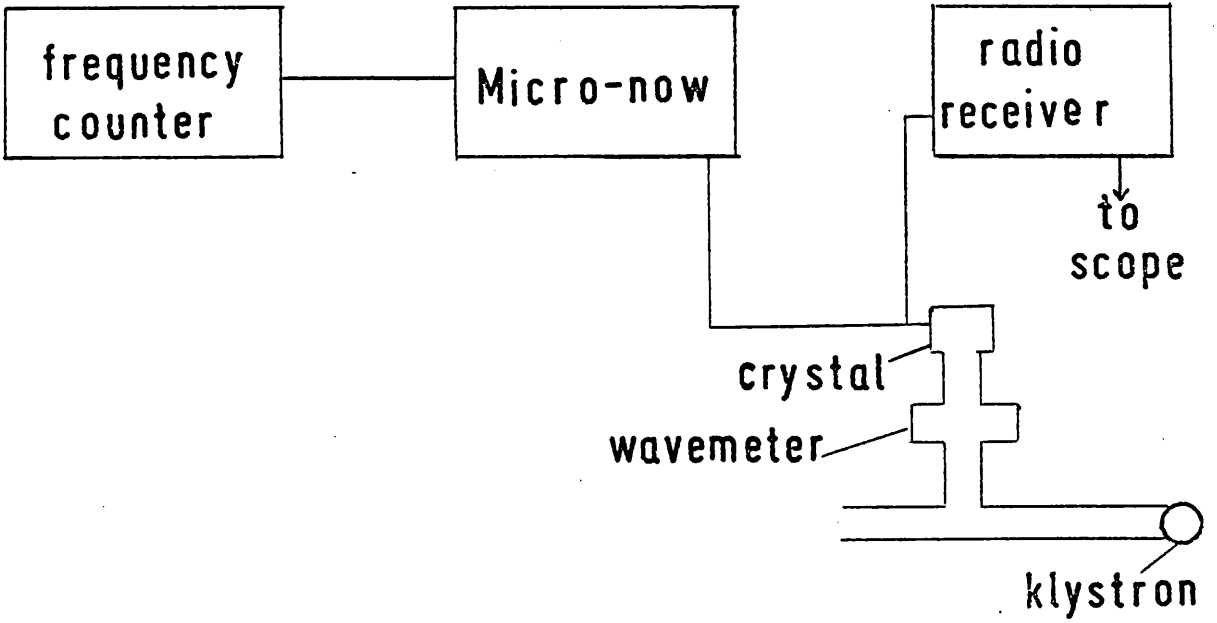
frequency counter
Micro-now
radio receiver
to scope
crystal
wavemeter
klystron

fig.1-2

the radio receiver setting a marker pip is observed on the second trace of the oscilloscope. Two markers emanate from each harmonic and the variable frequency oscillator of the Micronow is tuned until one of the markers is set on the line. The frequency of this oscillator is measured to $\pm$ 1 c/s using a Marconi frequency counter, and the frequency counter is periodically checked against the 200 kc/s Droitwich transmission of the B.B.C. In order to eliminate the radio receiver setting both markers are set on the line and to cancel delays measurements are made with the klystron sweeping from low to high frequency and then with the sweep reversed. The harmonic of the variable frequency oscillator used is determined from wave meter measurements.

Strong lines such as those of OCS have been measured to better than $\pm$ 0.05 mc/s using this system. The lines observed for many of the molecules studied in this work were often quite weak and broad and the measurements are probably accurate to $\pm$ 0.1 mc/s.

(2) The calculation of rigid asymmetric top energy levels.

The energy levels of a rigid asymmetric top may be written[1]

$$E_J = J(J+1)\,(A+C)/2 + (A-C)/2\; E_J(\kappa)$$

where $E_J(\kappa)$ is the reduced energy and

$$\kappa = \frac{2B - A - C}{A - C}$$

is Ray's asymmetry parameter. Tables[5] giving the reduced energies correct to eight significant figures and at intervals of 0.001 in κ have been used throughout this work for the calculation of rigid asymmetric rotor energy levels. For molecules such as aniline $(A - C)/2$ is of the order of two thousand mc/s and the accuracy of the reduced energy tables is such that errors of not more than 0.05 mc/s are introduced into calculated line frequencies. The small magnitudes of the second and higher differences show that linear interpolation

between adjacent entries in the reduced energy tables is a very good approximation.

(3) The location of atoms by isotopic substitution.

The rotational constants of a molecule are related to the corresponding moments of inertia by

$$B = \frac{h}{8\pi^2 I}$$

or, if B is in mc/s and I is in atomic mass units x Å^2

$$B \times I = 505531 \times 10^5 \text{ mc/s.(a.m.u. Å}^2\text{)}.$$

Because the atoms in a molecule are vibrating the rotational constants are essentially reciprocals of the moments of inertia averaged over the vibrational state. Costain[6] has shown how to calculate molecular structures from ground state moments of inertia in such a way that the effects of zero point

vibrations are minimised. He recommends locating each non-equivalent atom in the principal axis system of a parent isotopic species by making an isotopic substitution of each atom. The co-ordinates in the principal axis system are then calculated from Kraitchman's equations [7].

For a planar asymmetric top Kraitchman's equations may be written

$$x^2 = \frac{\Delta I_y}{\mu}\left[1 + \frac{\Delta I_x}{I_x - I_y}\right], \text{ etc.}$$

where

$$\mu = \frac{M \Delta M}{M + \Delta M}$$

~~where~~ ΔI_x and ΔI_y are the differences in moments of inertia of the substituted and parent isotopic species, M is the molecular weight of the parent molecule and ΔM is the difference in mass between

the two isotopes of the substituted atom.

In the case of a non-planar top the equations take the form

$$a^2 = \frac{1}{2\mu}\left[\Delta Ib + \Delta Ic - \Delta Ia\right]x$$

$$\left[1 + (\Delta Ia - \Delta Ib + \Delta Ic)/2(Ia - Ib)\right]x$$

$$\left[1 + (\Delta Ia + \Delta Ib - \Delta Ic)/2(Ia - Ic)\right]$$

Expressions for the b and c co-ordinates may be obtained by cyclic permutations of the subscripts of the inertial differences and moments of inertia.

Structures calculated by Costain's method are termed substitution structures (r_s) and are usually very good approximations to the equilibrium structures (r_e). In cases where comparisons can be made the r_s bond lengths are usually within 0.005 Å of the r_e bond lengths. Partial molecular structures can

be determined to the same degree of accuracy and the structure of the C - NH_2 group in aniline has been determined in this way.

REFERENCES

1. H.C. Allen Jr. and P.C. Cross, "Molecular Vib-rotors", John Wiley and Sons, Inc.1963

2. W. Gordy, W.V.Smith and R.F. Trambarulo, "Microwave Spectroscopy", John Wiley and Sons, Inc., 1953.

3. C.H. Townes and A.L. Schawlow, "Microwave Spectroscopy", McGraw-Hill Book Company, Inc., 1955

4. T.M. Sugden and C.N. Kenny, "Microwave Spectroscopy of Gases", D. Van Nostrand Company Ltd., 1965

5. M. Sidran, F. Nolan and J.W. Blaker, "Rotational Energy Levels of Asymmetric Top Molecules", Gramman Research Department, 1963

6. C.C. Costain, J.Chem.Phys., 1958, 29, 864

7. J. Kraitchman, Am. J. Phys., 1953, 21, 17

CHAPTER 2.

The microwave spectrum of aniline

(1) Introduction

The basicity constants of aromatic amines are usually lower than those of aliphatic amines and ammonia by a factor of nearly a million [1]. This is usually attributed to delocalisation of the lone pair of electrons on the nitrogen atom into the π-electron system of the benzene ring. Or, in valence bond language aniline is a resonance hybrid of the canonical forms (a) - (e).

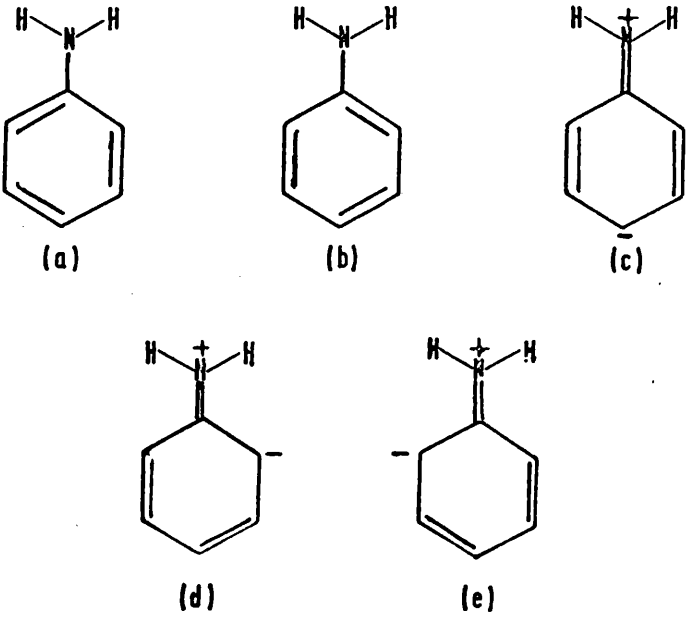

The enhanced reactivity of aniline compared to benzene in electrophilic substitution reactions and the ortho para directing nature of the amine group are further evidence for the contribution of structures (c) - (e) to the overall state of the molecule [2]. These structures can be visualised as being formed from nitrogen in an sp^2 hybridized state by overlap of the $2p_z$ orbital on the nitrogen atom with the $2p_z$ orbital of the 1 - carbon atom and they are therefore planar. Depending on the weights of these structures in the total molecular wave function the nitrogen atom in aniline might be expected to lose to a certain extent the pyrimidal configuration that is characteristic of ammonia [3] and methylamine [4].

There is a number of precedents for taking aniline to be non-planar e.g. dipole moment relaxation studies [5], Kerr constant measurements [6] and the dipole moment of p-phenylenediamine equal to 1.23D [7]. The infra-red[8] spectrum of aniline supports a molecule with Cs symmetry and recently it has been established from its ultra-violet

spectrum[9] that aniline is non-planar in its ground electronic state. None of these studies give a really accurate measure of the degree of the non-planarity of aniline.

The geometry of the benzene ring is likely to be altered when a hydrogen atom is replaced by a substituent. Inductive effects can change the hybridization of the 1 - carbon atom, but except for very electronegative groups such as fluorine these effects are expected to be small. Resonance effects change the π- bond orders within the benzene ring and this will also cause small distortions. The canonical forms (c) - (e) of aniline indicate that $r_{C_1 - C_2} > r_{C_3 - C_4} > r_{C_2 - C_3}$. Using the π-bond orders deduced from some Hückel calculations[10] in conjunction with the slope of a bond order - bond length curve[11] at the point corresponding to benzene the following deviations from the bond length in benzene are predicted for the carbon - carbon bond lengths in aniline.

$\Delta r\, C_1 - C_2 \sim + 0.005$ Å

$\Delta r\, C_2 - C_3 \sim - 0.001$

$\Delta r\, C_3 - C_4 \sim 0.000$

In order to obtain an accurate measure of the degree of non-planarity of aniline and to investigate the possibilities of distortions in the benzene ring the microwave spectra of the following ten isotopic species of aniline have been examined.

aniline - H_7	aniline - NHD
aniline - ^{15}N	aniline - $1\text{-}^{13}C$
aniline - 2 D_1	aniline - 4 D_1
aniline - 3,5 D_2	aniline - N D_2
aniline - 2,4,6 D_3	aniline - D_5

A planar structure with a regular six membered ring and

$r_{C-C} = 1.395$ Å $\qquad r_{C-H} = 1.084$ Å

$r_{C-N} = 1.350$ Å $\qquad r_{N-H} = 1.000$ Å

$\widehat{HNH} = 120^\circ$

was used as a model for predicting line frequencies. The model is a prolate asymmetric rotor with $\kappa = 0.55$ and the dipole moment lies along the a inertial axis. The most intense transitions in the microwave spectrum of such a molecule are the μ_a R branch lines with $\Delta K_{-1} = 0$ and $\Delta K_{1} = +1$.

(2) Analysis of spectra

A line diagram of the μ_a R branch spectrum of aniline - H_7 in the region 23,000 - 33,000 mc/s is shown in fig. 2.1. Similar patterns of lines are observed for the other isotopic species of aniline. A very striking feature of the microwave spectrum of aniline - H_7, aniline - ^{15}N, aniline - ^{13}C and the ring deuterated species of aniline is the presence to low frequency of lines due to molecules in the ground vibrational state (V = 0) of a satellite (V = 1) of appreciable intensity. The V = 0 and V = 1 lines of all of these isotopic species except aniline - $2D_1$ show alternations in intensity depending on the K_{-1} quantum number of the transitions.

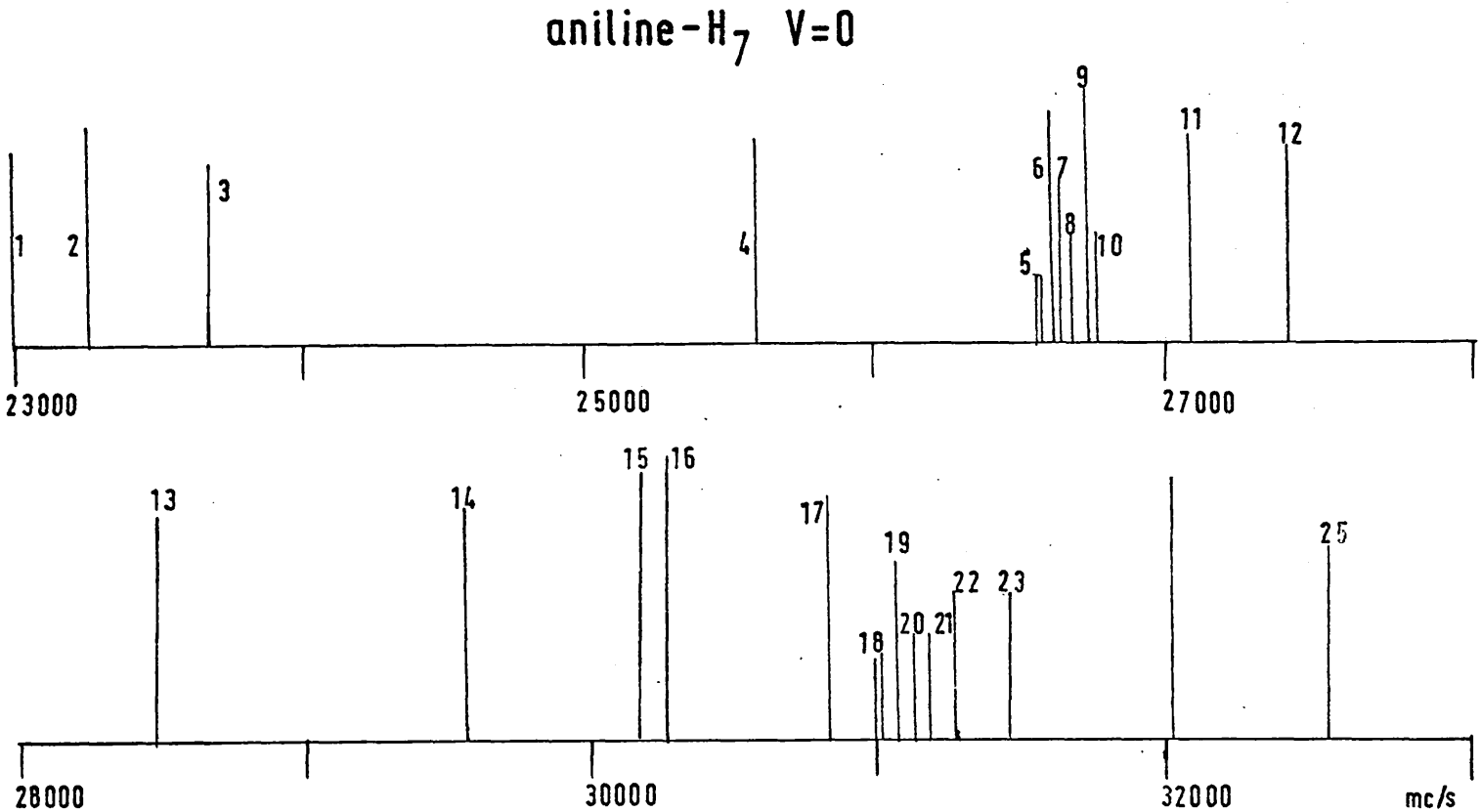
aniline-H_7 V=0
1
2
3
4
5
6
7
8
9
10
11
12
23000
25000
27000
13
14
15
16
17
18
19
20
21
22
23
25
28000
30000
32000
mc/s

fig. 2-1

Key to fig. 2.1

1. $5_{15} - 6_{16}$
2. $5_{05} - 6_{06}$
3. $4_{22} - 5_{23}$
4. $5_{24} - 6_{25}$
5. $5_{51} - 6_{52}$
   $5_{50} - 6_{51}$
6. $6_{16} - 7_{17}$
7. $5_{33} - 6_{34}$
8. $5_{42} - 6_{43}$
9. $6_{06} - 7_{07}$
10. $5_{41} - 6_{42}$
11. $5_{14} - 6_{15}$
12. $5_{32} - 6_{33}$
13. $5_{23} - 6_{24}$
14. $6_{25} - 7_{26}$
15. $7_{17} - 8_{18}$
16. $7_{07} - 8_{08}$
17. $6_{15} - 7_{16}$
    $6_{61} - 7_{62}$
18. $6_{60} - 7_{61}$
19. $6_{34} - 7_{35}$
20. $6_{52} - 7_{53}$
21. $6_{51} - 7_{52}$
22. $6_{43} - 7_{44}$
23. $6_{42} - 7_{43}$
24. $7_{26} - 8_{27}$
25. $6_{33} - 7_{34}$

These alternations in intensity are due to nuclear spin statistical weight effects of a number of pairs of equivalent nuclei.

Fig. 2.2 shows the $6_{06} - 7_{07}$ and $5_{33} - 6_{34}$ transitions of aniline - H_7. The vibration giving rise to the V = 1 state is very anharmonic since a series of vibrational satellites almost equally spaced and decreasing exponentially in intensity (apart from the nuclear spin statistical weight effects) is not observed to low frequency of the ground state lines. The spectra of the V = 1 states of aniline - NHD and aniline - N D_2 are somewhat anomolous and are discussed below.

The analysis of the spectra of the V = 0 and V = 1 states of all of the isotopic species of aniline except that of the V = 1 state of aniline - NHD and those of the V = 0 and V = 1 states of aniline - N D_2 followed much the same course as that of the V = 0 state of aniline - H_7. A spectrum was predicted from a model; our preliminary structure (appendix 2) was used

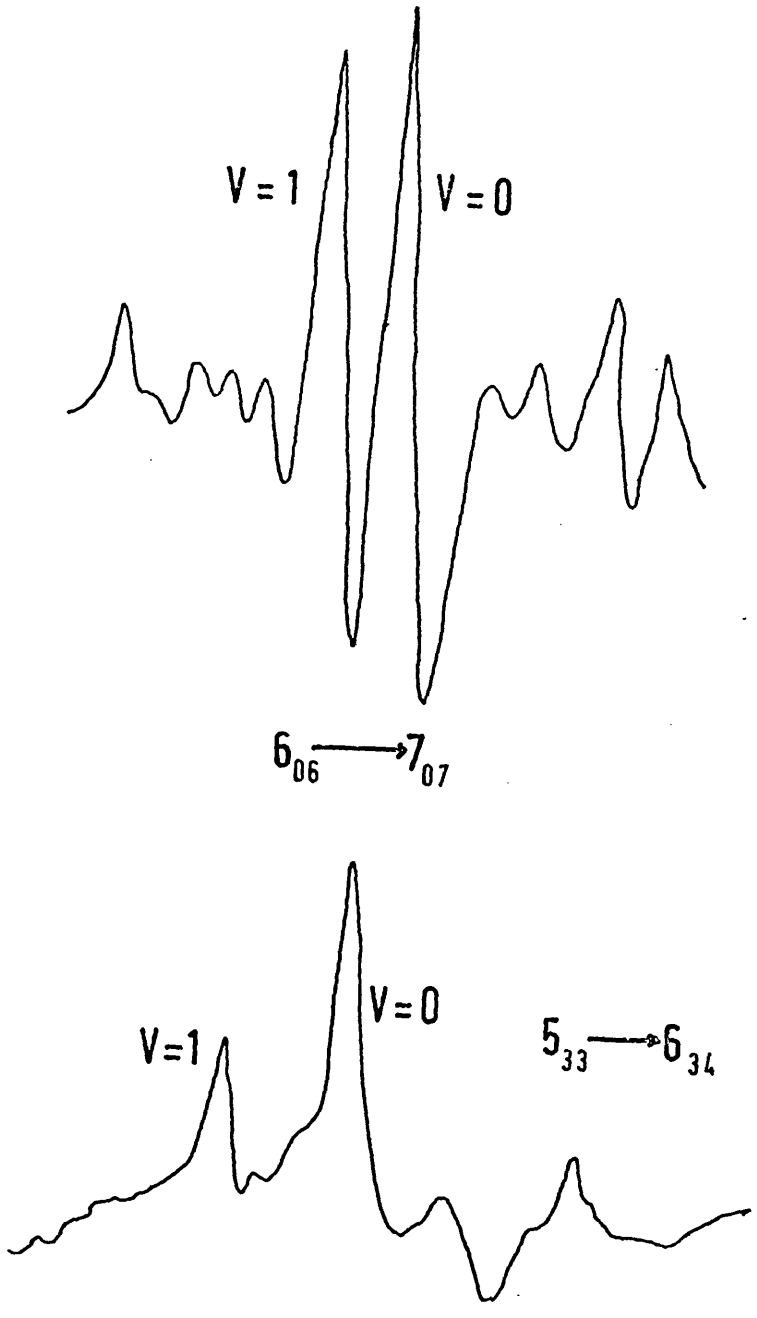

aniline-H_7 1600 volts/cm

fig.2·2

for this purpose for aniline - ^{15}N, aniline - ^{13}C and the ring deuterated species of aniline.

The vapour pressure of aniline at room temperature (0.5 torr) is more than adequate for microwave spectroscopy. Samples were admitted to the cell by filling a section of the manifold of the vacuum system with aniline vapour and then transferring this to the cell. Before work was started on any of the isotopic species of aniline the cell was flushed several times with normal aniline in order to remove traces of other compounds absorbed on the cell walls.

A search for lines was usually made in K band in the region where the $6_{06} - 7_{07}$, $6_{16} - 7_{17}$ and high K_{-1} lines of the J = 5 - 6 transition were expected to occur. Assignments were made on the basis of Stark effects and on separations expected from the model. The high K_{-1} lines are modulated at low Stark fields and the pattern of K_{-1} = 3, 4 and 5 lines is very characteristic. The search for lines was extended over a few thousand mc/s in order

to locate some of the $K_{-1} = 2$ transitions.

The assignments were confirmed and an improved set of constants was obtained by the following graphical procedure. If rigid rotor theory is obeyed the frequency of a R branch line is given by

$$\nu = 2(J+1)(A+C)/2 + (A-C)/2\,\Delta E(\kappa) \quad 2.1$$

The line frequencies were weighted and differences taken in such a way that the term in $(A + C)_{/2}$ in 2.1 was eliminated, giving

$$\Delta\nu = (A-C)/2\,\Delta(\Delta E(\kappa))$$

If the transitions have been assigned correctly then plots of $\Delta\nu/\Delta(\Delta E(\kappa))$ against κ for several pairs of transitions should have a common intersection. A plot over a wide range of κ for some of the transitions of aniline - ^{15}N is shown in fig. 2.3.

Other transitions were predicted from the new set of rotational constants and a number of lines

aniline-^{15}N R branch plot

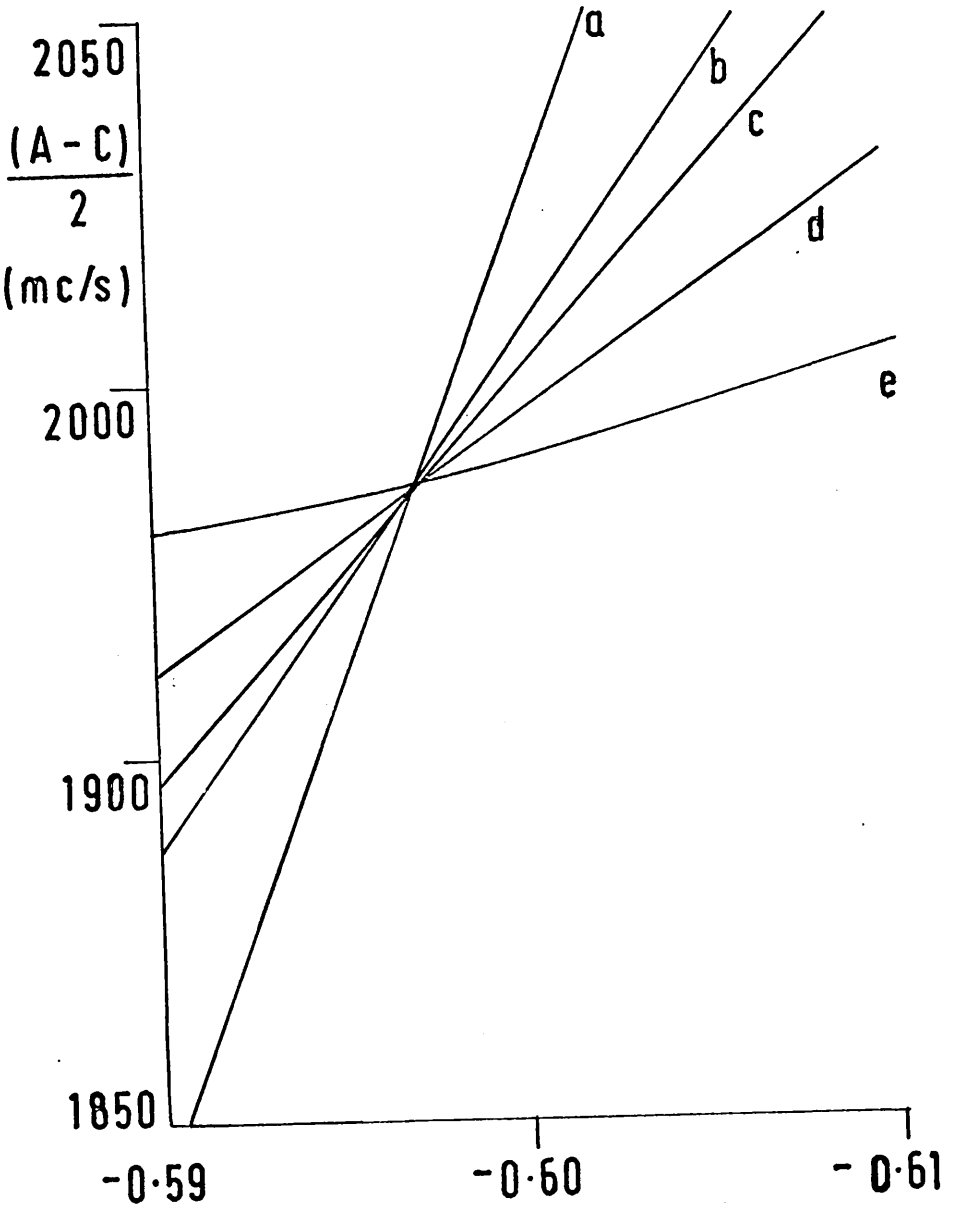

fig.2·3

spanning a range of 10,000 - 15,000 mc/s was measured accurately. The R branch plot was repeated over a smaller range of K (fig. 2.4) and the quality of the intersection shows that centrifugal distortion effects are negligible in the observed transitions. The final rotational constants were obtained by fitting the observed line frequencies by least squares to equation 2.1. A brief discussion of the procedure and computer programme used is given in appendix 1.

Because the amino-hydrogen atoms in aniline are very labile it is impossible to prepare a sample containing more than 50% aniline - NHD. As the deuterium content of the samples was increased large numbers of low field lines with symmetrical Stark effects were observed. These lines are thought to be due to aniline - N D_2. The V = 0 transitions of aniline - NHD with $K_{-1} \geqslant 2$ are accompanied by a vibrational satellite to low frequency. The separations between the ground state lines and these satellites are only half of those

aniline-^{15}N R branch plot

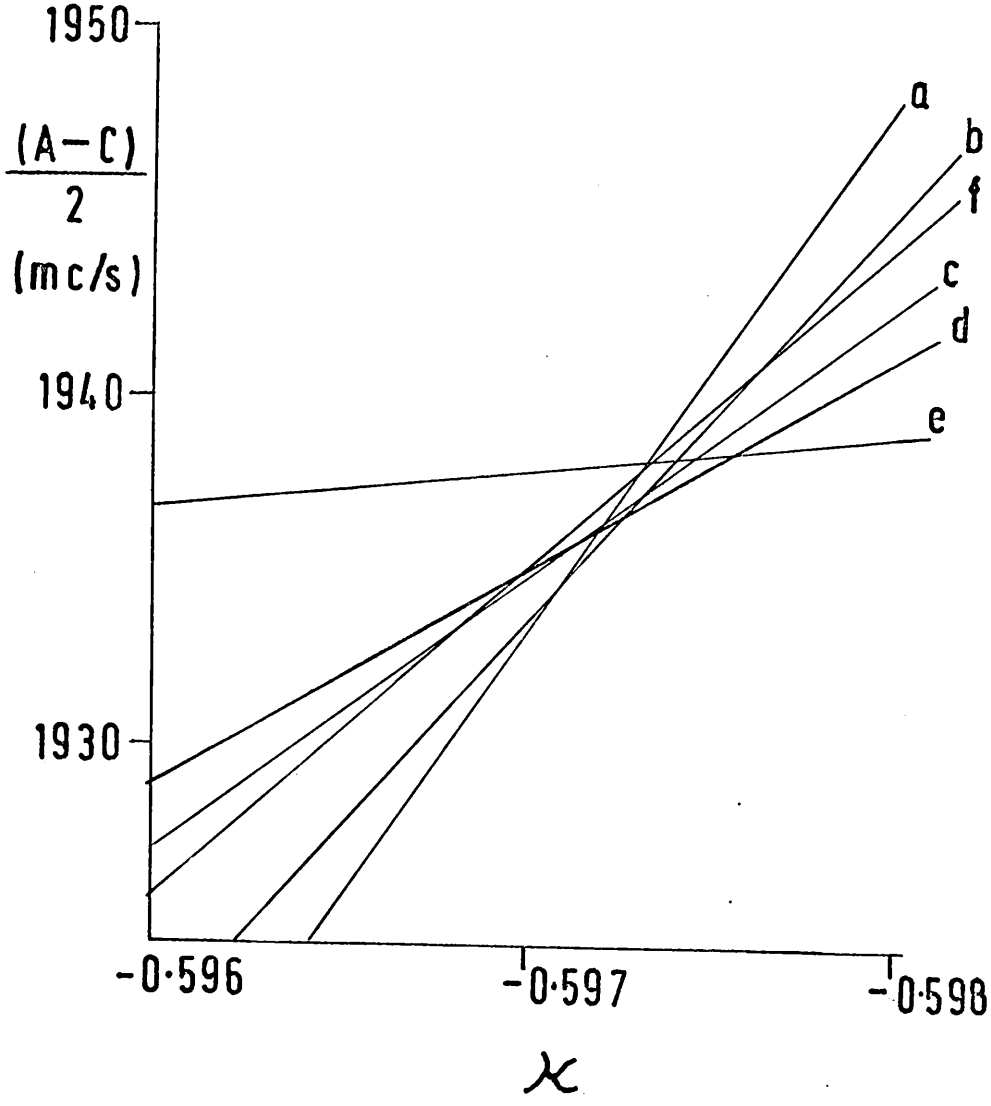

fig.2·4

Key to fig. 2.3 and fig. 2.4

a	$(5_{23} - 6_{24})$	-	$(5_{14} - 6_{15})$
b	$6/5\ (4_{22} - 5_{23})$	-	$(5_{05} - 6_{06})$
c	$(5_{23} - 6_{24})$	-	$6/7(6_{06} - 7_{07})$
d	$(5_{14} - 6_{15})$	-	$(5_{15} - 6_{16})$
e	$(5_{05} - 6_{06})$	-	$6/7(6_{06} - 7_{17})$
f	$(6_{33} - 7_{34})$	-	$(6_{43} - 7_{44})$

NOTE Since differences between line frequencies are taken in constructing an R branch plot the scatter in fig. 2.4 represents deviations of less than 0.5 mc/s from rigid rotor theory. The plot also illustrates the necessity of obtaining the rotational constants by least squares.

observed for the corresponding transitions of the other isotopic species of aniline. The $5_{05} - 6_{06}$, $6_{06} - 7_{07}$, $6_{16} - 7_{17}$ and $7_{17} - 8_{18}$ transitions of aniline - NHD do not have such a satellite and the $7_{07} - 8_{08}$ transition is a doublet whose lower frequency component is assigned to the V = 0 state. A set of rotational constants obtained from the satellites of the higher K_{-1} lines predicts that the satellites for the $5_{05} - 6_{06}$, $6_{06} - 7_{07}$, $6_{16} - 7_{17}$ and $7_{17} - 8_{18}$ transitions lie only 1 mc/s above the V = 0 lines. The satellite for the $7_{07} - 8_{08}$ transition is predicted at the frequency of the upper component of the doublet. The satellites in aniline - NHD are only slightly weaker than the V = 0 lines and it is reasonable to assign them to the V = 1 state. The isotope effect on the V = 1 lines on deuteration of the amine group indicates that the vibration responsible for this state involves primarily the amino-hydrogen atoms.

The very rich spectrum of aniline - $N D_2$ made the assignment of the μa R branch lines very difficult. The substitution co-ordinates of the amino-hydrogen atoms

obtained from the moments of inertia of aniline - NHD were used to predict the changes in moments of inertia of aniline - N D_2 relative to aniline - H_7. It was considered, provided there were no dramatic rotation-vibration interactions in aniline - N D_2, that the rotational constants obtained in this manner should predict lines to within 20 mc/s. Recordings of the region where the high K_{-1} lines of the J = 5 - 6 transition were expected to occur were made at several Stark voltages. A large number of low field lines with symmetrical Stark effects were observed but it was possible to pick out good candidates for the $5_{33} - 6_{34}$, $5_{42} - 6_{43}$ and $5_{41} - 6_{42}$ lines within 5 mc/s of the predicted frequency. The separation between the candidates for the $K_{-1} = 4$ lines (31.40 mc/s) is within 0.1 mc/s of that predicted by the model. Recordings of other regions were made and it was usually possible to pick out a line with the expected type of Stark effect within a few mc/s of the predicted frequency. The final least squares fit for aniline - N D_2 is

comparable in accuracy with those obtained for the other isotopic species of aniline.

The aniline - N D_2 lines so far assigned do not appear to be accompanied by a satellite of the intensity expected for the V = 1 state. The most likely explanation is that the rotational constants of the V = 0 and V = 1 states are so similar that their spectra are practically co-incident.

The measured and calculated line frequencies and the least squares rigid rotor constants for the various isotopic species of aniline are given in tables 2.1 - 2.10.

In an attempt to obtain the dipole moment and quadrupole coupling constants of aniline a search was made for the $1_{01} - 2_{02}$ and $1_{10} - 2_{11}$ transitions of aniline - H_7 at the predicted frequencies of

$1_{01} - 2_{02}$	8597.4 mc/s
$1_{10} - 2_{11}$	9558.5

The lines were very weak and were observed and measured

TABLE 2.1

Measured line frequencies for aniline - H_7

	V = 0		V = 1	
	observed (mc/s)	calculated (mc/s)	observed (mc/s)	calculated (mc/s)
$1_{10} - 2_{11}$	9558.65	9558.56	9553.20	9553.45
$5_{05} - 6_{06}$	23238.27	23238.26	23233.08	23232.89
$5_{15} - 6_{16}$	22983.70	22983.55		
$5_{14} - 6_{15}$	27107.50	27107.74	27097.05	27097.20
$5_{24} - 6_{25}$	25589.75	25589.75	25579.99	25580.04
$5_{23} - 6_{24}$	28524.56	28524.47	28508.85	28508.87
$5_{33} - 6_{34}$	26651.24	26651.14	26638,75	26638.77
$5_{32} - 6_{33}$	27426.56	27426.46	27411.21	27411.16
$5_{42} - 6_{43}$	26699.83	26699.80	26687.15	26686.95
$5_{41} - 6_{42}$	26751.96	26752.09	26738.87	26738.96
$5_{51} - 6_{52}$		26590.70		26578.20
$5_{50} - 6_{51}$	26591.01	26591.96	26578.75	26579.45
$6_{06} - 7_{07}$	26729.10	26729.14	26723.12	26723.12
$6_{16} - 7_{17}$	26596.42	26596.32	26590.05	26590.03
$6_{15} - 7_{16}$	30808.54	30808.36	30798.25	30798.14

TABLE 2.1 (Cont'd.)

	V = 0		V = 1	
	observed (mc/s)	calculated (mc/s)	observed (mc/s)	calculated (mc/s)
$6_{25} - 7_{26}$	29529.59	29529.63	29519.06	29519.11
$6_{34} - 7_{35}$	31034.94	31034.87	31020.85	31020.85
$6_{43} - 7_{44}$	31252.82	31252.84	31237.64	31237.66
$6_{42} - 7_{43}$	31419.81	31419.80	31403.78	31403.73
$6_{52} - 7_{53}$	31113.65	31113.47	31098.77	31098.53
$6_{51} - 7_{52}$	31119.90	31120.26	31104.99	31105.27
$6_{61} - 7_{62}$	31005.98	31005.93	30991.23	30991.39
$6_{60} - 7_{61}$		31006.06		30991.51
$7_{07} - 8_{08}$	30245.68	30245.68	30239.03	30238.96
$7_{17} - 8_{18}$	30180.88	30180.98	30173.87	30174.07
$(A + C)/2$		3697.22		3696.15
$(A - C)/2$		1920.18		1919.42
χ		- 0.574626		- 0.575128

TABLE 2.2

Measured line frequencies for aniline - NHD

	V = 0		V = 1	
	observed (mc/s)	calculated (mc/s)	observed (mc/s)	calculated (mc/s)
$4_{22} - 5_{23}$	22698.02	22697.94	22693.19	22693.12
$5_{05} - 6_{06}$	22856.59	22856.44		22587.59
$5_{14} - 6_{15}$	26262.94	26263.17	26259.62	26259.55
$5_{24} - 6_{25}$	24759.67	24759.73	24757.44	24757.40
$5_{23} - 6_{24}$	27451.83	27451.60		
$5_{33} - 6_{34}$	25708.52	25708.62	25704.94	25704.91
$5_{32} - 6_{33}$	26354.94	26355.11	26350.10	26350.19
$5_{42} - 6_{43}$	25735.91	25735.91	25732.23	25732.07
$5_{41} - 6_{42}$	25775.75	25775.81	25771.81	25771.88
$5_{51} - 6_{52}$	25638.47	25638.00		
$5_{50} - 6_{51}$		25638.89		
$6_{06} - 7_{07}$	25973.51	25973.61		26974.84
$6_{16} - 7_{17}$	25820.92	25820.83		25821.90
$6_{15} - 7_{16}$	29913.89	29913.70		
$6_{25} - 7_{26}$	28597.22	28597.32	28594.96	28595.02

Cont'd.

TABLE 2.2 (Cont'd.)

	v = 0		V = 1	
	observed (mc/s)	calculated (mc/s)	observed (mc/s)	calculated (mc/s)
$6_{24} - 7_{25}$	32033.33	32033.34	32026.76	32026.82
$6_{34} - 7_{35}$	29954.04	29954.02	29949.64	29949.82
$6_{33} - 7_{34}$	31228.95	31228.85	31222.38	31222.42
$6_{43} - 7_{44}$	30119.94	30120.03	30115.40	30115.43
$6_{42} - 7_{43}$	30248.23	30248.23	30243.53	30243.53
$7_{07} - 8_{08}$	29384.75	29384.77	29385.57	29385.66
$7_{17} - 8_{18}$	29307.31	29307.25		29308.03
$(A + C)/2$		3649.03		3647.72
$(A - C)/2$		1922.93		1921.44
κ		-0.600868		-0.601019

TABLE 2.3

Measured line frequencies for aniline - ^{15}N

	V = 0		V = 1	
	observed (mc/s)	calculated (mc/s)	observed (mc/s)	calculated (mc/s)
$4_{22} - 5_{23}$	22972.40	22972.35	22958.09	22958.07
$5_{05} - 6_{06}$	22820.08	22819.94	22813.83	22813.78
$5_{15} - 6_{16}$	22540.74	22540.71	22534.18	22534.12
$5_{14} - 6_{15}$	26551.08	26551.27	26539.28	26539.53
$5_{23} - 6_{24}$	27779.58	27779.52	27762.79	27762.73
$5_{24} - 6_{25}$	25034.14	25034.12	25023.46	25023.40
$5_{33} - 6_{34}$	26005.36	26005.33	25992.04	25991.96
$6_{06} - 7_{07}$	26242.38	26242.53	26235.39	26235.61
$6_{16} - 7_{17}$	26091.52	26091.54	26084.33	26084.24
$6_{15} - 7_{16}$	30231.98	30231.87	30220.50	30220.33
$6_{25} - 7_{26}$	28910.39	28910.40	28898.76	28898.74
$6_{24} - 7_{25}$	32408.68	32408.68	32390.14	32390.16
$6_{34} - 7_{35}$	30297.38	30297.45	30282.17	30282.23
$6_{33} - 7_{34}$	31611.82	31611.82	31591.57	31591.80

Cont'd.

TABLE 2.3 (Cont'd.)

	V = 0		V = 1	
	observed (mc/s)	calculated (mc/s)	observed (mc/s)	calculated (mc/s)
$6_{43} - 7_{44}$	30471.59	30471.48	30455.29	30455.19
$6_{42} - 7_{43}$	30605.42	30605.56	30588.45	30588.48
$7_{07} - 8_{08}$	29689.54	29689.53	29681.81	29681.80
$7_{17} - 8_{18}$	29613.37	29613.35	29605.36	29605.38
(A + C)/2		3680.52		3679.40
(A - C)/2		1936.58		1935.84
κ		-0.597244		- 0.59772

TABLE 2.4

Measured line frequencies for aniline - $1^{13}C$

	V = 0		V = 1	
	observed (mc/s)	calculated (mc/s)	observed (mc/s)	calculated (mc/s)
$4_{13} - 5_{14}$	23006.56	23006.49	22996.37	22996.29
$4_{23} - 5_{24}$	21455.46	21455.36	21446.89	21446.83
$4_{22} - 5_{23}$	23506.55	23506.36	23493.32	23493.14
$4_{32} - 5_{33}$	22114.48	22114.54	22104.18	22104.26
$4_{31} - 5_{32}$	22424.54	22424.57		
$5_{06} - 6_{06}$	23170.03	23169.92	23165.06	23164.78
$5_{15} - 6_{16}$	22911.27	22911.18		
$5_{14} - 6_{15}$	27017.08	27017.22	27006.66	27006.78
$5_{24} - 6_{25}$	25498.68	25498.75	25489.18	24589.20
$5_{23} - 6_{24}$	28401.94	28401.94	28386.62	28386.50
$5_{33} - 6_{34}$	26544.85	26544.85	26532.66	26532.60
$5_{32} - 6_{33}$	27301.60	27301.60	27286.45	27286.54
$6_{16} - 7_{17}$	26513.82	26513.86		
$6_{25} - 7_{26}$	29428.35	29428.35	29417.91	29418.05

Cont'd.

TABLE 2.4 (cont'd.)

	V = 0		V = 1	
	observed (mc/s)	calculated (mc/s)	observed (mc/s)	calculated (mc/s)
$6_{24} - 7_{25}$	33095.12	33095.07	33078.15	33078.15
$6_{33} - 7_{34}$	32380.85	32380.89	32362.09	32362.07
$6_{43} - 7_{44}$	31124.00	31123.95	31108.99	31109.01
$6_{42} - 7_{42}$	31284.90	31285.01	31269.15	31269.21
$7_{07} - 8_{08}$	30154.72	30154.73	30148.35	30148.36
$7_{17} - 8_{18}$	30088.17	30088.22	30081.50	30081.66
$(A + C)/2$		3694.60		3693.48
$(A - C)/2$		1922.97		1922.15
κ		-0.578430		-0.578927

TABLE 2.5

Measured line frequencies for aniline - $2D_1$

	V = 0		V = 1	
	observed (mc/s)	calculated (mc/s)	observed (mc/s)	calculated (mc/s)
$4_{22} - 5_{23}$	23538.36	23538.21		
$5_{05} - 6_{06}$	22799.41	22799.31	22794.46	22794.49
$5_{15} - 6_{16}$	22596.48	22595.80	22590.52	22590.43
$5_{24} - 6_{25}$	25264.66	25264.62	25255.52	25255.45
$5_{23} - 6_{24}$	28377.60	28377.45	28362.13	28362.17
$5_{33} - 6_{34}$	26436.31	26436.20	26424.02	26423.95
$6_{06} - 7_{07}$	26234.63	26234.64	26229.11	26229.12
$6_{16} - 7_{17}$	26135.10	26135.19	26129.36	26129.29
$6_{25} - 7_{26}$	29114.05	29114.03		
$6_{34} - 7_{35}$	30754.11	30754.31	30740.59	30740.64
$6_{43} - 7_{44}$	31049.61	31049.48		
$6_{42} - 7_{43}$	31279.42	31279.65	31263.30	31262.91
$6_{33} - 7_{34}$	32519.95	32519.95		

Cont'd.

TABLE 2.5 (Cont'd.)

	V = 0		V = 1	
	observed (mc/s)	calculated (mc/s)	observed (mc/s)	calculated (mc/s)
$7_{07} - 8_{08}$	29694.90	29695.08	29688.86	29688.86
$7_{17} - 8_{18}$	29649.40	29649.53	29642.97	29643.09
(A + C)/2		3545.90		3545.54
(A - C)/2		1800.60		1800.55
κ		-0.533358		-0.534050

TABLE 2.6

Measured line frequencies for aniline - $4D_1$

	V = 0		V = 1	
	observed (mc/s)	calculated (mc/s)	observed (mc/s)	calculated (mc/s)
$4_{04} - 5_{05}$	19198.88	19198.74	19194.45	19194.24
$4_{14} - 5_{15}$	18721.40	18721.15	18716.56	18716.42
$4_{23} - 5_{24}$	20768.72	20768.74	20760.87	20760.77
$4_{22} - 5_{23}$	22600.81	22600.66	22588.73	22588.48
$5_{05} - 6_{06}$	22574.14	22573.86	22569.12	22568.95
$5_{15} - 6_{16}$	22279.79	22279.98		
$5_{24} - 6_{25}$	24708.02	24708.02	24698.78	24699.04
$5_{23} - 6_{24}$	27344.40	27344.34	27329.91	27329.97
$5_{33} - 6_{34}$	25629.29	25628.90		
$6_{15} - 7_{16}$	29888.60	29888.51	29879.13	29878.75
$6_{25} - 7_{26}$	28545.93	28546.13	28536.00	28536.38
$6_{24} - 7_{25}$	31925.87	31926.33	31909.94	31910.44
$6_{34} - 7_{35}$	29866.59	29866.56	29853.63	29853.60
$6_{33} - 7_{34}$	31080.06	31080.07	31063.30	31062.96

Cont'd.

TABLE 2.6 (Cont'd.)

	V = 0		V = 1	
	observed (mc/s)	calculated (mc/s)	observed (mc/s)	calculated (mc/s)
$6_{43} - 7_{44}$	30017.89	30017.59	30003.81	30003.79
$6_{42} - 7_{43}$	30134.99	30135.20	30120.54	30120.80
$7_{07} - 8_{08}$	29362.69	29362.77	29356.82	29356.68
$7_{17} - 8_{18}$	29278.96	29279.20	29272.52	29272.87
(A + C)/2		3671.01		3670.04
(A - C)/2		1946.55		1945.87
κ		-0.61015		-0.610619

TABLE 2.7

Measured line frequencies for aniline - $3,5D_2$

	V = 0		V = 1	
	observed (mc/s)	calculated (mc/s)	observed (mc/s)	calculated (mc/s)
$4_{04} - 5_{05}$	18746.79	18746.65	18742.52	18742.29
$4_{14} - 5_{15}$	18409.94	18409.76	18705.15	18704.96
$4_{23} - 5_{24}$	20666.04	20665.87	20657.72	20657.60
$4_{22} - 5_{23}$	22945.10	22944.94	22931.97	22931.79
$4_{32} - 5_{33}$	21436.73	21436.50	21426.22	21426.55
$4_{31} - 5_{32}$	21867.86	21867.85		
$4_{40} - 5_{41}$	21443.24	21443.57		
$5_{05} - 6_{06}$	22046.31	22046.16	22041.39	22041.22
$5_{24} - 6_{25}$	24505.37	22505.25	24496.22	24496.12
$5_{23} - 6_{24}$	27629.01	27629.09	27614.06	27614.15
$5_{33} - 6_{34}$	25705.94	25705.96		
$6_{06} - 7_{07}$	25373.33	25373.26	25367.79	25367.66
$6_{16} - 7_{17}$	25290.13	25290.13	25284.05	25284.24
$6_{25} - 7_{26}$	28217.74	28218.06	28208.09	28208.37

Cont'd.

TABLE 2.7 (Cont'd.)

	V = 0		V = 1	
	observed (mc/s)	calculated (mc/s)	observed (mc/s)	calculated (mc/s)
$6_{34} - 7_{35}$	29887.53	29887.51	29874.06	29874.04
$6_{43} - 7_{44}$	30219.13	30219.16	30203.98	30204.08
$6_{42} - 7_{43}$	30482.78	30482.83	30466.32	30466.30
$7_{07} - 8_{08}$	28723.79	28724.10	28717.63	28717.83
$7_{17} - 8_{18}$	28687.25	28687.21	28680.81	28680.80
(A + C)/2		3391.05		3390.31
(A - C)/2		1702.60		1702.16
κ		-0.511275		-0.511892

TABLE 2.8

Measured line frequencies for aniline $-ND_2$

	observed	calculated
$5_{05} - 6_{06}$	21982.07	21981.84
$5_{14} - 6_{15}$	25478.19	25478.21
$5_{23} - 6_{24}$	26482.88	26482.91
$5_{33} - 6_{34}$	24856.43	24856.39
$5_{32} - 6_{33}$	25404.84	25404.89
$5_{42} - 6_{43}$	24868.89	24868.96
$5_{41} - 6_{42}$	24900.31	24900.35
$6_{06} - 7_{07}$	25274.04	25274.40
$6_{25} - 7_{26}$	27739.63	27739.76
$6_{24} - 7_{25}$	30943.55	30943.43
$6_{34} - 7_{35}$	28973.14	28973.18
$6_{42} - 7_{43}$	29202.55	29202.45
$7_{07} - 8_{08}$	28588.92	28588.70
$(A + C)/2$		3599.39
$(A - C)/2$		1920.35
κ		-0.622616

TABLE 2.9

Measured line frequencies for aniline - 2,4,6 D_3

	V = 0		V = 1	
	observed (mc/s)	calculated (mc/s)	observed (mc/s)	calculated (mc/s)
$4_{12} - 5_{14}$	21770.24	21770.30		
$4_{23} - 5_{24}$	20313.17	20312.93	20305.49	20305.54
$4_{22} - 5_{23}$	22466.03	22466.09	22454.14	22454.21
$5_{05} - 6_{06}$	21745.51	21745.24	21740.62	21740.94
$5_{15} - 6_{16}$	21552.96	21552.90	21548.21	21548.16
$5_{14} - 6_{15}$	25460.93	25461.01	25452.37	25452.86
$5_{24} - 6_{25}$	24103.11	24103.33	24094.80	24095.19
$5_{23} - 6_{24}$	27082.43	27082.29	27068.61	27068.79
$5_{32} - 6_{33}$	26135.22	26135.39	26121.32	26121.19
$6_{16} - 7_{17}$	24928.49	24928.40	24923.34	24923.20
$6_{25} - 7_{26}$	27773.78	27774.02		
$6_{24} - 7_{25}$	31456.15	31456.20		
$6_{34} - 7_{35}$	29345.87	29345.63	29333.07	29333.54
$6_{33} - 7_{34}$	31042.61	31042.70		

Cont'd.

TABLE 2.9 (Cont'd)

	V = 0		V = 1	
	observed (mc/s)	calculated (mc/s)	observed (mc/s)	calculated (mc/s)
$6_{43} - 7_{42}$	29631.11	29630.90		
$6_{42} - 7_{43}$	29853.55	29853.67	29838.93	29838.93
$7_{07} - 8_{08}$	28322.65	28322.94	28316.84	28317.43
$7_{17} - 8_{18}$	28280.19	28280.12	28274.43	28274.44
$(A + C)/2$		3379.01		3378.54
$(A - C)/2$		1714.35		1715.16
κ		-0.531528		-0.532120

TABLE 2.10

Measured line frequencies for aniline - D_5

	V = 0		V = 1	
	observed (mc/s)	calculated (mc/s)	observed (mc/s)	calculated (mc/s)
$4_{13} - 5_{14}$	20906.32	20906.17		
$4_{22} - 5_{23}$	21862.91	21862.76	21851.04	21851.05
$4_{32} - 5_{33}$	20352.25	20352.26		
$4_{31} - 5_{32}$	20852.01	20851.94	20840.74	20840.91
$5_{05} - 6_{06}$	20706.74	20706.51	20702.56	20702.56
$5_{15} - 6_{16}$	20573.72	20573.48	20569.16	20569.09
$5_{14} - 6_{15}$	24317.71	24317.70		
$5_{23} - 6_{24}$	26261.36	26261.19		
$5_{33} - 6_{34}$	24386.87	24386.84		
$5_{32} - 6_{33}$	25531.17	25531.13	25516.77	25516.64
$5_{41} - 6_{42}$	24638.63	24638.90		
$6_{06} - 7_{07}$	23840.55	23840.52	23835.77	23835.91
$6_{16} - 7_{17}$	23781.53	23781.47	23776.79	23776.67
$6_{24} - 7_{25}$	30358.47	30358.77		

Cont'd.

TABLE 2.10 (Cont'd.)

	V = 0		V = 1	
	observed (mc/s)	calculated (mc/s)	observed (mc/s)	calculated (mc/s)
$7_{07} - 8_{08}$	26994.91	26995.21	26989.94	26990.07
$7_{17} - 8_{18}$	26970.47	26970.55	26965.33	26965.31
$(A + C)/2$		3123.08		3122.41
$(A - C)/2$		1535.91		1535.48
κ		-0.469162		-0.469779

for the first time using the recorder. The lines were too weak to resolve any quadrupole fine structure and the Stark lobes too indefinite to make dipole moment measurements.

(3) Excited vibrational states : the inversion and torsional motions of the amine group

A very anharmonic vibration involving primarily the amino-hydrogen atoms and giving rise to a low lying first excited state has been observed in formamide [12], cyanamide [13], and nitramide [14]. These facts have been interpreted in terms of a pyrimidal configuration about the nitrogen atom and an inverting NH_2 group.

If aniline were planar the potential describing the NH_2 wagging vibration would be nearly parabolic and the vibrational energy levels would be evenly spaced (fig. 2.5a). The symmetry of the vibrational wave function for this vibration with respect to inversion is even for V = 0, 2, 4 $^{\circ\circ}$ and odd for V = 1, 3, 5 $^{\circ\circ}$.

(a)

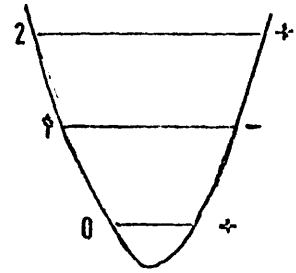

planar molecule

(b)

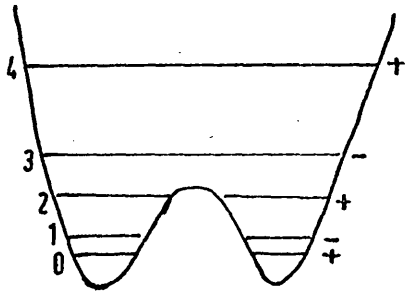

intermediate barrier

(c)

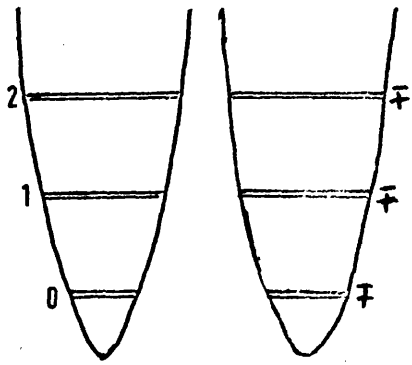

high barrier

fig.2·5

If the potential function for the N H_2 wagging vibration is distorted by raising a hump the energy levels approach each other in pairs (fig. 2.5b). When the potential barrier is very high and the two conformations cannot interconvert by tunnelling through the barrier the energy levels are again evenly spaced but are doubly degenerate (fig. 2.5c). In the case of barriers of intermediate height the vibrational wave functions retain the same symmetry with respect to inversion as the corresponding wave functions of the planar molecule.

An idea of the separation between the V = 0 and V = 1 states of aniline can be obtained from the relative intensities of their spectra.

In aniline - H_7 and the symmetrically substituted isotopic species the nuclear spin statistical weight effects due to a number of pairs of equivalent hydrogen or deuterium atoms must be allowed for. The overall wave function for a molecule must be either symmetric or antisymmetric depending on the number of pairs of

nuclei and their spins. The wave function may be written as a product of electronic, vibrational, rotational and nuclear spin wave functions.

$$\Psi_{total} = \Psi_e \times \Psi_{vib} \times \Psi_{rot} \times \Psi_{N.S.}$$

Aniline has a symmetric ground electronic state (A_g) and the symmetries of the vibrational wave functions have been given above. The symmetry of the rotational wave function with respect to the operation C_{2a} depends on K_{-1} and is

K_{-1}	even	symmetric
K_{-1}	odd	antisymmetric

The allowed combinations of vibrational, rotational and nuclear spin wave functions are given in table 2.11. The statistical weight effects ($g_{N.S.}$) have been calculated from the formulae[15]

$$g_{symmetrical} = 1/2 \left[\prod_1^n (2I_i+1)\right] \times \left[\prod (2I_i+1) + 1\right]$$

$$g_{antisymm.} = 1/2 \left[\prod_1^n (2I_i+1)\right] \times \left[\prod_1^n (2I_i+1) - 1\right]$$

TABLE 2.11

Allowed combinations of vibrational, rotational and nuclear spin wave functions for aniline.

	Ψ total	K_{-1}	V = 0 $\Psi_{N.S.}$	V = 0 $g_{N.S.}$	V = 1 $\Psi_{N.S.}$	V = 1 $g_{N.S.}$
aniline -H_7						
aniline -^{15}N		even	antisymmetric	28	symmetric	36
aniline -1^{13}C	antisymmetric					
aniline -4 D_1		odd	symmetric	36	antisymmetric	28
aniline -N D_2	symmetric	even	symmetric	78	antisymmetric	66
aniline -3,5 D_2						
aniline -2,4,6 D_3		odd	antisymmetric	66	symmetric	78
aniline D_5	antisymmetric	even	antisymmetric	135	symmetric	171
		odd	symmetric	171	antisymmetric	135

where Ii is the spin of one of the i th pair of nuclei and n is the number of pairs of equivalent nuclei. The V = 1 lines of the various isotopic species of aniline never appear stronger than the V = 0 lines even when the V = 1 state has the larger statistical weight. If the μ_a components of the dipole moments of the V = 0 and V = 1 states are equal then the separation between these states is less than 100 cm^{-1}.

From the ultra-violet spectrum of aniline Brand, Williams and Cook [8] deduce a separation of 34 cm^{-1}. They have fitted the lower energy levels of the inversion modes of aniline - H_7 and aniline - N D_2 to a double minimum potential

$$V/hc = 1/2 q^2 \nu_0 + \alpha \nu_0 \exp(-\beta q^2)$$

where q is the normal co-ordinate and α, β and ν_0 are arbitrary constants. In this way they obtained a value of the degree of non-planarity of aniline and obtained a barrier to inversion of 565 cm^{-1}. However if their inversion splittings are fitted, assuming the

geometry of the CNH_2 group given in the next section, to a Manning potential

$$V/hc = A\,\mathrm{sech}^4(X/\rho) + B\,\mathrm{sech}^2(X/\rho)$$

(where X is the normal co-ordinate and A, B and ρ are arbitrary constants) a barrier of 970 cm^{-1} is obtained [16]. These values may be compared with the barriers in ammonia [17] (V = 2000 cm^{-1}), formamide [12] (V = 310 cm^{-1}), cyanamide [13] (V = 710 cm^{-1}) and nitramide [13] (V = 950 cm^{-1}) that have been obtained by fitting the vibrational energy levels of the inversion modes of those molecules to a Manning potential.

μ_C transitions occur with a change in parity of the K_{-1} quantum number and must therefore involve states with vibrational wave functions of different symmetries. For such transitions to occur in the microwave region the changes in vibrational and rotational energies must almost cancel each other. The inversion splitting in aniline - $N D_2$ has been estimated to be 7 cm^{-1} and the low field lines in the microwave spectrum of this isotopic

species are thought to be μ_c transitions between the V = 0 and V = 1 states. An estimate of the J and K_{-1} quantum numbers involved in these transitions may be obtained by equating the change in rotational energy to the inversion splitting. For high J and K_{-1} the energy levels of a prolate asymmetric top are given quite accurately by

$$W_J, K_{-1} = J(J + 1)(B + C)/2 + (A - (B + C)/2) K_{-1}^2$$

If a $\Delta K_{-1} = +1$, $\Delta K_1 = 0$ Q branch line is to occur in the microwave region

$$(A - (B + C)/2) (K_{-1} + 1) \sim 7 \text{ cm}^{-1}$$

giving $K_{-1} \sim 35$. Although the analysis of such lines would lead to an accurate value of the inversion splitting the assignment of lines with very high J and K_{-1} quantum numbers is very difficult.

The internal rotation of the amine group in aniline is hindered by a potential of the form

$$V = V_2/2(1 - \cos\alpha)$$

where α is the torsional angle (fig. 2.6). If the internal rotation of the amine group can be separated from the other motions of the molecule the energy levels are solutions of the Mathieu equation and are given by [18]

$$br(s) = \frac{8\pi^2 c\, Ieff}{h}\left[\frac{E(r) - V_2}{hc}\right]$$

$$s = \frac{8\pi^2 c\, Ieff\,(V_2/hc)}{h}$$

$E(r)/hc$ are the term values, the br(s) are eigenvalues of the Mathieu equation and

$$Ieff = I_1 I_2 / I_\alpha$$

where I_1 and I_2 are the moments of inertia of the amine and phenyl group and I_α is the a moment of inertia of aniline. If the barrier to internal rotation is very high the energy levels are doubly degenerate and evenly spaced and when the barrier is low the upper energy levels correspond to free rotation. The two situations

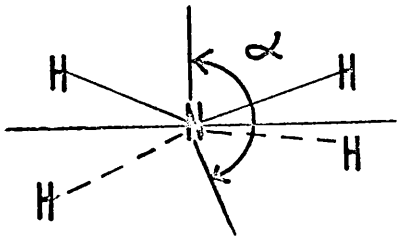

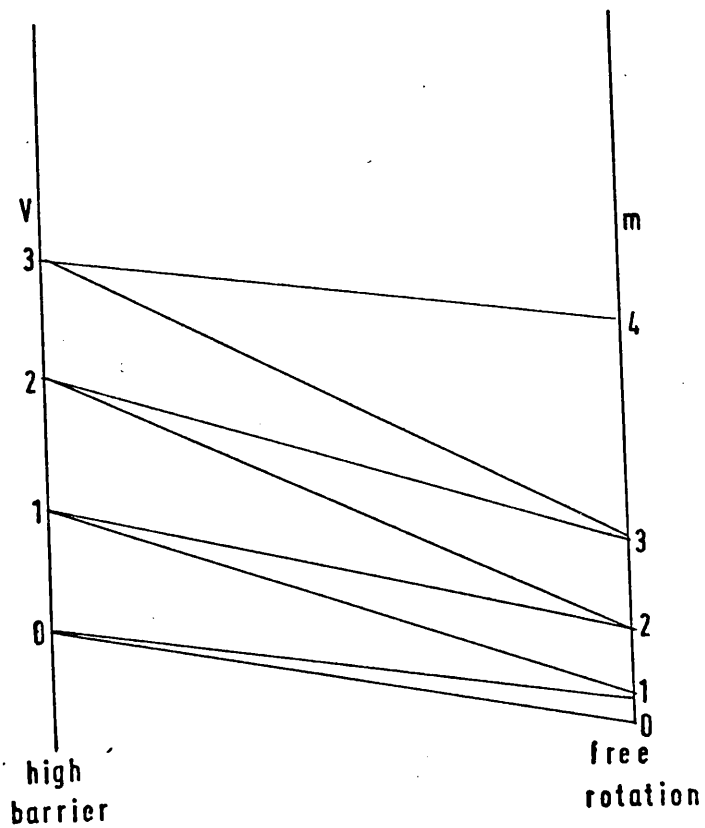

fig. 2·6

are shown in fig 2.6.

Evans [8] has assigned an infra-red band at 420 cm^{-1} to the 0 - 2 transition of the torsional mode of aniline and calculates the barrier to internal rotation to be 1247 cm^{-1}. The splitting of the lowest energy level ($\Delta b_{0^{\pm}}$) can be estimated from the formula [18]

$$\Delta b_{0^{\pm}} = 7.6788(s)^{0.75} \exp[-1.9860\, s^{0.5}]$$

and is found to be less than 1 mc/s. The degeneracy of the vibrational levels of aniline due to the internal rotation is therefore not effectively lifted. There is some uncertainty about the infra-red band at 420 cm^{-1} since Brand, Williams and Cook calculate the 0 - 2 transition of the inversion mode at 423 cm^{-1}. However the similarity of the barriers to internal rotation in methylamine [4] (V_3 = 691 cm^{-1}) and methyl alcohol [19] (V_3 = 375 cm^{-1}) indicate that the barrier in aniline should be similar to that in phenol [18] (V_2 = 1215 cm^{-1}).

The vibrational satellites in the microwave spectrum of aniline are consistent with a non-planar molecule and

considerable barriers preventing the inversion and internal rotation of the amine group.

4. Structure

(a) Inertial defects

The inertial defect, defined by

$$\Delta^{\circ} = I_c - I_b - I_a,$$

is zero for a rigid lamina and for a rigid non-planar body

$$\Delta^{\circ} = -2\sum mc^2.$$

These expressions are not strictly valid for the effective moments of inertia obtained from the ground state rotational constants of a molecule. The corrections due to Coriolis coupling and the inversion and averaging of the moments of inertia have been discussed but are too complicated to be applied to heavy molecules[20]. In a planar molecule the in-plane vibrations make a positive and the out of plane vibrations a negative contribution to Δ°. Planar aromatic molecules have a number of low frequency out

of plane vibrations and the inertial defects of this type of molecule are usually of the order of +0.05 a.m.u. $\AA^2$. Variations of $\pm$ 0.02 a.m.u. $\AA^2$ are generally found amongst the various isotopic species of a given molecule.

The ground state and first excited vibrational state moments of inertia for the ten isotopic species of aniline whose microwave spectra have been investigated are given in tables 2.12 and 2.13. The inertial defects (Δ°) for aniline $-^{15}N$, aniline $-1^{13}C$ and the ring deuterated species of aniline are similar to that of aniline $-H_7$. The ratios of Δ° for aniline -NHD and aniline $-ND_2$ to that of aniline $-H_7$ are 1.42:1 and 1.97:1 respectively. Such behaviour is consistent with a planar C_6H_5N fragment and the amino-hydrogen atoms lying out of the plane of the rest of the molecule.

The amino-hydrogen atoms were located in the principal axis system of aniline $-H_7$ using Kraitchman's equations and the moments of inertia of aniline -NHD and aniline $-H_7$.

TABLE 2.12

V = 0 moments of inertia for aniline

	Ia (a.m.u. Å^2)	Ib (a.m.u. Å^2)	Ic (a.m.u. Å^2)	Δ (a.m.u. Å^2)
aniline -H_7	89.9938	194.8968	284.4792	-0.4114
aniline - NHD	90.7277	202.7314	292.8747	-0.5844
aniline -^{15}N	89.9986	200.2968	289.8787	-0.4167
aniline -1-^{13}C	89.9910	195.7681	285.3481	-0.4110
aniline -2 D_1	94.5536	195.5224	289.6528	-0.4232
aniline -4 D_1	89.9912	203.5706	293.1532	-0.4086
aniline -3,5 D_2	99.2473	200.5638	299.4054	-0.4057
aniline -N D_2	91.5871	210.3096	301.0849	-0.8118
aniline -2,4,6 D_2	99.2529	204.8525	303.6842	-0.4214
aniline - D_5	108.5066	210.4196	318.5109	-0.4153

TABLE 2.13

V = 1 moments of inertia for aniline

	Ia (a.m.u. Å^2)	Ib (a.m.u. Å^2)	Ic (a.m.u. Å^2)	Δ (a.m.u. Å^2)
aniline -H_7	90.0231	195.0171	284.5289	-0.5113
aniline -NHD	90.7758	202.7898	292.8424	-0.7231
aniline -^{15}N	90.0444	200.4318	289.9942	-0.4820
aniline -1^{13}C	90.0222	195.8891	285.3952	-0.5160
aniline -2 D_1	94.5609	195.6420	289.7052	-0.4977
aniline -4 D_1	90.0176	203.6904	293.2025	-0.5055
aniline -3,5 D_2	99.2703	200.6880	299.4586	-0.4997
aniline -N D_2	-	-	-	-
aniline -2,4,6 D_3	99.2660	204.9663	303.7335	-0.4988
aniline -D_5	108.5322	210.5440	318.5591	-0.5171

$$a_{NH} = 2.7801 \quad (\text{Å})$$

$$b_{NH} = 0.8352$$

$$c_{NH} = 0.3016$$

The principal moments of inertia of the C_6H_5N fragment were calculated using the following expressions for the differences in moments of inertia between aniline $-H_7$ and C_6H_5N

$$\Delta I_a = \Delta' I_a - 2 M_H b^2_{NH}$$

$$\Delta I_c = \Delta' I_c - 2 M_H b^2_{NH}$$

$$\Delta I_b = \Delta' I_a + \Delta' I_c$$

$\Delta' I_a$ and $\Delta' I_c$ are roots of equations 2.2 and 2.3.

$$\Delta' I_a^2 - [\mu(a^2_{NH} + c^2_{NH}) - (I_a - I_c)]\Delta' I_a - \mu c^2_{NH}(I_a - I_c) = 0 \qquad 2.2$$

$$\Delta' I_c^2 - [\mu(a^2_{NH} + c^2_{NH}) - (I_c - I_a)]\Delta' I_c - \mu a^2_{NH}(I_c - I_a) = 0 \qquad 2.3$$

$$\mu = -\frac{2 M M_H}{M - 2M_H}$$

and M is the molecular weight of aniline. Equations

2.2 and 2.3 are derived from Kraitchman's equations for a planar asymmetric top.

The inertial defect of C_6H_5N was found to be -0.0034 a.m.u. $\AA^2$ and this is good evidence for the planarity of that fragment. Table 2.13 shows that Δ' is smaller than Δ° and the contribution from the inversion vibration causes the inertial defect of the C_6H_5N fragment to have a negative rather than the expected small positive value.

The c co-ordinates of the amino-hydrogen atoms confirm that aniline has the configuration (fig.2.7a). In configuration (b) the distance between the amino-hydrogen atoms ($\sim$0.60 $\AA$) is only twice the covalent radius of hydrogen and such a small separation between non-bonded atoms is unlikely. The other possible configuration for non-planar aniline (c) is excluded because such a molecule would not show the observed inversion doubling.

Possible configurations for aniline

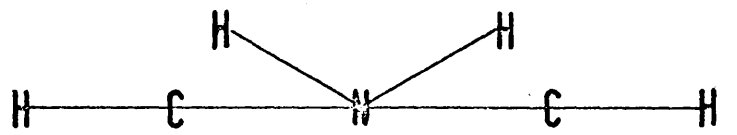

(a)

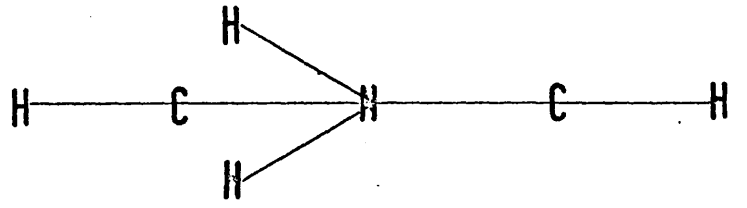

(b)

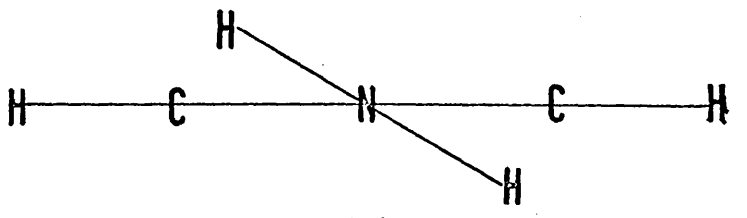

(c)

fig.2-7

(b) The structure of the C-NH_2 fragment

Lide[21] has shown that interactions between the inversion of the amine group and the overall rotation of the molecule can lead to appreciable contributions to the rotational constants. The data for aniline -ND_2 thus provides a useful check on the accuracy of the location of the amino-hydrogen atoms. The differences in moments of inertia of aniline -ND_2 and aniline -H_7 are given by the following expressions

$$\Delta I_a = \Delta' I_a + 2\Delta M_b^2{}_{NH} \quad - 2.4$$

$$\Delta I_c = \Delta' I_c + 2\Delta M_b^2{}_{NH} \quad - 2.5$$

$$\Delta I_b = \Delta' I_a + \Delta' I_c \quad - 2.6$$

$$\Delta M = M_D - M_H$$

and $$b^2_{NH} = \frac{1}{4\Delta M}(\Delta I_a + \Delta I_c - \Delta I_b) \quad - 2.7$$

The a and b co-ordinates were obtained by substituting $\Delta' I_a$ and $\Delta' I_c$ into Kraitchman's equations for a

planar asymmetric top.

$$a_{NH} = 2.7770$$

$$b_{NH} = \pm 0.8320$$

$$c_{NH} = 0.3305$$

The a and b co-ordinates determined from the singly and doubly deuterated isotopic species show the variations expected from zero point vibrational effects. The difference between the c co-ordinates is somewhat larger, but this is the least well determined co-ordinate.

The nitrogen and 1-carbon atoms were located in the principal axis system of aniline $-H_7$ by substituting the appropriate values of ΔI_a and ΔI_c into Kraitchman's equations for a planar top.

$a_N = 2.3390$ $\qquad$ $c_N = 0.0707$

$a_{C_1} = 0.9365$ $\qquad$ c_{C_1} = imaginary.

In view of the expected small values of the C

co-ordinates of the atoms of the C_6H_5N fragment the imaginary value of C_{C_1} is not surprising.

As the C_6H_5N fragment is planar there is a linear relationship between the a and c co-ordinates of its atoms

$$C_i = Xa_i + y \qquad 2.8$$

The constants X and y can be obtained from the first moment conditions ($\Sigma ma = 0$, $\Sigma mc = 0$) and the product of inertia condition ($\Sigma mac = 0$). These conditions take the form

$$-2M_H a_{NH} X + (M - 2M_H) y = -2M_H c_{NH}$$

$$(Ib + 1/2\,\Delta^\circ - 2M_H a^2_{NH})\,X - 2M_H a_{NH} = -2M_H a_{NH} c_{NH}$$

where Σma^2 over the atoms of C_6H_5N has been replaced by

$$I_b - 1/2\,\Delta^\circ - 2\,M_H\,a^2_{NH}$$

The degree of non-planarity (ϕ) is defined as the angle between the extension of the C - N bond and the

bisector of the HNH angle (fig.2.8a).

$$\phi = \alpha + \beta$$

$$\alpha = \tan^{-1} (c_{NH} - c_N) / (a_{NH} - a_N)$$

$$\beta = -\tan^{-1} X$$

The geometry of the C-NH_2 group calculated using the co-ordinates of the amino-hydrogen atoms obtained from the moments of inertia of the pairs of isotopic species

aniline - NHD / aniline - H_7

aniline - ND_2 / aniline - H_7

are shown in fig 2.8b and fig. 2.8c. Because the rotational constants for aniline -ND_2 might well be an average for the V = 0 and V = 1 states of that isotopic species the structure calculated from the single deuterium substitution is considered more reliable.

The degree of non-planarity is somewhat less than that obtained by Brand, Williams and Cook ($\phi \sim 46^\circ$) from their study of the ultra-violet spectrum of aniline. The N - H bond length is comparable with those in

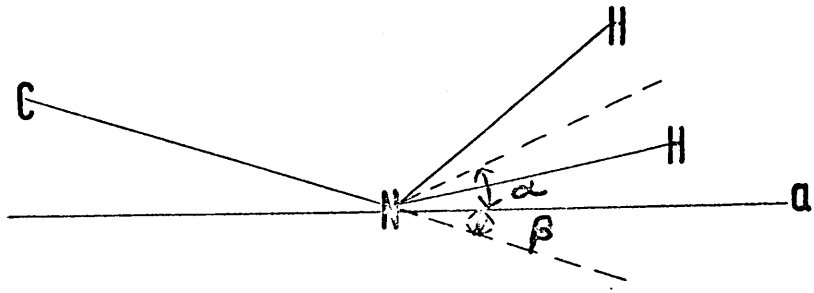

(a)

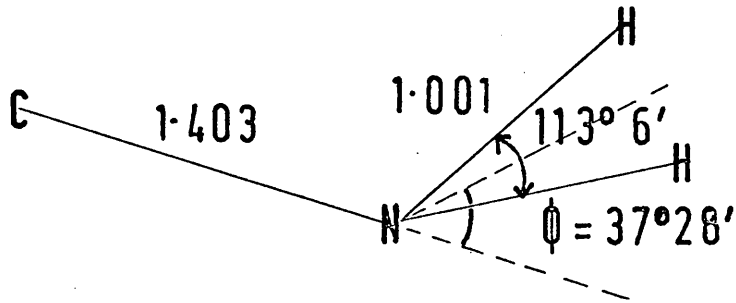

α = 36° 53′

β = 33′

(b)

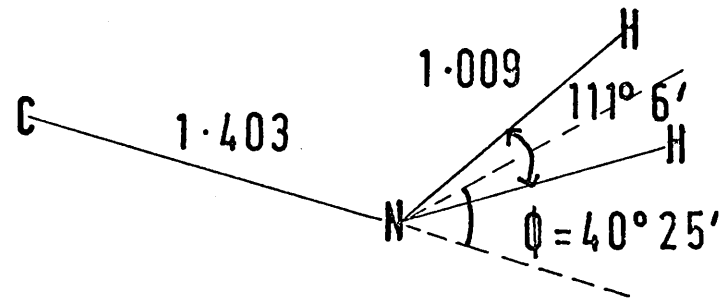

α = 39° 47′

β = 38′

(c)

fig.2.8

nitramide[14] (r_{N-H} = 1.005 Å) and cyanamide[13] (r_s N - H = 0.990 Å) but slightly shorter than that in ammonia[3] (r_s = 1.014 Å).

The degrees of non-planarity and C - N bond lengths in a number of amines are given in table 2.14a. The short bonds in aniline, formamide and cyanamide relative to that in methylamine are expected for two reasons

(i) changes in the hybridization of the carbon atom from sp^3 in methylamine to sp^2 in aniline and formamide to sp in cyanamide

(ii) contributions from structures of the type $N^+H_2=\bar{X}$ to the overall state of the molecule. These effects are difficult to separate but the variations in the C - C bonds of the analogous methyl compounds (table 2.14b) indicate the hybridization effects may be responsible for a large portion of the bond shortenings found in these amines. The degree of non-planarity is therefore perhaps a better measure of the contributions from the structures $N^+H_2=\bar{X}$ than the length of the C - N bond.

TABLE 2.14a

	ϕ (°)	r_{C-C} (Å)
methyl amine [4]	55	1.474
aniline	38	1.403
formamide [12]	17	1.376
cyanamide [13]	38	1.346

TABLE 2.14b

	r_{C-C} (Å)	Δr (Å)
ethane [22]	1.536	
toluene [23]	1.51	0.03
acetaldehyde [24]	1.501	0.035
methyl cyanide [25]	1.458	0.078

Δr is the difference between the C - C bond in ethane and that in CH_3X.

(c) The location of the ring hydrogen atoms

The ortho and para hydrogen atoms were located in the principal axis system of aniline $-H_7$ using the moments of inertia of aniline $-2D_1$ and aniline $-4D_1$. The meta hydrogen atoms were located using aniline - 3,5 D_2 and equations 2.4 - 2.7. The c co-ordinates were calculated from equation 2.8 and a list of the substitution co-ordinates is given in table 2.15.

A check on the b co-ordinates of the ortho and meta hydrogen atoms was made using equation 2.7 and the pairs of isotopic species given below

aniline - D_5/ aniline - 3,5 D_2 $\quad b_{H2} = \pm 2.1440$

aniline - D_5/ aniline - 2,4,6 D_3 $\quad b_{H3} = \pm 2.1443$

The agreement with the values given in table 2.13 is very good.

Before the sample of aniline - $4D_1$ was available the a co-ordinate of the para hydrogen atom was found from the following calculation. The intermediate

TABLE 2.15

Isotopic substitution co-ordinates for aniline

	a (Å)	b (Å)	c (Å)
NH	2.7801	0.8352	0.3016
N	2.3390	0	-0.0299[1]
C_1	0.9365	0	-0.0163
H_2	0.7714	2.1442	-0.0148
H_3	-1.6958	2.1444	0.0091
H_4	-2,9513	0	0.0213

The c co-ordinates of the atoms except for c_{NH} have been calculated from equation 2.8 .

moment of inertia of aniline - 2, 6 D_2 is given by

$$I'_b = I_b + \Delta'I_a + \Delta'I_c$$

where $\Delta'I_a$ and $\Delta'I_c$ are solutions of the appropriate forms of equations 2.3 and 2.4. The co-ordinates of the ortho hydrogen atoms about axes parallel to the principal axes of aniline - 2, 6 D_2 were calculated from the first moment conditions, giving

$$a'_{H2} = 0.7551$$
$$c'_{H2} = -0.0117$$

Allowing for the small rotation to the principal axis system of aniline - 2, 6 D_2 makes negligible differences to these co-ordinates. In the remainder of this calculation the effects of the small rotations of principal axis systems relative to each other have been neglected. The para hydrogen atom was located in the principal axis system of aniline - 2, 6 D_2 using aniline - 2,4,6 D_3 and

$$\Delta I_b = \mu(a^2_{H_4} + c^2_{H_4}) \qquad 2.9$$

C'_{H4} was estimated using a_{H4} from our preliminary structure. The co-ordinate of the para hydrogen atom in the principal axis system of aniline - H_7 is given by

$$a_{H4} = a_{H2} + a'_{H4} - a'_{H2} = -2.9526 .$$

The a co-ordinate of the meta hydrogen atom was calculated in a similar manner. The co-ordinate of the para hydrogen atom (a''_{H4}) in the principal axis system of aniline - 2,4,6 D_3 was calculated using equation 2.9 and the appropriate reduced mass. The meta hydrogen atoms were located in this system of axes using the inertial data for aniline -D_5 and equations 2.5 - 2.7. The a co-ordinate of the meta hydrogen atom is given by

$$a_{H3} = a_{H4} + a''_{H3} - a''_{H4} = -1.6949$$

The good agreement with the values given in table 2.15 indicates the reliability of the rotational constants of the various isotopic species of aniline.

(d) The location of the remaining atoms.

In order to determine the structure of aniline completely the a and b co-ordinates of the ortho and meta carbon atoms and the a co-ordinate of the para carbon atom remain to be fixed. The second moment condition for I_a, the first moment condition ($\sum ma = 0$) and the second moment condition for I_b mean it is necessary to assume one a and one b co-ordinate. If the reasonable assumption is made that the $C_2 - C_3$ and $C_5 - C_6$ bonds are parallel then the second moment condition for I_a may be rewritten to give

$$b_C^2 = (I_a + 1/2\,\Delta^\circ - 2m\,(b_{NH}^2 + b_{H_2}^2 + b_{H_3}^2))/2m_C \qquad 2.10$$

where $\sum mc^2$ has been replaced by $-1/2\,\Delta^\circ$. Equations similar to 2.10 hold for all of the isotopic species with C_s symmetry and solution of these equations gives

$$b_c = 1.2060 \pm 0.0002\ \text{Å}$$

The first moment condition may be rewritten to give

$$2a_{C_2} + 2a_{C_3} + a_{C_4} = -\frac{\Sigma' ma}{m_C} \qquad 2.11$$

and the second moment condition to give

$$2a_{C_2}^2 + 2a_{C_3}^2 + a_{C_4}^2 = 1/m_C[Ib + 1/2\,\Delta^\circ - \Sigma' ma^2] \quad 2.12$$

where Σ' indicates a summation over atoms located by isotopic sybstitution. In benzene[26] the C – H bond is 1.084 Å and setting C_4 – H equal to this gives

$$a_{C_4} = -1.8673\,,$$

substitution of this value into 2.11 and 2.12 and solution of the resulting simaltaneous equations gives

$$a_{C_2} = +0.2395$$

$$a_{C_3} = -1.1712$$

The C_2 – C_3 bond length of 1.411 Å is much longer than the C – C bond in benzene[26] (1.397 Å). The replacement of a hydrogen atom by an amine group is not expected to have such a large effect on the geometry of the benzene ring. Substitution co-ordinates are known to place atoms too close to the centre of mass. The use of the second moment condition

in conjunction with the substitution co-ordinates can lead to serious errors in the location of atoms especially if these atoms are close to a principal axis.

When an isotopic substitution is made in a molecule the average bond lengths around the atom in question change slightly. The substitution of deuterium for hydrogen causes a shortening of approximately 0.003 Å and the changes for heavier atoms such as carbon or nitrogen are of the order of 0.00005 Å. Laurie and Herschbach[27] have discussed the effects of such shortenings on the moments of inertia of a linear molecule.

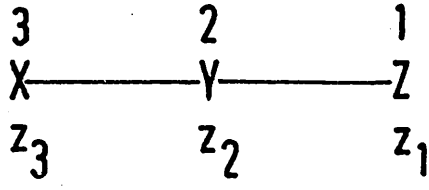

If no bond shortenings occur on isotopic substitution then the change in moment of inertia is related to the co-ordinate of the atom with respect to the centre of mass of the parent molecule by

$$\Delta I_i = \sum z_i^2 \qquad 2.13$$

If the X - Y bond length changes by δ_1 on substitution of the atom X then 2.13 must be replaced by

$$\Delta I_1 = \mu z_1^2 + 2m_1' z_1' \delta_1 \qquad 2.14$$

where the primes refer to the substituted molecule. The substitution co-ordinate is defined by

$$z_{is} = \left(\frac{\Delta I_i}{\mu}\right)^{1/2}$$

and provided z_1 is much greater than δ_1 equation 2.14 gives

$$z_1 = z_{1s} + m_1' \delta_1 \qquad 2.15$$

When the atom Y is substituted the changes in the X - Y bond (δ_1) and Y - Z bond (δ_3) must be taken into account and 2.13 must be replaced by

$$\Delta I_2 = \mu z_2^2 + 2(m_1 z_1' - m_3 z_3' \delta_3) \qquad 2.16 .$$

If the co-ordinates are large compared to the δs then equation 2.16 gives

$$z_2 = z_{2s} + (m_1 z_1 \delta_1 - m_3 z_3' \delta_3) / z_{2s} \qquad 2.17 .$$

Equation 2.15 was used to calculate the corrections to the co-ordinates of the hydrogen and nitrogen atoms in

aniline. The following σ_s were assumed for the hydrogen atoms

$$\sigma_a = 0.0015 \text{ Å}$$
$$\sigma_b = 0.0026$$

The HNH group was treated as a single mass and σ_N was assumed to be 0.00005 Å. The correction to the co-ordinate of the 1 - carbon atom was estimated using equation 2.17 assuming

$$m_1 = 16 \qquad \sigma_1 = 0.00005 \text{ Å}$$
$$m_3 = 26 \qquad \sigma_3 = 0.00003 \text{ Å}$$
$$z_3' = 0.25 \text{ Å}$$

The remaining carbon atoms were located using equations 2.10 - 2.13 and assuming $C_4 - H = 1.084$ Å. The co-ordinates of the atoms are given in table 2.16 and the resulting structure is shown in fig. 2.9a.

The geometry of the phenyl group was also fixed using the substitution co-ordinates, equations 2.10 and 2.11, and assuming that $r_{c_2 - c_3}$ and $r_{c_3 - c_4}$ are equal to 1.397 Å. The resulting structure is

TABLE 2.16

Co-ordinates corrected for bond shortening effects.

	a	b	c
NH	2.7816	$\pm$0.8378	0.3024
N	2.3398	0	-0.0300[1]
C_1	0.9387	0	-0.0164
H_2	0.7729	$\pm$2.1468	-0.0148
H_3	-1.6973	$\pm$2.1470	0.0092
H_4	-2.9573	0	0.0213
C_2	0.2347	$\pm$1.2056	-0.0096
C_3	-1.1644	$\pm$1.2056	0.0040
C_4	-1.8733	0	0.0109

1. The c co-ordinates of the atoms except for 1 c_{NH} have been calculated from equation 2.8.
2. The a and b co-ordinates for C_2 - C_4 have been calculated from equations 2.10 - 2.13 assuming C_4 - H = 1084 Å .

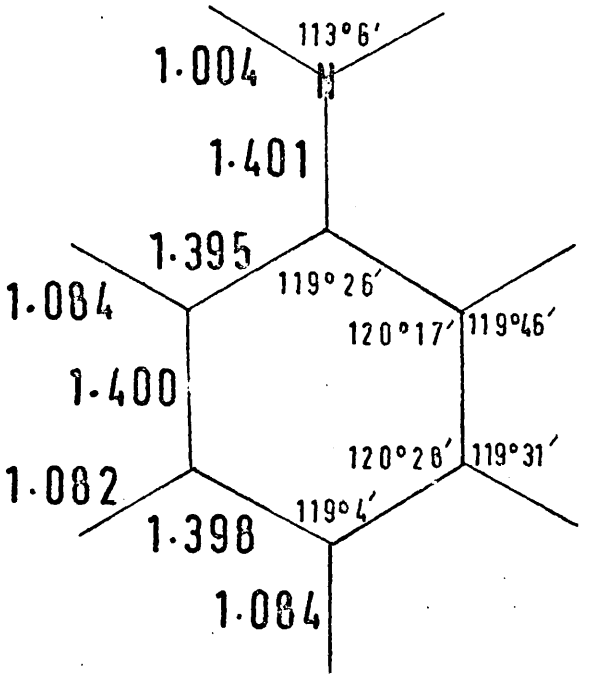
113°6′
1·004
1·401
1·395
119°26′
1·084
120°17′
119°46′
1·400
120°26′
119°31′
1·082
119°4′
1·398
1·084

(a)

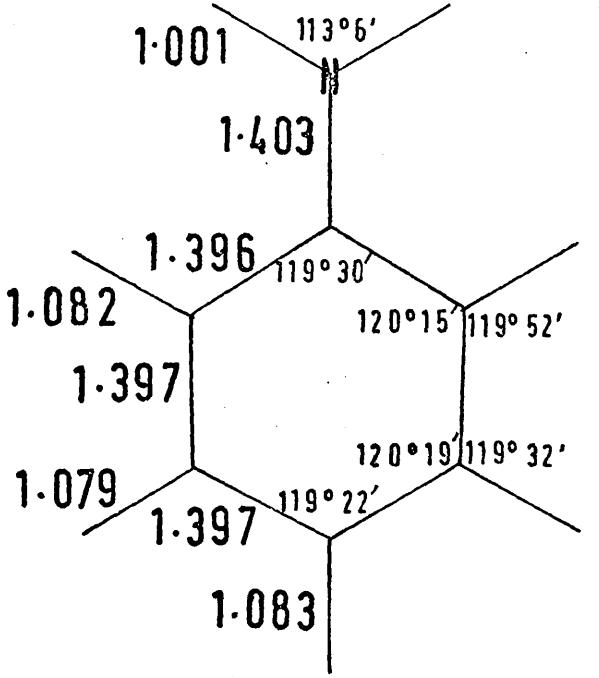
1·001
113°6′
1·403
1·396
119°30′
1·082
120°15′
119°52′
1·397
120°19′
119°32′
1·079
119°22′
1·397
1·083

(b)

fig.2·9

shown in fig. 2.9b and the calculated I_b is lower than the observed by a factor of 1.002. Moments of inertia calculated from r_s structures are usually smaller than the observed values by a factor of up to 1.005.

Both of the structures shown in fig. 2.9 indicate that the carbon-carbon bond lengths in aniline do not differ by more than 0.005 Å from that in benzene. The phenyl group appears to be somewhat narrower and elongated compared to that in benzene and this is reflected in the substitution co-ordinates of H_3 and H_4. The $H_2 - H_3$ distance in aniline (2·467 Å) is slightly shorter than that in benzene (2·488 Å) but this might be due to repulsions between the amino and ortho hydrogen atoms rather than a short $C_2 - C_3$ bond. A detailed discussion of the distortions to the phenyl group in aniline must await the location of the remaining atoms by isotopic substitution.

REFERENCES

1. A. Albert and E.P. Serjeant, "Ionization Constants of Acids and Bases", Methven and Co. Ltd., 1962, 139.

2. C. K. Ingold, "Structure and Mechanism in Organic Chemistry", G. Bell and Sons Ltd., 1953, Chapter 6, 223.

3. W. S. Benedict and E.K. Plyler, Canad.J.Phys., 1957, 35, 1235

4. D. R. Lide Jr., J.Chem.Phys., 1957, 27, 343

5. T. J. Bhattachanya, Indian J.Phys., 1962, 36, 533

6. M. Aroney and R.J.W. LeFevre, J.Chem.Soc., 1956, 2775

7. A. Weissenberger and R. Sangewald, Z.Physik. Chem. 1929, 35, 237

8. J. C. Evans, Spectrochim. Acta, 1960, 16, 428

9. J.C.D. Brand, D.R. Williams and T.J. Cook, J. Mol. Spectroscopy, 1966, 20, 359

10. I. Fischer - Hjalmers, Arkiv Fysik, 1962, 21,123

11. C. A. Coulson, "Valence", Oxford University Press, 1961, 270

12. C. C. Costain and J.M. Dowling, J.Chem.Phys., 1960, 32, 158

13. J.K. Tyler, C.C. Costain and J. Sheridan, to be published

14. J. K. Tyler, J.Mol. Spectroscopy, 1963, 11, 39

15. C.H. Townes and A.L. Schawlow, "Microwave Spectroscopy", McGraw-Hill Book Company, Inc., 1955, 104

16. J. N. Macdonald, B.Sc., Thesis, University of Glasgow, 1966

17. M.F. Manning, J.Chem.Phys., 1935, 3, 136

18. H.D. Bist, J. C. Brand and D.R. Williams, J. Mol. Spectroscopy, 1967, 24, 402

19. E. V. Ivash and D.M. Dennison, J.Chem.Phys., 1953, 21, 1804

20. D. R. Herschbach and V.W. Laurie, J.Chem.Phys., 1964, 40, 3142

21. D.R.Lide,J.Mol. Spectroscopy, 1962, 8, 142

22. H. C. Allen and E.K. Plyler, J.Chem.Phys., 1959, 31, 1062

23. F. A. Keidel and S.H. Bauer, J.Chem.Phys., 1956, 25, 1218

24. R. W. Kilb, C.C Lin and E. B. Wilson, Jr., J. Chem. Phys., 1957, 26, 1695

25. C. C. Costain, J.Chem.Phys., 1958, 29, 864

26. A. Langseth and B.P. Stoicheff, Canad.J.Phys., 1956, 34, 350

27. V.W. Laurie and D. R. Herschbach, J.Chem.Phys., 1962, 37, 1687

CHAPTER 3.

Propiolic acid : centrifugal distortion and dipole moment

(1) Introduction

Propiolic acid may be regarded as belonging to a series of compounds derived from simple single carbon atom molecules by replacing a hydrogen atom by an acetylene group. A number of such compounds have been studied and the bond lengths in the acetylene groups have been shown to be nearly constant. The possibility of conjugation between the π-electron systems of the acetylene and carboxylic acid groups and the effect of this on the molecular geometry and the magnitude and direction of the dipole moment are of interest in propiolic acid.

Because of strong intra-molecular hydrogen bonding it is usually assumed that the cis conformation (a) of carboxylic acids is the only minimum in the potential function for the internal rotation of the hydroxyl group.

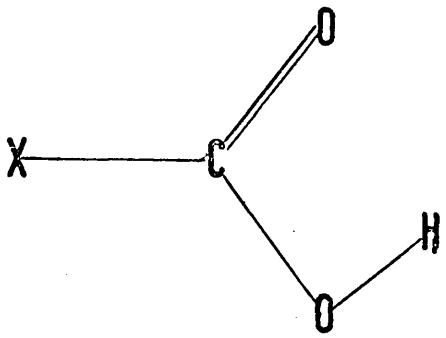

(a)

If minima corresponding to the other rotamers exist, then since their moments of inertia are different from that of the cis form it should be possible to detect their microwave spectra provided the Boltzman factors are not too small. Propiolic acid is a suitable molecule for this type of study because the only kind of rotational isomerism is associated with the hydroxyl group and a number of low J transitions occur in the microwave region.

A structure derived by replacing the hydrogen atom in formic acid[1] by the acetylene group of propynal[2] was used as a model for predicting lines (fig 3.1). Models for the trans and gauche rotamers were obtained by making suitable rotations

of the hydroxyl group of the structure shown in fig 3.1. The models were found to be prolate tops with $\kappa \sim -0.7$ and the most intense transitions expected were the μ_a R branch lines and a μ_b Q branch series of the type $J_{1,\ J-1} - J_{2,\ J-2}$.

Three isotopic species of propiolic acid, HCCCOOH, HCCCOOD and DCCCOOH have been studied. The spectrum of the normal isotopic species is too weak and complicated to observe lines due to ^{13}C species in their natural abundances. Uncertainty about the chemistry of propiolic acid has meant that the preparation of ^{18}O species has not been attempted.

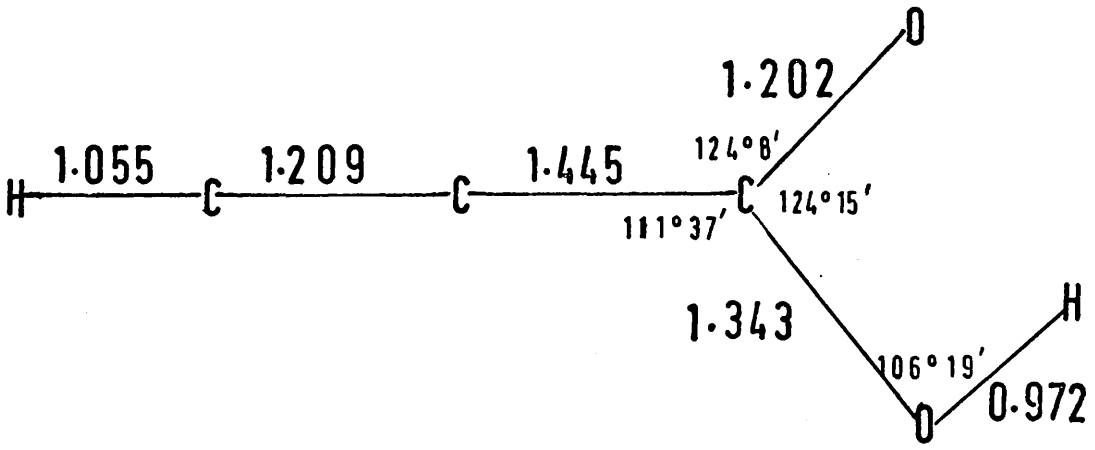

fig.3.1

(2) Analysis of spectra

(a) HCCCOOH

A sample of laboratory grade pripiolic acid (supplied by Koch-Light Laboratories Ltd.) was pumped under reduced pressure for half an hour to remove volatile impurities and then distilled into a sample tube. When freshly distilled the acid is colourless, but if left at room temperature and exposed to daylight it turns yellow and gradually polymerises. A preliminary search for lines was made in K band in the region where the $J = 2 - 3$ μa R branch and $J_{1,\ J-1} - J_{2,\ J-2}$ μb Q branch lines were expected to occur.

A number of moderately strong Q branch lines was located and recordings were made at several Stark voltages in order to determine the J values involved in the transitions. Assignments were made and these were confirmed from a Q branch plot. It was possible to assign the $2_{02} - 3_{03}$ and $1_{01} - 2_{12}$ R branch lines from the recordings (fig 3.2).

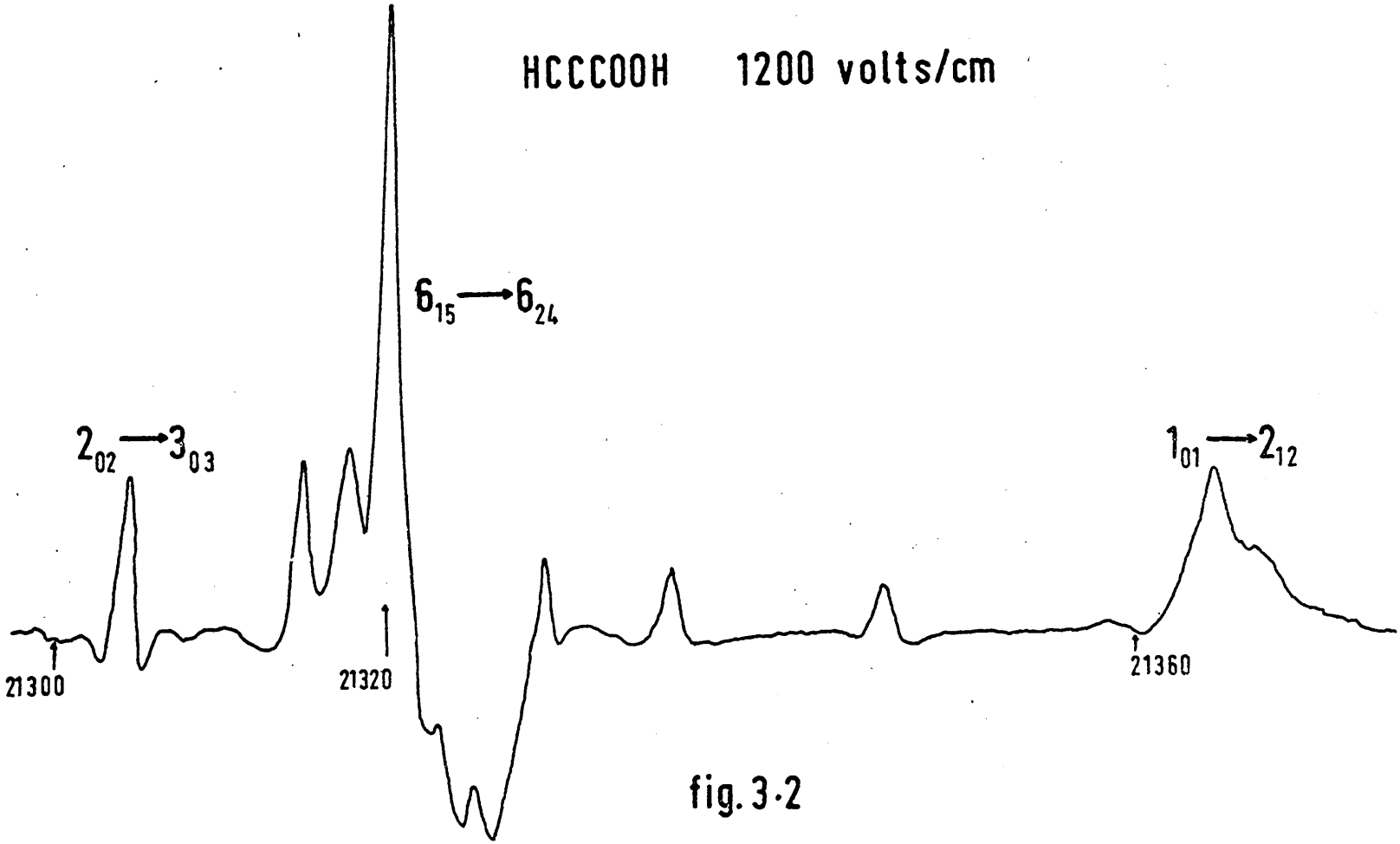
HCCCOOH 1200 volts/cm
$6_{15} \longrightarrow 6_{24}$
$2_{02} \longrightarrow 3_{03}$
$1_{01} \longrightarrow 2_{12}$
21300
21320
21360

fig. 3·2

A set of rigid rotor constants was obtained and these predicted other lines to within a few mc/s.

An estimate of the ratio of the μa to μb components of the dipole moment was obtained from the relative intensities of the $2_{02} - 3_{03}$ and $6_{15} - 6_{24}$ lines (fig 3.2).

The ratio of the intensities is given by

$$R = \frac{\mu_a^2}{\mu_b^2} \times \frac{S_{2_{02} \rightarrow 3_{03}}}{S_{6_{15} \rightarrow 6_{24}}} \times \exp(\Delta W/kT)$$

where S is the line strength and ΔW is the difference between the 2_{02} and 6_{15} energy levels. The ratio of the μa to μb calculated in this way is 0.7 and indicates that the dipole moment makes an angle of 60° with the spine of the molecule.

In order to allow for centrifugal distortion some thirty lines were measured accurately and a list of line frequencies is given in table 3.1.

(b) Excited vibrational states and spectra due to other rotamers

A number of vibrational satellites was observed around each of the stronger Q branch lines, but none of these was comparable in intensity to the ground state lines. A search for spectra due to other rotamers was unsuccessful and it must be concluded that if such rotamers exist there must be a considerable energy difference between them and the cis form.

(c) HCCCOOD

Attempts to prepare this isotopic species by exchange with D_2O and extraction into ether were not successful. It was prepared in the cell by alternately admitting doses of D_2O and propiolic acid vapours. After the cell had become acclimatised the spectrum of the deuterated species attained approximately half the intensity of that of the normal isotopic species.

Lines for HCCCOOD were predicted from a set

of rotational constants obtained by adding the changes in moments of inertia expected on deuteration of the model to the experimental moments of inertia of the normal isotopic species. Recordings of regions where lines due to HCCCOOD were predicted to occur were made with ordinary propiolic acid and then with the acid/D_2O mixture in the cell. Lines due to HCCCOOD were picked out by comparison of the two series recordings. Better values of $(A - C)/2$ and κ were obtained from a Q branch plot and $(A + C)/2$ was calculated from the $1_{01} - 2_{12}$ R branch line. Other lines were predicted and accurate measurements were made (table 3.2).

(d) DCCCOOH

This isotopic species was prepared by the method given in chapter 6. A spectrum was predicted from a set of rotational constants which were obtained in a similar manner to those of HCCCOOD.

TABLE 3.1

Line frequencies for HCCCOOH

	observed (mc/s)	rigid rotor (mc/s)	centrifugal distortion energy (mc/s)	calculated (mc/s)
$0_{00} - 1_{11}$	15194.50	15194.59	- 0.04	15194.55
$1_{01} - 2_{12}$	21363.44	21363.57	- 0.11	21363.47
$1_{10} - 2_{11}$	15525.22	15525.32	- 0.16	15525.16
$2_{02} - 3_{03}$	21302.43	21302.47	- 0.08	21302.40
$2_{02} - 3_{13}$	27041.23	27041.28	- 0.22	27041.06
$2_{12} - 2_{21}$	27076.23	27076.78	- 0.66	27076.12
$2_{12} - 3_{03}$	14302.49	14302.40	0.00	14302.40
$2_{12} - 3_{13}$	20041.03	20041.20	- 0.14	20041.07
$2_{11} - 2_{20}$	23988.45	23988.81	- 0.54	23988.27
$2_{11} - 3_{12}$	23222.36	23222.70	- 0.31	23222.40
$2_{21} - 3_{22}$	21693.73	21694.33	- 0.58	21693.75
$2_{20} - 3_{21}$	22085.47	22086,18	- 0.64	22085.54
$3_{03} - 4_{04}$	27979.80	27980.32	- 0.18	27980.14
$3_{13} - 4_{04}$	22241.36	22241.51	- 0.05	22241.47
$3_{12} - 3_{21}$	22851.45	22852.29	- 0.87	22851.42
$3_{12} - 4_{13}$	30832.75	30833.42	- 0.54	30932.88

Cont'd.

TABLE 3.1 (Cont'd.)

	observed (mc/s)	rigid rotor (mc/s)	centrifugal distortion energy (mc/s)	calculated (mc/s)
$3_{22} - 4_{23}$	28847.55	28848.31	- 0.85	28847.45
$3_{21} - 4_{22}$	29792.68	29793.47	- 0.99	29792.48
$3_{31} - 4_{32}$	29106.63	29108.17	- 1.73	29106.44
$3_{30} - 4_{31}$	29141.26	29143.01	- 1.74	29141.27
$4_{04} - 4_{13}$	14959.83	14960.74	- 0.79	14959.95
$4_{13} - 4_{22}$	21810.89	21812.34	- 1.33	21811.01
$5_{05} - 5_{14}$	18886.81	18888.10	- 1.29	18886.81
$5_{14} - 5_{23}$	21199.49	21201.48	- 1.92	21199.57
$6_{15} - 6_{24}$	21320.67	21323.56	- 2.66	21320.90
$7_{16} - 7_{25}$	22416.27	22419.85	- 3.59	22416.26
$8_{17} - 8_{26}$	24667.72	24672.32	- 4.75	24667.57
$9_{18} - 9_{27}$	28195.47	28201.73	- 6.20	28195.53

TABLE 3.2

Line frequencies for HCCCCOD

	observed (mc/s)	rigid rotor (mc/s)	centrifugal distortion energy (mc/s)	calculated (mc/s)
$1_{01} - 2_{12}$	20845.10	20845.10	+ 0.01	20845.04
$2_{02} - 3_{03}$	20666.18	20666.10	+ 0.13	20666.23
$2_{12} - 2_{21}$	26588.00	26588.25	- 0.20	26588.05
$2_{12} - 3_{13}$	19447.89	19447.80	+ 0.08	19447.87
$2_{11} - 2_{20}$	23621.02	23621.11	- 0.07	23621.04
$2_{11} - 3_{12}$	22502.86	22502.86	- 0.09	22502.77
$3_{03} - 4_{14}$	31530.83	31530.84	+ 0.14	31530.98
$3_{13} - 4_{04}$	21459.46	21549.16	+ 0.37	21459.53
$3_{13} - 4_{14}$	25833.68	25833.43	+ 0.22	25833.64
$3_{12} - 3_{21}$	22519.44	22519.75	- 0.37	22519.39
$3_{31} - 4_{32}$	28215.40	28216.38	- 1.08	28215.30
$3_{30} - 4_{31}$	28247.20	28248.28	- 1.09	28247.30
$4_{13} - 4_{22}$	21497.65	21498.36	- 0.80	21497.56
$5_{14} - 5_{23}$	20871.06	20872.41	- 1.38	20871.03
$6_{06} - 6_{15}$	23099.55	23100.96	- 1.43	23099.53
$6_{15} - 6_{24}$	20931.01	20933.14	- 2.09	20931.05

Cont'd.

TABLE 3.2 (Cont'd.)

	observed (mc/s)	rigid rotor (mc/s)	centrifugal distortion energy (mc/s)	calculated (mc/s)
$7_{07} - 7_{16}$	28856.67	28858.49	- 1.80	28856.69
$7_{16} - 7_{25}$	21910.79	21913.78	- 2.93	21910.85
$8_{17} - 8_{26}$	23987.28	23991.25	- 3.88	23987.37
$9_{18} - 9_{27}$	27281.69	27286.53	- 4.99	27281.63

TABLE 3.3

Line frequencies for DCCCOOH

	observed (mc/s)	rigid rotor (mc/s)	centrifugal distortion energy (mc/s)	calculated (mc/s)
$1_{01} - 2_{12}$	20808.69	20808.80	- 0.13	20908.67
$2_{02} - 3_{03}$	19871.11	19871.29	- 0.19	19871.10
$2_{02} - 3_{13}$	26176.60	26176.82	- 0.33	27176.49
$2_{21} - 3_{22}$	20157.31	20158.00	- 0.69	20157.31
$2_{20} - 3_{21}$	20443.84	20444.70	- 0.72	20443.98
$3_{03} - 4_{04}$	26178.12	26178.74	- 0.45	26178.30
$3_{13} - 4_{04}$	19873.04	19873.21	- 0.30	19872.91
$3_{12} - 3_{21}$	23896.40	23896.85	- 0.46	23896.39
$3_{12} - 4_{13}$	28560.70	28561.44	- 0.74	28560.69
$3_{31} - 4_{32}$	27010.11	27012.02	- 1.96	27010.06
$5_{14} - 5_{23}$	22076.74	22078.22	- 1.45	22076.78
$6_{15} - 6_{24}$	21821.64	21823.70	- 2.01	21821.60
$7_{16} - 7_{25}$	22305.57	22308.43	- 2.86	22305.57
$8_{17} - 8_{26}$	23699.09	23702.77	- 3.75	23699.02
$9_{18} - 9_{27}$	26131.11	26135.94	- 4.80	26131.13

The lines were generally found to be within 20 mc/s of the predicted frequency and a list of measured lines is given in table 3.3.

(3) Centrifugal Distortion

The effect of centrifugal distortion in propiolic acid can be seen in the Q branch plot shown in fig. 3.3. There is an uncertainty in (A - 0)/2 of 0.25 mc/s and 0.0001 in κ and this places a limitation on the usual method of deriving the rotational constants from a rigid rotor least squares fit. It is possible to derive an accurate set of rotational constants for the normal isotopic species from three lines, which if rigid rotor theory is obeyed, are simple functions of the rotational constants. Three such lines and the expressions for their frequencies are

$0_{00} - 1_{11}$	A + C	15194.50 (mc/s)
$1_{10} - 2_{11}$	3B + C	15525.22
$2_{12} - 2_{21}$	3(A - C)	27076.23

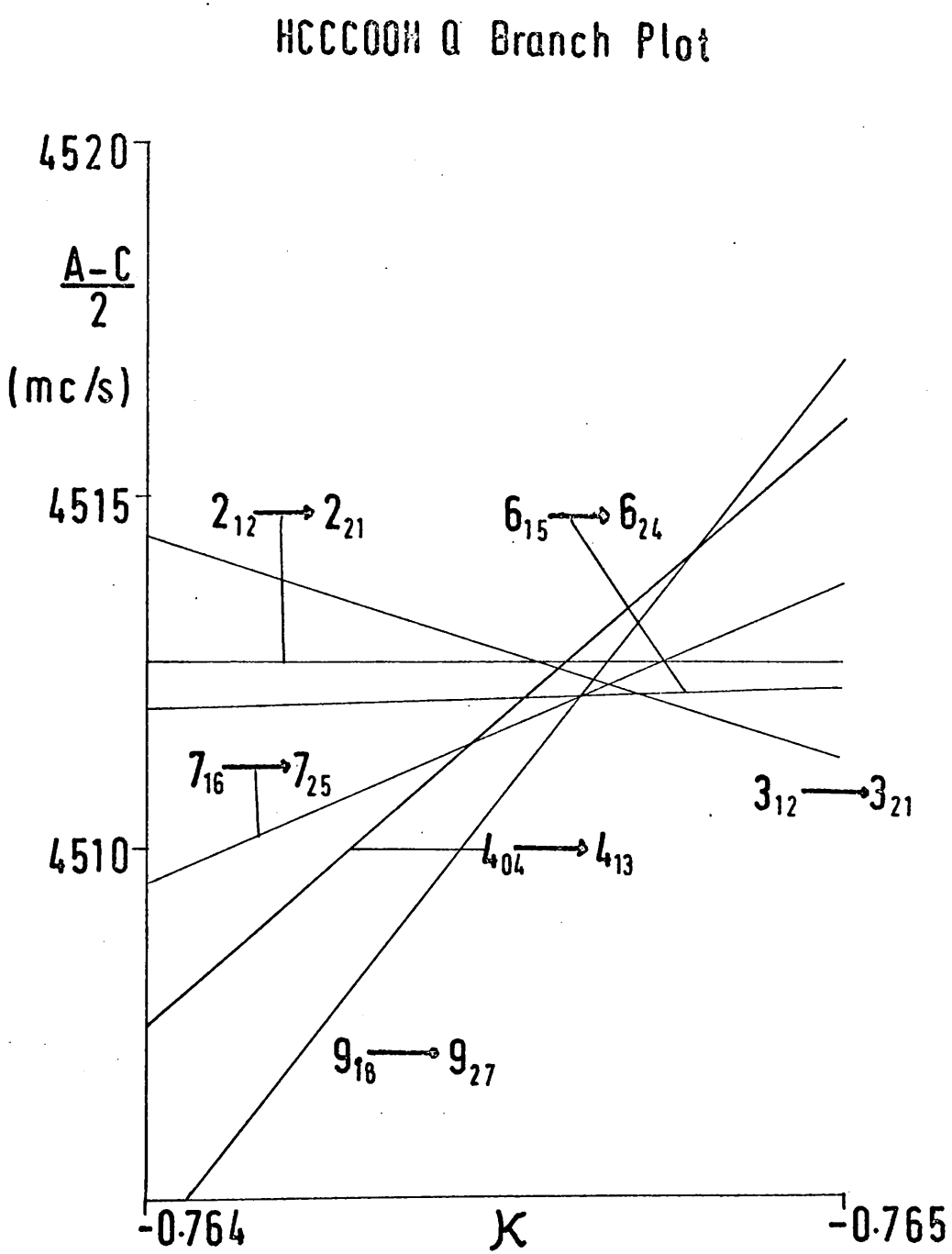
HCCCOOH Q Branch Plot
4520
A-C
2
(mc/s)
4515
4510
$2_{12} \rightarrow 2_{21}$
$6_{15} \rightarrow 6_{24}$
$7_{16} \rightarrow 7_{25}$
$3_{12} \rightarrow 3_{21}$
$4_{04} \rightarrow 4_{13}$
$9_{18} \rightarrow 9_{27}$
-0.764
K
-0.765

fig.3·3

The rotational constants derived from these expressions are (in mc/s)

A = 12109.96 B = 4146.86 C = 3084.65

For the other two species of propiolic acid it was not possible to measure all three lines and the rotational constants had to be obtained from higher J lines by allowing for centrifugal distortion.

The centrifugal distortion in many slightly asymmetric top molecules has been treated using the expression for a symmetric top. An attempt was made to fit the data for propiolic acid using the following formula for the energy levels.

$$W_{J\tau} = J(J+1)\times(A+C)/2 + E(\kappa)\times(A-C)/2$$
$$-J(J+1)K_1^2\times D_{JK} - K_1^4\times D_K$$

The D_J term has been omitted, since for molecules of similar molecular weight it only makes a significant contribution to high J lines.

$A - C_{/2}$ and κ were obtained from an R branch plot by taking differences between the J = 2 - 3 μ_a lines so that the centrifugal distortion terms were eliminated. $(A + C)_{/2}$ was calculated from $2_{02} - 3_{03}$ and a constant value of D_{JK} was obtained from the other four lines. D_K was obtained by substituting the values of the other constants into the expressions for higher J lines. The value of D_K depends on the line chosen and this indicates that the symmetric top expression is no longer a good approximation for molecules of this asymmetry. The results of these calculations are given in table 3.4.

A first order perturbation theory treatment of centrifugal distortion in asymmetric top molecules has been given by Kivelson and Wilson[3], Watson[4] has recently shown that the number of independent centrifugal distortion constants in Kivelson and Wilson's expression may be reduced from six to five by application of an additional angular momentum

TABLE 3.4

Rotational and centrifugal distortion constants for HCCCOOH using the symmetric top expression for the centrifugal distortion energy.

$(A + C)/2 = 7598.07$ (mc/s)

$(A - C)/2 = 4513.57$ (mc/s)

$= - 0.764623$

$D_{JK} = + 0.0187$ (mc/s) from J = 2 - 3 μ a lines

$D_K = + 0.275$ from $6_{15} - 6_{24}$

$+ 0.299$ from $5_{14} - 5_{23}$

$+ 0.325$ from $3_{12} - 3_{21}$

$A = 12111.64$ (mc/s)

$B = 4146.89$

$C = 3084.50$

commutation relationship. This provides a theoretical explanation of the indeterminacies which arise in the application of the original equation. In the case of planar molecules further constraints can be applied to reduce the number of independent coeffecients to four[5].

The Hamiltonian of reference 3 is usually written as

$$H = H^{o} + H'$$

$$H^{o} = A' P_a^2 + B' P_b^2 + C' P_c^2$$

$$H' = 1/4 \sum_{\alpha\beta} \tau'_{\alpha\alpha\beta\beta} \qquad (\alpha\beta = a,b,c)$$

$$\tau'_{\alpha\alpha\alpha\alpha} = \tau_{\alpha\alpha\alpha\alpha}\pi$$

$$\tau'_{\alpha\alpha\beta\beta} = (\tau_{\alpha\alpha\beta\beta} + 2\tau_{\alpha\beta\alpha\beta})\pi$$

A small amount of the centrifugal distortion has been absorbed into H^{o}. The τs are constants for a particular vibrational state and depend on

the molecular geometry and vibrational frequencies[6]. Application of first order perturbation theory gives

$$\Delta W = 1/4 \sum_{\alpha\beta} \tau'_{\alpha\alpha\beta\beta} \langle P_\alpha^2 P_\beta^2 \rangle \quad 3.1$$

where $\langle P_\alpha^2 P_\beta^2 \rangle$ is the average or expectation value of the quartic angular momentum operator $P_\alpha^2 P_\beta^2$

For planar molecules the six constants in 3.1 can be reduced to four by application of Dowling's relations. These may be written in the form

$$\tau'_{aacc} = 1/2 A^2 C^2 [\tau'_{aaaa}/A^4 - \tau'_{bbbb}/B^4 + \tau'_{cccc}/C^4] \quad 3.2$$

$$\tau'_{bbcc} = 1/2 A^2 C^2 [-\tau'_{aaaa}/A^4 + \tau'_{bbbb}/B^4 + \tau'_{cccc}/C^4] \quad 3.3$$

$$\tau_{acac} = \tau_{bcbc} = 0 \quad 3.4$$

$$\tau_{aabb} = 1/4 [A^2 B^2/C^2 \tau_{cccc} - A^2/B^2 \tau_{bbbb} - B^2/A^2 \tau_{aaaa}] \quad 3.5$$

Substitution of equation 3.2 and 3.3 into 3.1 gives

$$\Delta W = 1/4[\langle P_a^4\rangle + C^2/A^2(\langle P_a^2 P_c^2\rangle - B^2/A^2\langle P_b^2 P_c^2\rangle)]\ T'_{aaaa}$$

$$+1/4[\langle P_b^4\rangle - C^2/B^2(A^2/B^2\langle P_a^2 P_b^2\rangle - \langle P_b^2 P_c^2\rangle)]\ T'_{bbbb}$$

$$+1/4[\langle P_c^4\rangle + A^2/C^2\langle P_a^2 P_b^2\rangle + B^2/C^2\langle P_b^2 P_c^2\rangle]\ T'_{cccc}$$

$$+1/2\langle P_a^2 P_b^2\rangle\ T'_{aabb} \qquad 3.6$$

Using 3.4 and 3.5 and assuming a zero inertial defect so that C may be replaced by $AB/(A+B)$, Sorensen's[8] expression may be derived

$$W = 1/4[\langle P_a^4\rangle - B^2/A^2(\langle P_a^2 P_b^2\rangle - (A/A+B)^2\langle P_a^2 P_c^2\rangle + (B/A+B)^2\langle P_b^2 P_c^2\rangle)]\ T_{aaaa}$$

$$+1/4[\langle P_b^4\rangle - A^2/B^2(\langle P_a^2 P_b^2\rangle + (A/A+B)^2\langle P_a^2 P_c^2\rangle - (B/A+B)^2\langle P_b^2 P_c^2\rangle)]\ T_{bbbb}$$

$$+1/4[\langle P_c^4\rangle + (A+B)^4/A^2B^2(\langle P_a^2 P_b^2\rangle + (A/A+B)^2\langle P_a^2 P_c^2\rangle + (B/A+B)^2\langle P_b^2 P_c^2\rangle)]\ T_{cccc}$$

$$+\langle P_a^2 P_b^2\rangle\ T_{abab} \qquad 3.7$$

In 3.7 the τs are in units of $\hbar^4$ and this equation has the advantage that all of the constants are by definition negative quantities. This provides an immediate check on the results of least squares calculations.

Formulae for expressing the quartic angular momentum averages in terms of the quadratic averages are given in reference 4. The expression of these quantities in terms of the reduced energy and its derivitive with respect to the asymmetry parameter and a discussion of the least squares programme is given in appendix 1.

The effective rotational constants A, B and C may be expressed in terms of the constants of H^o and τ_{abab} using the relations given in the appendix of reference 3.

$$A = A' + \tfrac{1}{2}\,\tau_{abab}$$

$$B = B' + \tfrac{1}{2}\,\tau_{abab}$$

$$C = C' - \tfrac{2}{4}\,\tau_{abab}$$

The rotational and centrifugal distortion

constants obtained by least squares fits to equations 3.6 and 3.7 are given in table 3.5. The rigid rotor frequencies, centrifugal distortion energies and calculated line frequencies are given in tables 3.1, 3.2 and 3.3, Fig.3.4 shows that when the line frequencies are corrected for centrifugal distortion the intersection of the Q branch plot is improved. The values of 4512.80 mc/s for $(A - C)_{/2}$ and -0.76457 for κ agree very well with those obtained from the least squares fits.

The positive values obtained for τbbbb and τcccc in the case of HCCCOOD and the large variations in the centrifugal distortion constants between the three isotopic species show that the centrifugal distortions constants are not well determined from the available data. This is confirmed by the standard deviations and correlation coeffecients for HCCCOOH derived from equation 3.7 (table 3.6). A correlation coeffecient of 0.9 to 1.0 between two parameters means it is impossible

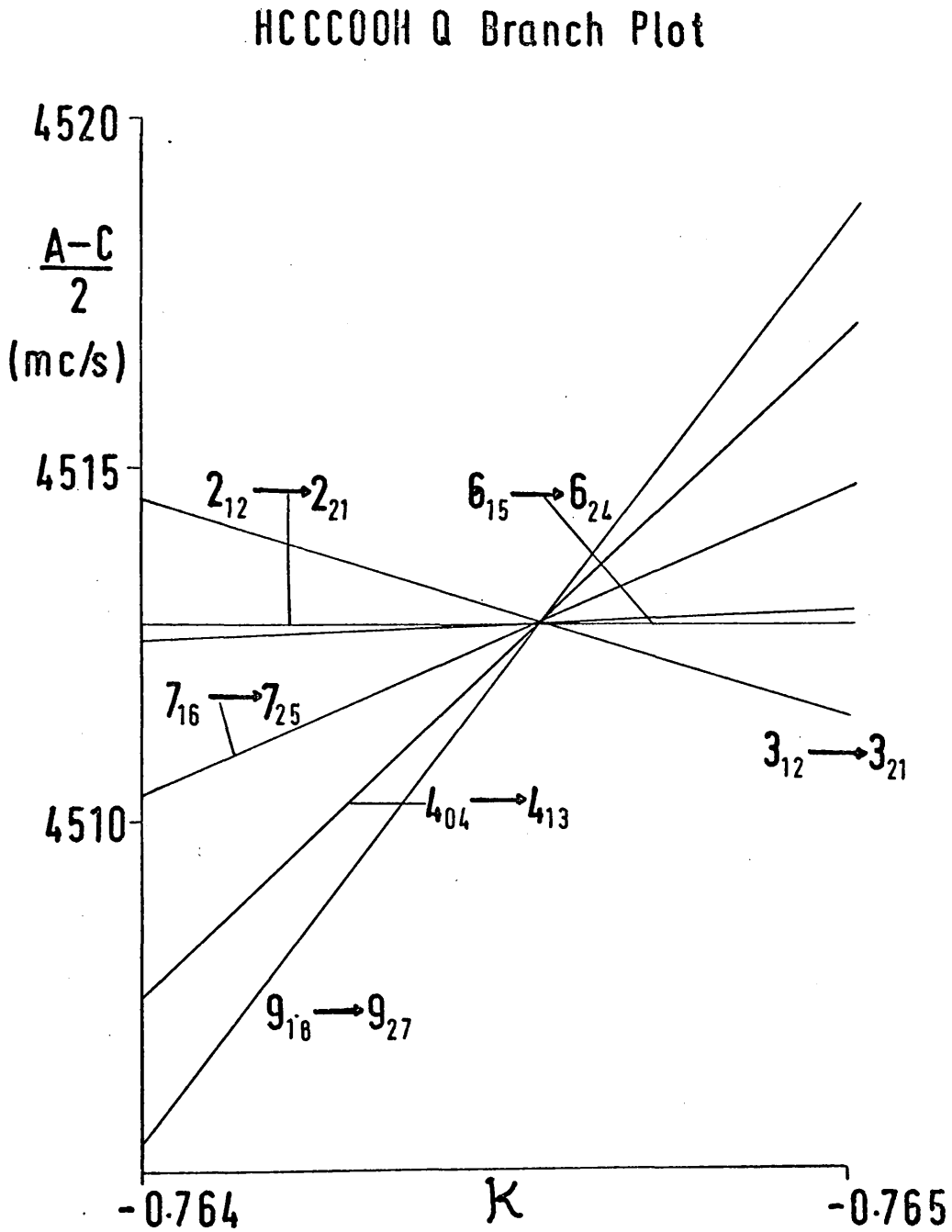
HCCCOOH Q Branch Plot
4520
A−C
2
(mc/s)
4515
4510
$2_{12} \rightarrow 2_{21}$
$6_{15} \rightarrow 6_{24}$
$7_{16} \rightarrow 7_{25}$
$3_{12} \rightarrow 3_{21}$
$4_{04} \rightarrow 4_{13}$
$9_{18} \rightarrow 9_{27}$
-0.764
K
-0.765

fig.3.4

TABLE 3.5

Least squares parameters for propiolic acid

	equation 3.6 (mc/s)		equation 3.7 (mc/s)
HCCCOOH			
$(A + C)_{/2}$	7597.29		7597.29
$(A - C)_{/2}$	4512.80		4512.80
	-0.764570		-0.764570
T'_{aaaa}	-0.1477	T_{aaaa}	-0.1476
T'_{bbbb}	-0.0075	T_{bbbb}	-0.0076
T'_{cccc}	-0.0025	T_{cccc}	-0.0025
T'_{aabb}	-0.0793	T_{abab}	-0.0426
HCCCOOD			
$(A + C)_{/2}$	7426.95		7426.95
$(A - C)_{/2}$	4431.37		4431.37
	-0.769799		-0.769799
T'_{aaaa}	-0.0169	T_{aaaa}	-0.0172
T'_{bbbb}	+0.0013	T_{bbbb}	+0.0013
T'_{cccc}	+0.0028	T_{cccc}	+0.0028
T'_{aabb}	-0.0776	T_{abab}	-0.0563

(cont'd.)

TABLE 3.5 (Cont'd.)

	equation 3.6 (mc/s)	equation 3.7 (mc/s)
DCCCOOH		
$(A + C)_{/2}$	7504.78	7504.78
$(A - C)_{/2}$	4605.15	4605.15
	- 0.800206	- 0.800206
T'_{aaaa}	- 0.0357	T_{aaaa} - 0.0355
T'_{bbbb}	- 0.0101	T_{bbbb} - 0.0101
T'_{cccc}	- 0.0060	T_{cccc} - 0.0060
T'_{aabb}	- 0.0702	T_{abab} - 0.0160

TABLE 3.6

Standard deviations and correlation coefficients for HCCCOOH

	standard deviations (mc/s)	correlation coefficients						
(A + C)/2	0.0403	1.000						
(A - C)/2	0.0360	0.890	1.000					
	0.000004	0.693	0.661	1.000				
τ_{aaaa}	0.0628	0.871	0.928	0.747	1.000			
τ_{bbbb}	0.0027	0.207	0.177	0.246	0.107	1.000		
τ_{cccc}	0.0019	0.292	0.129	0.088	0.050	0.972	1.000	
τ_{abab}	0.0086	0.258	0.179	0.032	0.054	0.914	0.972	1.000

to determine them accurately. The correlation coeffecients indicate that τ_{aaaa} should be well determined, but the small contributions made by this parameter to the centrifugal distortion energy (table 3.7) show why this is not the case. The more usual centrifugal distortion constants D_J, D_{JK} and D_K were derived using Dowling's relations and the formulae of reference 3. The following constants were obtained for HCCCOOH

$$D_J = -0.012 \pm 0.012 \text{ mc/s}$$

$$D_{JK} = -0.040 \pm 0.070$$

$$D_K = 0.089 \pm 0.140$$

The negative value of D_J and the large errors on the constants show that the centrifugal distortion constants cannot be used to give reliable information about the molecular force field.

TABLE 3.7

Contributions to the centrifugal distortion energy of HCCCOOH from the coefficients of equation 3.7

	τ_{aaaa} (mc/s)	τ_{bbbb} (mc/s)	τ_{cccc} (mc/s)	τ_{abab} (mc/s)
$0_{00} - 1_{11}$	- 0.04	+ 0.01	- 0.01	0.00
$1_{01} - 2_{12}$	- 0.04	+ 0.05	- 0.07	- 0.04
$1_{10} - 2_{11}$	+ 0.01	+ 0.03	- 0.07	- 0.13
$2_{02} - 3_{03}$	- 0.01	- 0.08	- 0.04	- 0.05
$2_{02} - 3_{13}$	- 0.05	+ 0.11	- 0.18	- 0.99
$2_{12} - 2_{21}$	- 0.54	+ 0.05	- 0.04	- 0.13
$2_{12} - 3_{03}$	+ 0.03	- 0.15	+ 0.02	+ 0.11
$2_{12} - 3_{13}$	- 0.01	+ 0.03	- 0.12	- 0.04
$2_{11} - 2_{20}$	- 0.56	+ 0.06	- 0.03	- 0.02
$2_{11} - 3_{12}$	+ 0.01	- 0.04	- 0.11	- 0.17
$2_{21} - 3_{22}$	+ 0.03	+ 0.26	- 0.35	- 0.51
$2_{20} - 3_{21}$	+ 0.04	+ 0.24	- 0.35	- 0.56
$3_{03} - 4_{04}$	- 0.28	- 0.14	- 0.12	+ 0.10
$3_{13} - 4_{04}$	+ 0.01	- 0.32	+ 0.02	+ 0.25
$3_{12} - 3_{21}$	- 0.53	+ 0.34	- 0.26	- 0.41
$3_{12} - 4_{13}$	+ 0.01	- 0.20	- 0.17	- 0.18
$3_{22} - 4_{23}$	+ 0.03	+ 0.25	- 0.51	- 0.62

Cont'd.

TABLE 3.7 (Cont'd.)

	τ_{aaaa} (mc/s)	τ_{bbbb} (mc/s)	τ_{cccc} (mc/s)	τ_{abab} (mc/s)
$3_{21} - 4_{22}$	+ 0.05	+ 0.15	- 0.47	- 0.72
$3_{31} - 4_{32}$	+ 0.09	+ 0.81	- 1.03	- 1.60
$3_{30} - 4_{31}$	+ 0.10	+ 0.80	- 1.03	- 1.61
$4_{04} - 4_{13}$	+ 0.04	+ 0.05	- 0.19	- 0.68
$4_{13} - 4_{22}$	- 0.48	+ 0.68	- 0.56	- 0.96
$5_{05} - 5_{14}$	+ 0.08	- 0.21	- 0.18	- 0.98
$5_{14} - 5_{23}$	- 0.42	+ 0.99	- 0.87	- 1.62
$6_{15} - 6_{24}$	- 0.32	+ 1.12	- 1.10	- 2.36
$7_{16} - 7_{25}$	- 0.21	+ 0.86	- 1.16	- 3.08
$8_{17} - 8_{26}$	- 0.08	- 0.04	- 0.92	- 3.72
$9_{18} - 9_{27}$	+ 0.04	- 1.82	- 0.26	- 4.16

4. Structure.

The rotational constants corrected for the contribution from τ_{abab} and the moments of inertia for the three isotopic species of propiolic acid are given in table 3.8. The agreement between the observed moments of inertia and those calculated from the model (table 3.9) shows that the molecule has the expected cis conformation. The positive inertial defects are good evidence for propiolic acid having a planar structure. The difference in Δ^{o} between DCCCOOH and HCCCOOH (+0.0066 a.m.u.Å^2) is very similar to that found in the corresponding isotopic species of propynal (+0.0070 a.m.u.Å^2). The difference for HCCCOOD and HCCCOOH (-0.0061 a.m.u.Å^2) is probably due to the torsional vibration of the hydroxyl group.

The hydrogen atoms were located in the principal axis system of HCCCOOH. The co-ordinates obtained by substituting ΔIa and ΔIb into Kraitchman's equations are given in the first row of table 3.9 and

TABLE 3.8

Rotational constants and moments of inertia of three isotopic species of propiolic acid.

	(mc/s)		(a.m.u. $Å^2$)
HCCCOOH			
A	12110.07	Ia	41.7447
B	4146.92	Ib	121.9052
C	3084.52	Ic	163.8929
		Δ°	0.2430
HCCCOOD			
A	11858.36	Ia	42.6308
B	4015.67	Ib	152.8897
C	2995.62	Ic	168.7590
		Δ°	0.2369
DCCCOOH			
A	12109.92	Ia	41.7452
B	3819.70	Ib	132.3484
C	2899.63	Ic	174.3432
		Δ°	0.2496

TABLE 3.9

Moments of inertia and co-ordinates of the hydrogen atoms of propiolic acid

	H_1			H_2	
	a (Å)	b (Å)		a (Å)	b (Å)
Experimental	1.993	-0.968		-3.244	-0.024
	1.989	-0.966		-3.245	-0.090
(a.m.u. $Å^2$)	Ia = 41.7447		Ib = 121.9052	Ic = 163.8929	
Model	1.963	-1.022		-3.232	-0.052
(a.m.u. $Å^2$)	Ia = 42.1126		Ib = 120.9109	Ic = 163.0235	
Structure fig. 3.5	1.997	-0.966		-3.246	-0.078
(a.m.u. $Å^2$)	Ia = 41.6286		Ib = 120.8760	Ic = 162.5046	

those obtained using $\Delta Ic - \Delta Ib$ and $\Delta Ic - \Delta Ia$ are given in the second row of that table. Except for the b co-ordinate of the acetylenic hydrogen atom which is too small to be determined by isotopic substitution the two sets of figures show the variations expected from zero point vibrational effects. The co-ordinates calculated from the model are in reasonable agreement with the experimental values.

An attempt to improve the agreement between the observed and calculated moments of inertia and co-ordinates was made by varying the bond angles of the carboxylic acid group. The structure giving closest agreement with the observed data is shown in fig.3.5. The acetylene and carboxylic groups in propiolic acid do not seem to have a marked structural effect on each other.

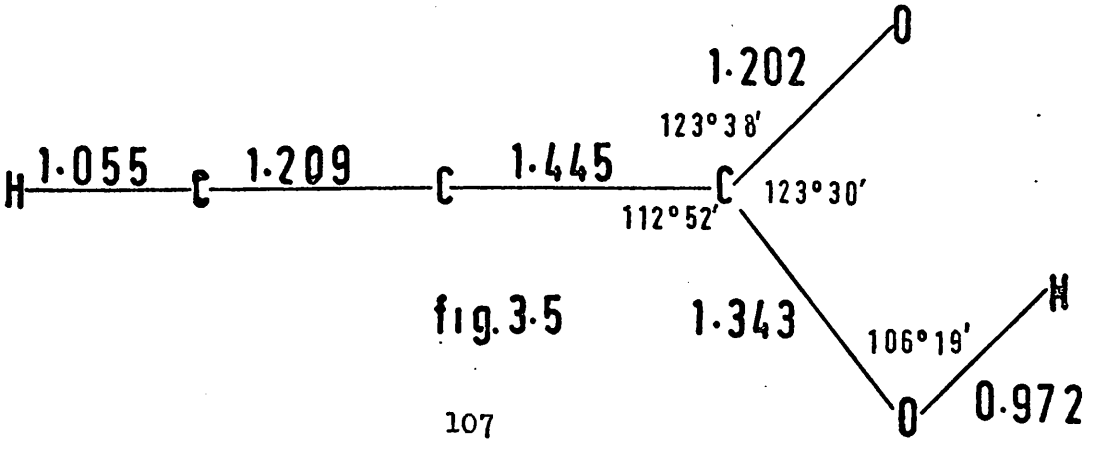

fig.3.5

5. Dipole moment and discussion.

The Stark effects of a number of lines were examined to see if they were suitable for dipole moment measurements and the $0_{00} - 0_{11}$ and $3_{12} - 3_{21}$ transitions of HCCCOOH and the $1_{01} - 2_{12}$ and $3_{12} - 3_{21}$ transitions of HCCCOOD were finally selected. The frequency displacements ($\Delta\nu$) of the Stark components were measured at several values of the applied modulation voltage (V) (table 3.10). Plots of $\Delta\nu$ against V^2 are shown in fig. 3.6 and 3.7 and the straight lines verify the quadratic nature of the Stark effects.

If no accidental degeneracies between rotational energy levels occur the Stark effect of an asymmetric rotor may be expressed in the form [9]

$$\Delta\nu/E^2 = A + B M_J^2$$

or since the electric field strength is proportional to the applied voltage

$$\Delta\nu/V^2 = A' + B' M_J^2$$

If $\Delta\nu/V^2$ is written as N and the Stark components are

TABLE 3.10

Frequency displacements of Stark components for HCCCOOH and HCCCOOD.

HCCCOOH

$0_{00} - 1_{11}$	$M_J = 0$	$\Delta\upsilon$
$V \times 10^{-2}$(Volts)	$V^2 \times 10^{-4}$(Volts)^2	(mc/s)
2.00	4.00	3.13
2.50	6.25	4.94
3.00	9.00	6.81
3.50	12.25	9.53
4.00	16.00	12.41
$3_{12} - 3_{21}$	$M_J = 3$	
1.28	1.64	5.41
1.50	2.25	7.23
2.00	4.00	12.78
2.50	6.25	20.58
$3_{12} - 3_{21}$	$M_J = 2$	
1.50	2.25	4.27
2.00	4.00	7.56
2.40	5.76	10.75
2.83	8.01	14.54
3.00	9.00	15.77

Cont'd.

TABLE 3.10 (Cont'd.)

HCCCOOH

$3_{12} - 3_{21}$	$M_J = 1$	$\Delta\nu$
$V \times 10^{-2}$(Volts)	$V^2 \times 10^{-4}$(Volts)^2	(mc/s)
3.00	9.00	9.15
3.50	12.25	12.44

HCCCOOD

$1_{01} - 2_{12}$	$M_J = 1$	
1.10	1.21	1.02
2.00	4.00	2.85
2.88	8.29	5.87
3.40	11.56	8.32
$3_{12} - 3_{21}$	$M_J = 3$	
1.00	1.00	2.76
1.50	2.25	7.09
2.00	4.00	12.26
2.50	6.25	18.85

HCCCOOH Dipole Moment Plots

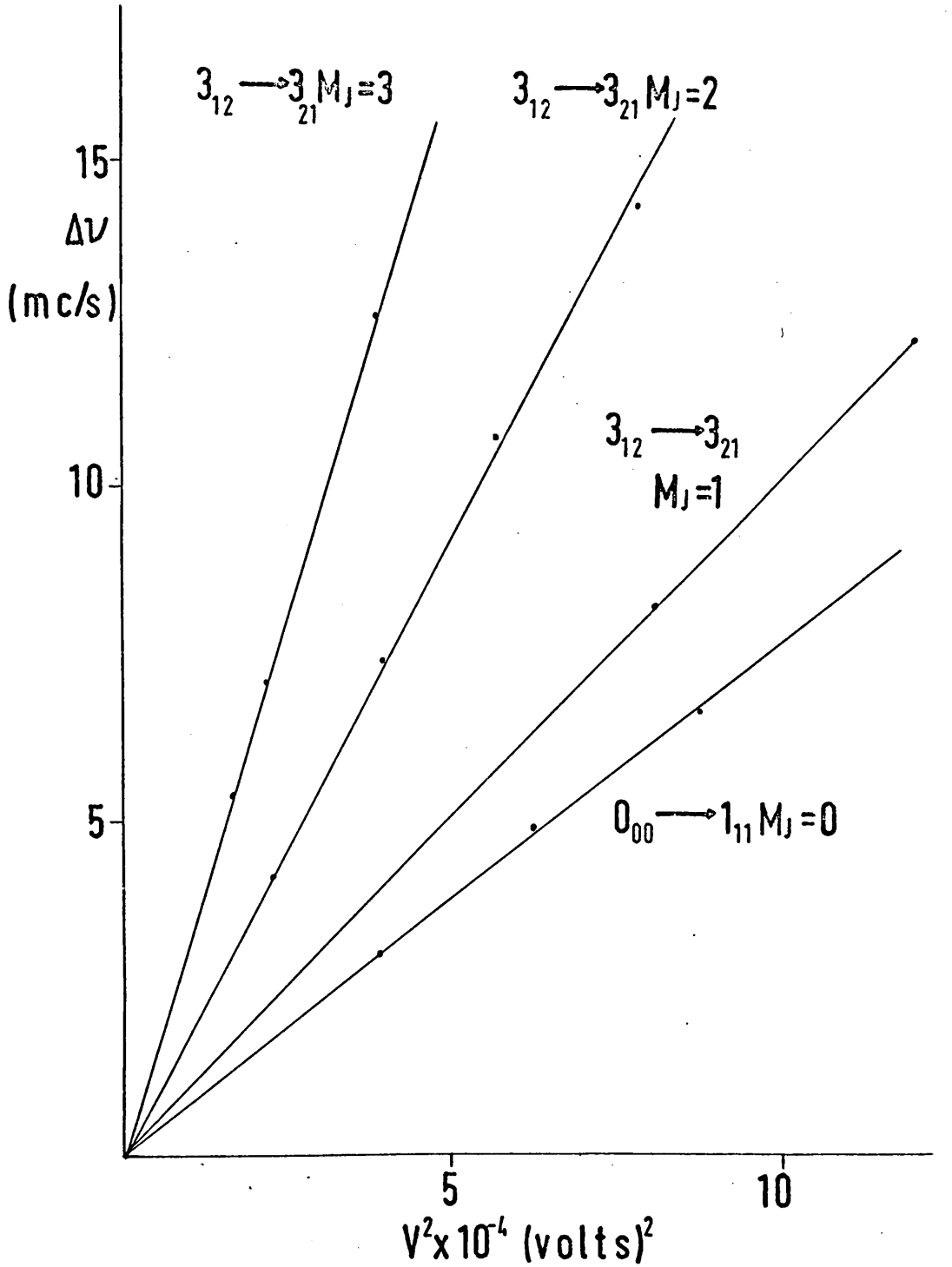

fig.3·6

HCCCOOD Dipole Moment Plots

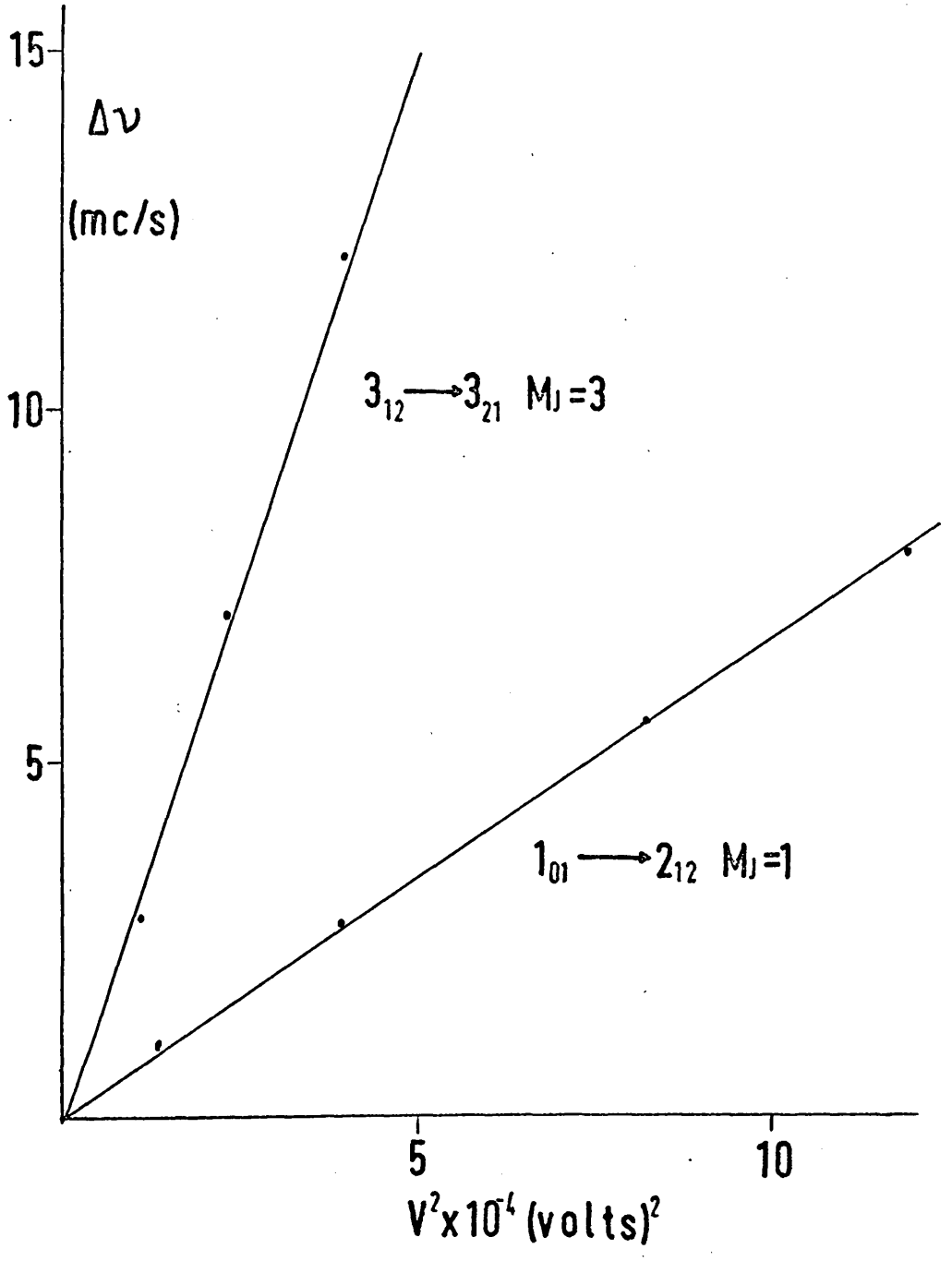

fig.3.7

labelled by their M_J values the following relation should hold for the $3_{12} - 3_{21}$ transition.

$$\frac{N_3 - N_1}{N_2 - N_1} = 2.667$$

The observed value is 2.665 and this indicates that the usual second order perturbation theory treatment is valid.

At the end of each set of measurements the apparatus was calibrated against the J = 1 - 2 transition of OCS (table 3.11 and fig. 3.8). This amounts to finding the electrode to cell spacing in order to determine the proportionality constant between the electric field strength and the applied voltage. The calculations are simplified if a constant (K) is derived instead. Division of $\Delta\nu/V^2$ by K converts the former quantity into $D^2(mc/s)^{-1}$. In deriving K an average value for the $M_J = 0$ and $M_J = 1$ lobes was taken and the dipole moment of OCS [10] was assumed to be 0.712D. The values of K used in the determinations

TABLE 3.11

OCS CALIBRATION FOR HCCCOOH

$J = 1 - 2$	$M_J = 1$	$\Delta\nu$
$V \times 10^{-2}$ (Volts)	$V^2 \times 10^{-4}$ (Volts)^2	(mc/s)
4.00	16.00	0.91
5.00	25.00	1.40
6.00	36.00	2.04
8.00	64.00	3.64
$J = 1 - 2$	$M_J = 0$	
4.00	16.00	1.15
5.00	25.00	1.78
6.00	36.00	2.57
8.08	64.00	4.52

OCS CALIBRATION FOR HCCCOOD

$J = 1 - 2$	$M_J = 1$	
4.00	16.00	0.92
5.00	25.00	1.32
6.00	36.00	1.95
8.00	64.00	3.49
$J = 1 - 2$	$M_J = 0$	
4.00	16.00	1.15
5.00	25.00	1.68
6.00	36.00	2.64
8.00	64.00	4.30

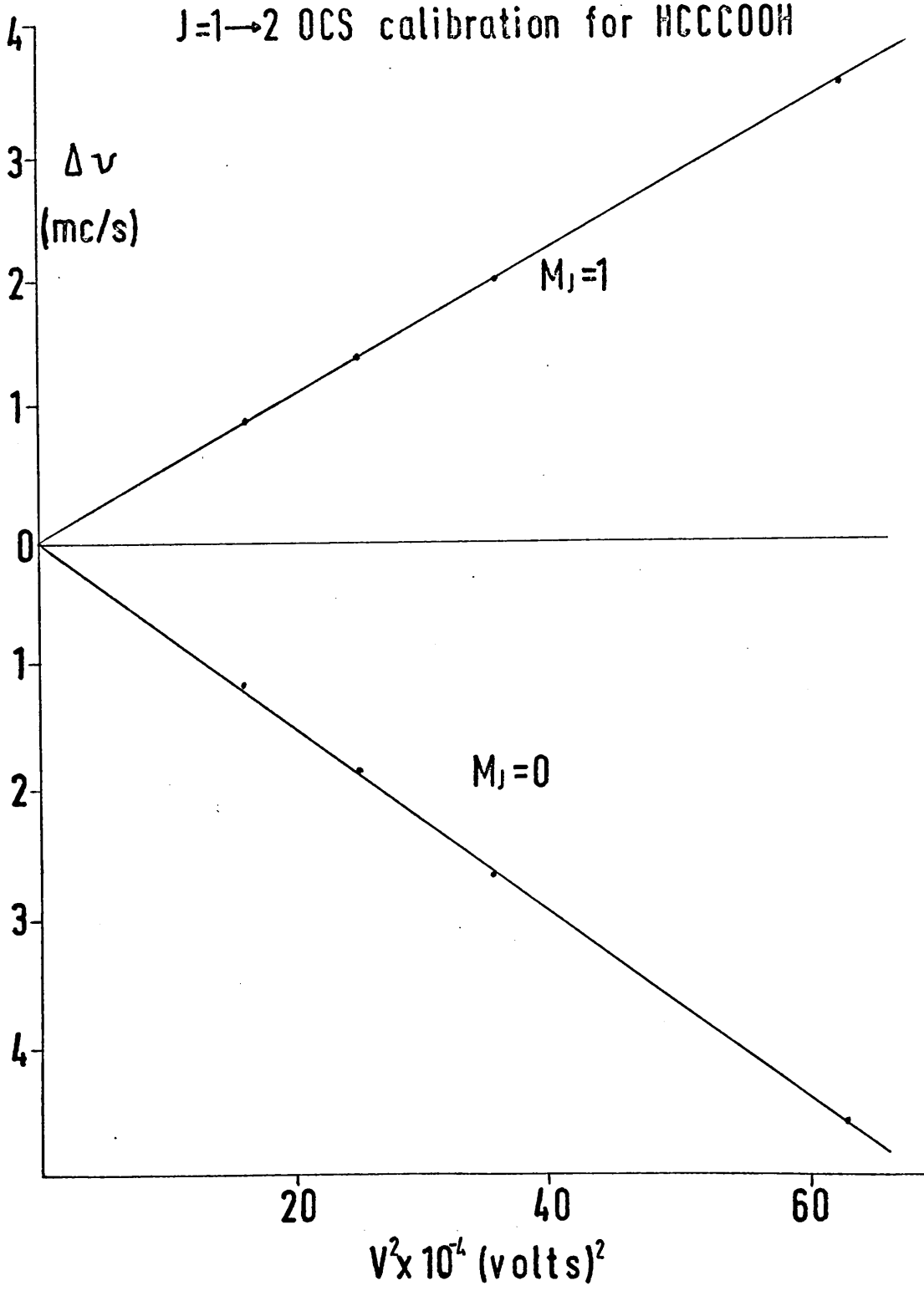
J=1→2 OCS calibration for HCCCOOH
Δν
(mc/s)
4
3
2
1
0
1
2
3
4
$M_J=1$
$M_J=0$
20
40
60
$V^2 \times 10^{-4}$ (volts)^2

fig.3·8

were

HCCCOOH $K = 1.121\ (mc/s)\ D^{-2}(volts)^{-2}$

HCCCOOD $K = 1.069$

Table 3.12 gives the values of $\Delta\nu/V^2$ and $\Delta\nu/KV^2$ for the measured Stark components of HCCCOOH and HCCCOOD.

The Stark effect for a molecule with μa and μb components of the dipole moment may be written

$$\Delta\nu/E^2 = \Delta X a \mu a^2 + \Delta X b \mu b^2$$

where $\Delta X_g = X_{J,\tau,g^{M_J}} - X_{J',\tau',g^{M_J}}$ and J,τ and J',τ' are the energy levels of the transition. $X_{J,\tau,g^{M_J}}$ is the second order perturbation theory coefficient and may be expressed in terms of tabulated line strengths in the following way[11].

$$X_{J\tau g}^{M_J} = \frac{1}{2J+1}\left[\sum \frac{J^2 - M_J^2}{J(2J-1)} \frac{S_{J\tau,J-1\tau'}}{W^o_{J\tau} - W^o_{J-1\tau'}} + \sum_{\tau' \neq \tau} \frac{M_J^2}{J(J+1)} \frac{S_{J\tau,J\tau'}}{W^o_{J\tau} - W^o_{J\tau'}} + \sum \frac{(J+1)-M_J}{(J+1)(2J+3)} \frac{S_{J\tau,J+1\tau'}}{W^o_{J\tau} W^o_{J+1\tau'}}\right]$$

TABLE 3.12

		$\Delta\nu/V^2$ (mc/s volts^{-1}) $\times 10^{-4}$	$\Delta\nu/KV^2$ (observed)	$\Delta\nu/KV^2$ (calculated)
HCCCOOH				
$0_{00} - 1_{11}$	$M_J = 0$	7.800	6.958	7.060
$3_{12} - 3_{21}$	$M_J = 1$	10.190	9.090	8.923
	2	18.680	16.664	16.553
	3	32.602	29.083	29.551
HCCCOOD				
$1_{01} - 2_{12}$	$M_J = 0$	7.130	6.670	6.674
$3_{12} - 3_{21}$	$M_J = 3$	30.940	28.943	28.794

In calculating ΔX_a and ΔX_b the line strengths (S) were obtained by graphical interpolation of tables [12] and the energy differences were calculated from the rigid rotor constants given in table 3.5.

The following expressions for the Stark components of HCCCOOH were obtained.

$$3.117\,\mu_a^2 + 2.682\,\mu_b^2 = 6.958 \quad 0_{00} - 1_{11},\ M_J = 0$$

$$5.290\,\mu_a^2 + 2.942\,\mu_b^2 = 9.090 \quad 3_{12} - 3_{21},\ M_J = 1$$

$$21.573\,\mu_a^2 + 1.559\,\mu_b^2 = 16.664 \quad 3_{12} - 3_{21},\ M_J = 2$$

$$49.159\,\mu_a^2 - 0.747\,\mu_b^2 = 29.083 \quad 3_{12} - 3_{21},\ M_J = 3$$

These equations were solved graphically, fig. 3.9, with the following results.

$\mu_a = 0.63 - 0.05$ D

$\mu_a^2 = 0.63 \pm 0.05$ D^2 $\qquad$ $\mu_a = 0.80 \pm 0.02$ D

$\mu_b^2 = 1.90 \pm 0.07$ $\qquad$ $\mu_b = 1.38 \pm 0.02$

$\mu^2 = 2.53 \pm 0.12$ $\qquad$ $\mu = 1.59 \pm 0.03$

The errors have been estimated from the intersection shown in fig. 3.9.

HCCCOOH Plots of μ_b^2 against μ_a^2

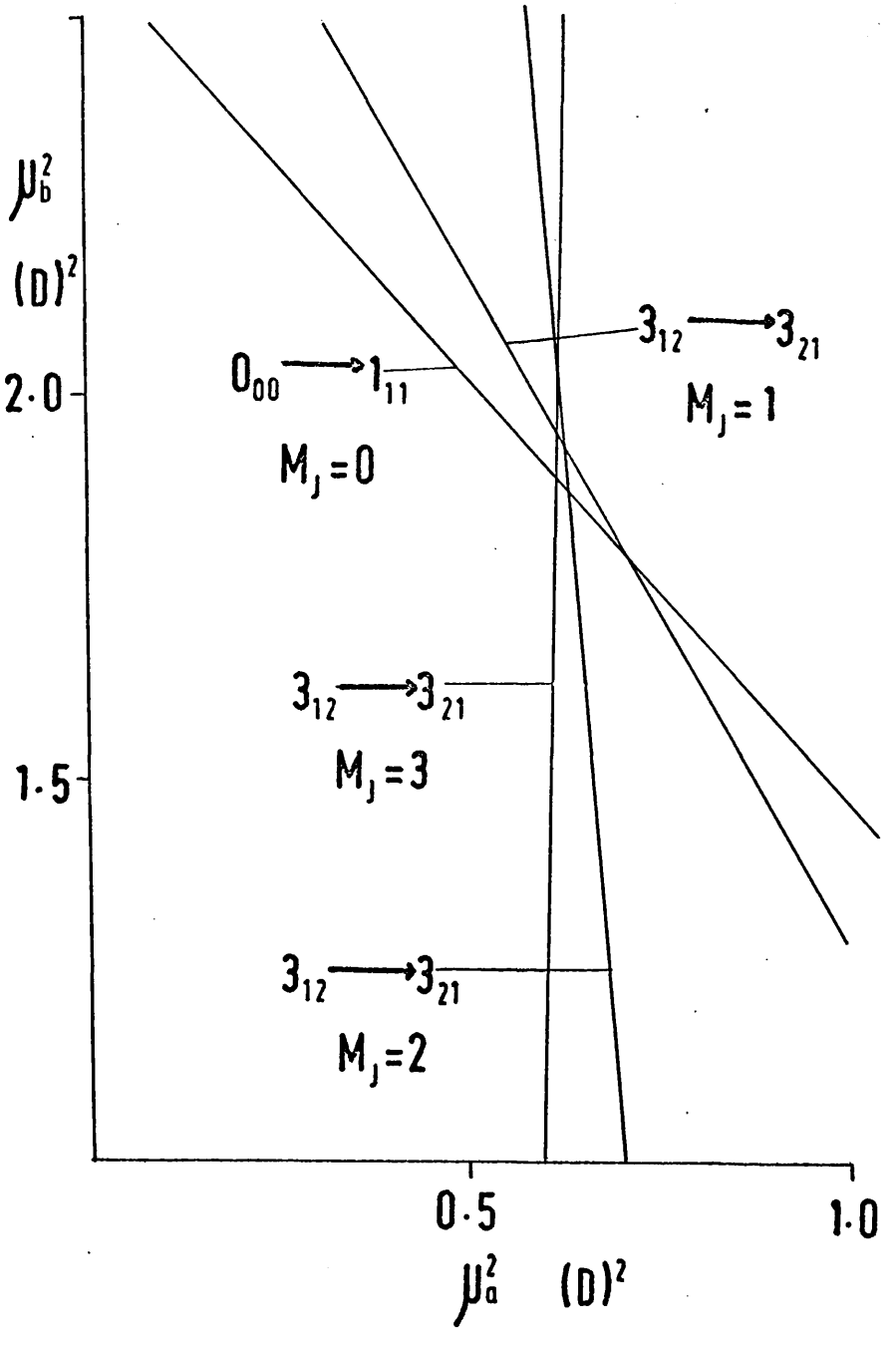

fig.3·9

The corresponding equations for HCCCOOD are

$$0.635\ \mu a^2 + 3.217\ \mu b^2 = 26.670\ \ 1_{01} - 2_{12},\ M_J = 1$$
$$52.611\ \mu a^2 - 0.878\ \mu b^2 = 28.943\ \ 3_{12} - 3_{21},\ M_J = 3$$

If the dipole moment of propiolic acid does not change in magnitude on deuteration a third equation may be added

$$\mu a^2 + \mu b^2 = 2.53$$

These equations were solved graphically (fig.3.10) with the following results

$\mu a^2 = 0.58\ D^2$	$\mu a = 0.76\ D$
$\mu b^2 = 1.96$	$\mu b = 1.40$
$\mu^2 = 2.54$	$\mu = 1.59$

The angle between the dipole moment and the a inertial axis is given by $\tan^{-1}(\mu b/\mu a)$ and the angles for the two isotopic species of propiolic acid are

HCCCOOH	$59^\circ\ 54'$
HCCCOOD	$61^\circ\ 30'$

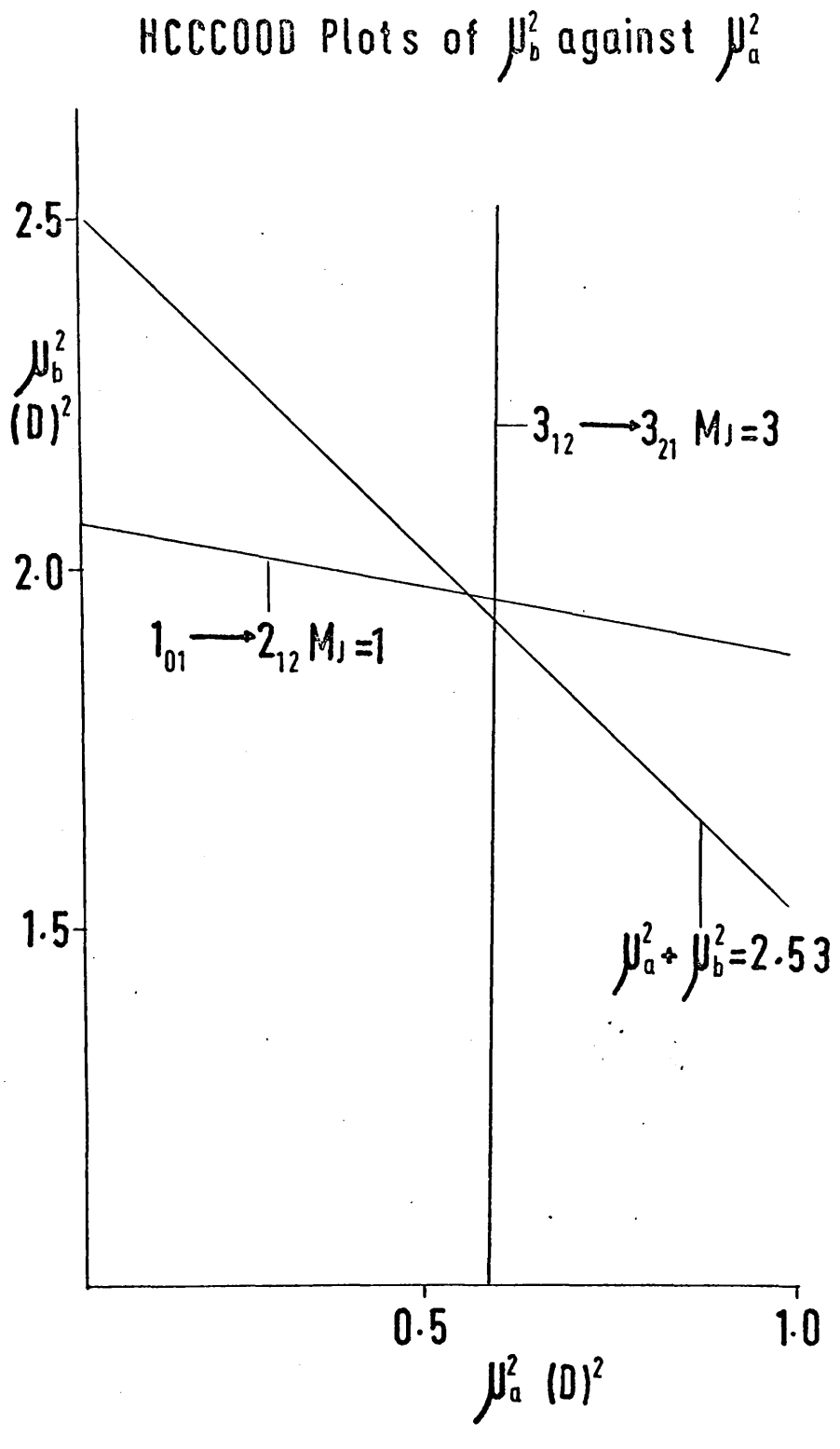
HCCCOOD Plots of μ_b^2 against μ_a^2
2·5
2·0
1·5
μ_b^2
$(D)^2$
$3_{12} \longrightarrow 3_{21}$ $M_J=3$
$1_{01} \longrightarrow 2_{12}$ $M_J=1$
$\mu_a^2+\mu_b^2=2.53$
0·5
1·0
μ_a^2 $(D)^2$

fig.3·10

If the small changes in the components of the dipole moment are significant then the angle of rotation of the principal axes on deuteration of the hydroxyl group is $-1^{\circ}\ 36'$. This angle may be calculated from the co-ordinates of the hydrogen atom and the moments of inertia of HCCCOOH. The condition that the products of inertia about principal axes are zero leads to the following expression.

$$\tan 2\Theta = \frac{-2 I_{XY}}{I_X - I_Y}$$

I_{XY}, I_X and I_Y are the product and moments of inertia of HCCCOOD about axes parallel to the principal axes of HCCCOOH but with origin at the centre of mass of HCCCOOD. The product and moments of inertia are given by

$$I_{XY} = -\mu ab$$
$$I_X = Ia + \mu b^2$$
$$I_Y = I_b + \mu a^2$$

where I_a and I_b are the moments of inertia of HCCCOOH,

a and b are the co-ordinates of the hydrogen atom and μ is the reduced mass used in Kraitchman's equations. The angle of rotation found in this way is - 1^{o} 26' and agrees well with that found from the components of the dipole moment.

The changes in the components of the dipole moment on deuteration are consistent with that vector lying in the first or third quadrant of the principal axis system shown in fig. 3.5. Considerations of bond moments [13] (fig.3.11a) favour the first quadrant and the dipole moment in propiolic acid is therefore almost parallel to the C = O bond.

The dipole moments of formaldehyde, [14] propynal, [15] formic acid, [16] and propiolic acid are shown in fig.3.11 b. The small increase and considerable change in direction of the dipole moments of the substituted molecules indicate that the acetylene group has an electron donating effect. On the basis of the small increase in the dipole moment relative to that of formaldehyde Howe and Goldstein in reference 15 argue against structure (a) contributing

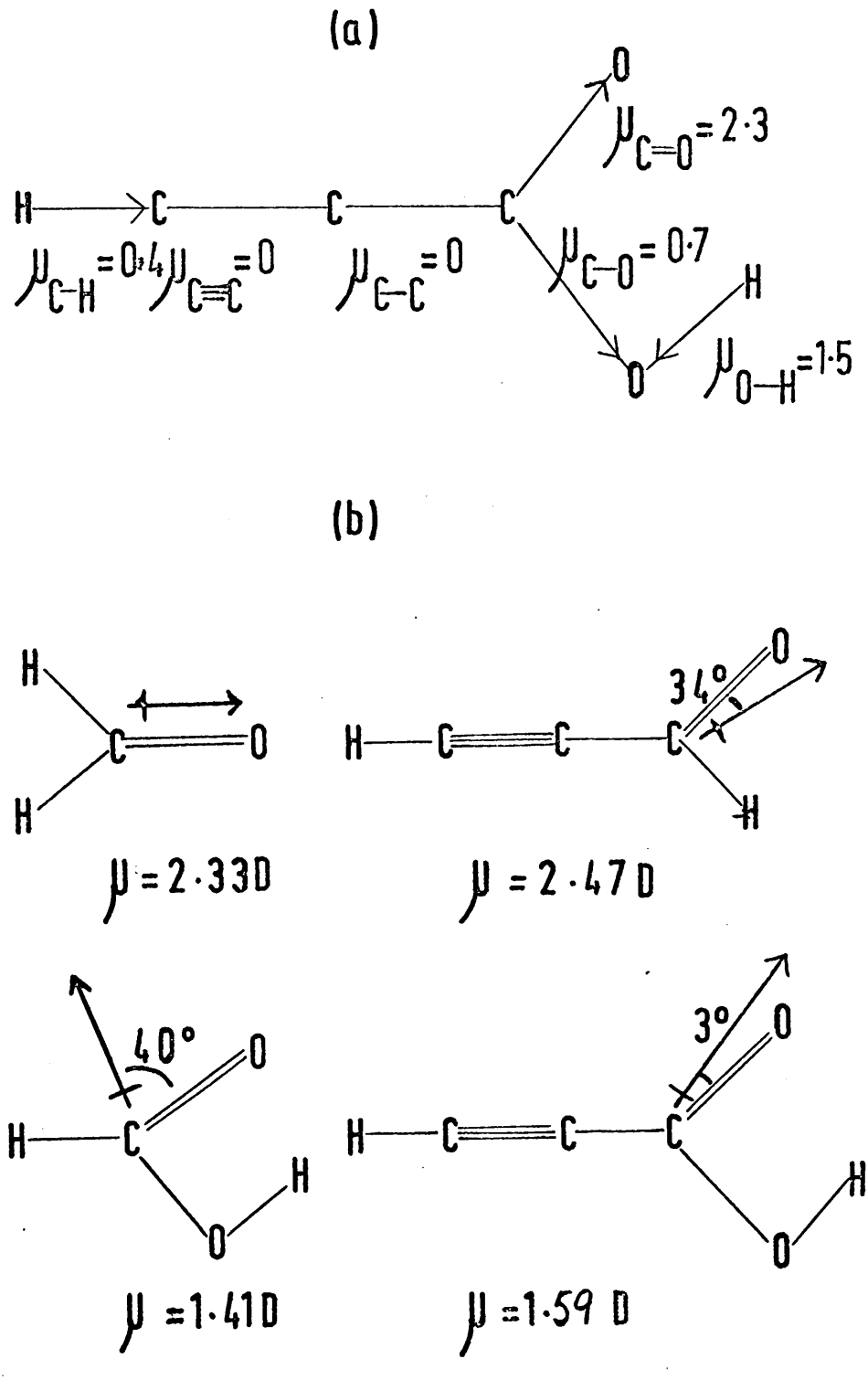
(a)
H
C
C
C
O
$\mu_{C=O}$ = 2·3
μ_{C-H} = 0·4
$\mu_{C\equiv C}$ = 0
μ_{C-C} = 0
μ_{C-O} = 0·7
H
O
μ_{O-H} = 1·5
(b)
H
C
O
H
μ = 2·33D
H
C
C
C
34°
O
H
μ = 2·47 D
40°
O
H
C
H
O
μ = 1·41D
3°
O
H
C
C
C
H
O
μ = 1·59 D

fig.3·11

significantly to the resonance hybrid of propynal.

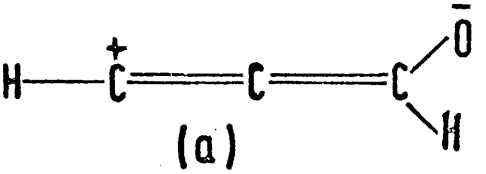

(a)

This view is supported by the C - C bonds in propynal and propiolic acid being some 0.02Å longer than the "normal" value of Stoicheff [17]. Stoicheff's formula is based on data in which carbon and hydrogen atoms are adjacent to the bonds under consideration. The C - C - H angle in propynal (114°) and the C - C - OH angle in propiolic acid (111°) are rather narrow for sp^2 hybridization and the long C - C bonds in these molecules might be due to the oxygen of the carbonyl group altering the hybridization of the carbon atom to which it is attached.

REFERENCES

1. G.H. Kwei and R.F. Curl, J.Chem.Phys., 1960 32, 1592

2. C.C. Costain and J.R. Morton, J.Chem.Phys., 1959, 31, 389

3. D. Kivelson and E.B. Wilson Jr., J.Chem.Phys., 1952, 20, 1575

4. J.K.G. Watson, J.Chem.Phys., 1967, 46, 1935

5. R.A. Hill and T.E. Edwards, J. Mol. Spectroscopy, 1962, 9, 494

6. E.B. Wilson Jr., J.Chem.Phys., 1937, 5, 617

7. J.M.Dowling, J.Mol. Spectroscopy, 1961, 6, 550

8. G.O. Sørensen, J.Mol. Spectroscopy, 1967, 22, 325

9. S. Golden and E.B. Wilson Jr., J.Chem.Phys., 1948, 7, 669

10. R. Weiss, Phys. Rev., 1963, 131, 659

11. C.H. Townes and A.L. Schawlow, "Microwave Spectroscopy", McGraw-Hill Book Company, Inc., 1955, 255

12. P.F. Wacker and Marlene R. Pratto, "Microwave Spectral Tables, Line Strengths of Asymmetric Rotors", N.B.S. Monograph 70 - Volume 2, 1964

13. C.P. Smythe, "Dielectric Behaviour and Structure", McGraw-Hill Book Company, Inc., 1955, 244

14. K. Kondo, J.Phys.Soc. Japan, 1960, 15, 307

15. J.A. Howe and J.H. Goldstein, J.Chem.Phys., 1955, 23, 1223

16. H. Kim, R. Kellar, and W.D. Gwinn, J.Chem.Phys. 1962, 37, 2748

17. B.P. Stoicheff, Tetrahedron, 1962, 17, 135

Double bond fixation in the six membered rings of 2,1,3 - benzoxadiazole and 2,1,3 - benzothiadiazole

(1) Introduction

The chemical properties of 2, 1, 3 - benzoxadiazole and those of the analogous sulphur and selenium compounds[1](a) indicate that the degree of double bond fixation in the six membered rings is somewhere between that in butadiene and that in naphthalene.

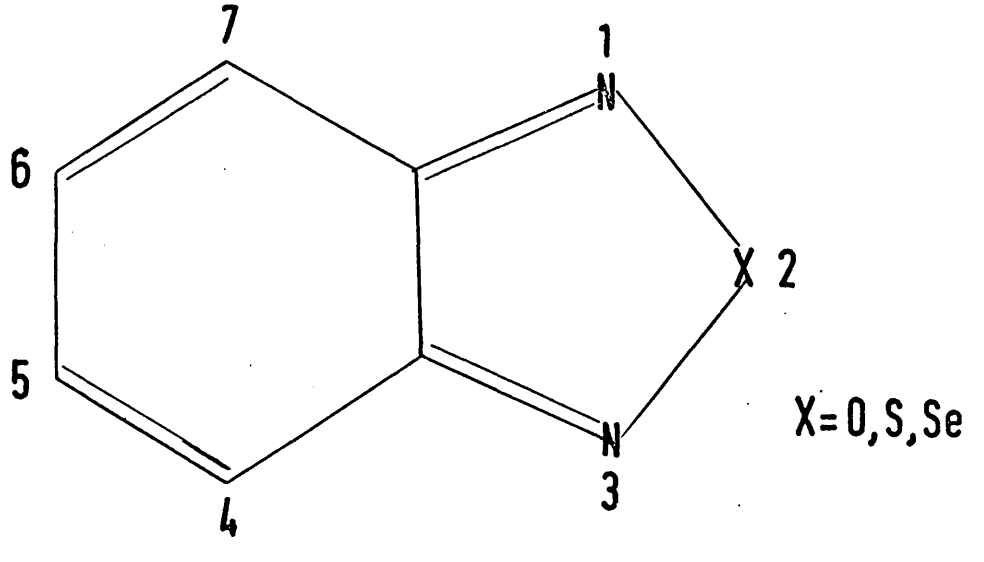

(a)

(The ring numbering system is that used in reference 2)

All three compounds undergo electrophilic substitution reactions, such as nitration [3], that are characteristic of aromatic compounds. The quinonoid nature of the six membered rings is shown by the addition, in the absence of a catalyst, of four atoms of halogen to the "butadiene" grouping. The compound formed by the addition of four atoms of bromine to 2, 1, 3 - benzoxadiazole is quite stable and only loses two molecules of hydrogen bromide on treatment with alkali [4].

The X - ray structures [5] of the three compounds are shown in fig 4.1. 2, 1, 3 - benzothiadiazole (b) and 2, 1, 3 - benzoselenadiazole (c) show considerable double bond fixation in the six membered rings. In view of its chemistry, the regular six membered ring in 2, 1, 3 - benzoxadiazole (a) appears anomolous. A n.m.r. study of these compounds [6] suggests that the degree of double bond fixation in 2, 1, 3 - benzoxadiazole is very similar to that in 2, 1, 3 - benzothiadiazole. The π - bond orders

(a)

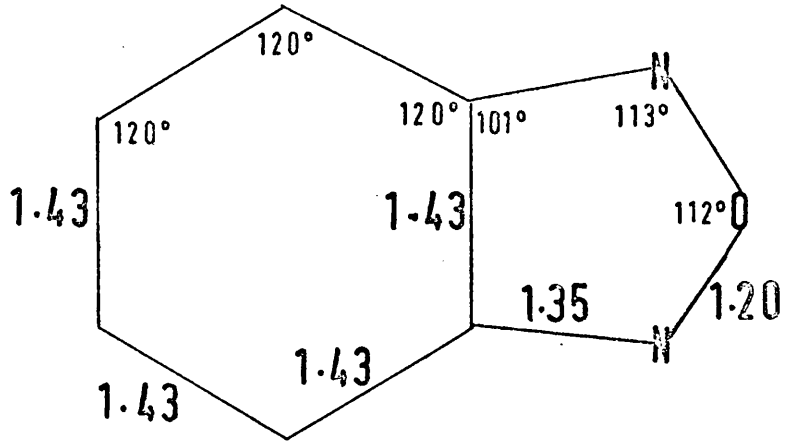
120°
120°
120°
101°
113°
N
1·43
1·43
112°O
1·35
1·20
N
1·43
1·43

(b)

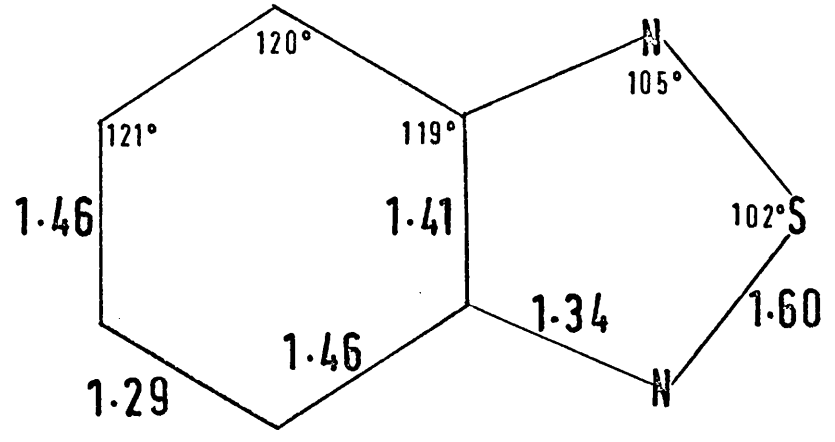
120°
N
105°
121°
119°
1·46
1·41
102°S
1·34
1·60
1·46
1·29
N

(c)

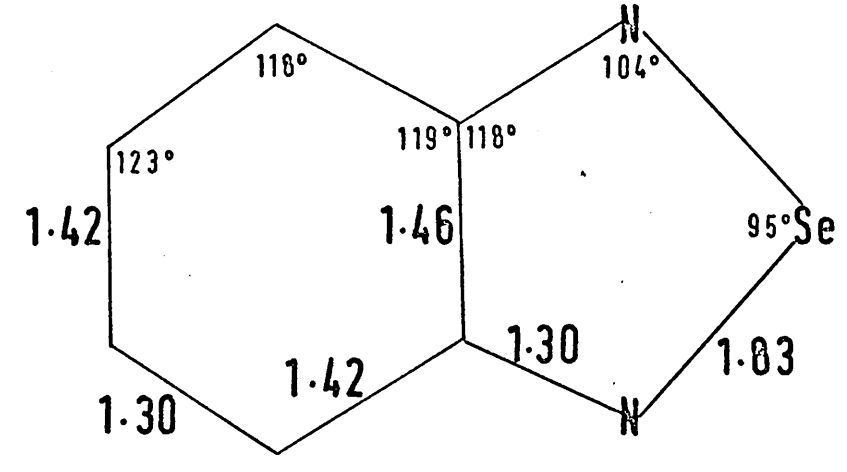
N
118°
104°
123°
119°
118°
1·42
1·46
95°Se
1·30
1·03
1·42
1·30
N

fig. 4.1

from this study agree with those obtained from a simple Hückel calculation [7]. The resonance integrals used in this calculation were those used to interpret the e.s.r. spectra of the radical anions of 2, 1, 3 - benzoxadiazole and 2, 1, 3 - benzothiadiazole [8]. The predicted bond lengths [6] are very close to those found in the corresponding part of naphthalene[9].

2, 1, 3 - benzoxadiazole and 2, 1, 3 - benzothiadiazole are rather heavy for a complete structural determination by microwave spectroscopy. However, it was thought that a study of the normal isotopic species of these compounds would show whether the X - ray structure of 2, 1, 3 - benzoxadiazole is in error and also help to confirm the n.m.r. work.

The X - ray structures of the two compounds were used as models to predict approximate rotational constants. In these and all subsequent calculations the following assumptions were made.

(i) the lengths of the C - H bonds were 1.084 Å.

(ii) the C - H bonds to C_4 and C_7 were perpendicular to the symmetry axis of the molecule.

(iii) the C - H bonds to C_5 and C_6 made angles of 120° with the bond between those atoms.

Both molecules were found to be prolate tops with $\kappa \sim 0.7$ and with the dipole moment along the **a** inertial axis. The most intense transitions for this type of molecule are the μ_a R branch lines. Apart from a shift to lower frequencies due to the increased molecular weight the spectra are similar to that of aniline (fig. 2.1).

(2) Analysis of spectra

Although they are solids, the vapour pressures (0.05 torr) at room temperature of 2, 1, 3 -

benzoxadiazole and 2, 1, 3 - benzothiadiazole are adequate for microwave spectroscopy. Samples were admitted into the cell in the usual way. Both compounds were very stable in the cell and it was possible to work for up to an hour without the lines deteriorating.

The dipole moments [10] of 2, 1, 3 - benzoxadiazole and 2, 1, 3 - benzothiadiazole are 4.03D and 1.73D respectively, and the intensities of their microwave spectra support these figures. It was decided to look at the oxygen compound first because the greater inherent intensity of the spectrum and lower J values of the transitions should make analysis more simple.

A preliminary search was made in K band and a number of strong lines were located. Groups of lines with fast Stark effects were found near 23,500 mc/s and 20,300 mc/s and were identified as the high K -1 lines which occur close to $(J + 1) \times (B + C)$. Several tentative assignments were made on the basis

of Stark effects and separations expected from the model. A set of rigid rotor constants was obtained from wavemeter measurements and an R branch plot. The assignments were confirmed by predicting other lines and these were generally found within 30 mc/s of the predicted frequency. A number of lines was measured accurately and a set of rigid rotor constants was obtained from a least squares fit. The observed and calculated line frequencies and rotational constants are given in table 4.1. Although the lines were quite broad, no quadrupole fine structure was observed even with low pressures in the cell. The high J values of the lines and the presence of vibrational satellites to high and low frequencies meant that it was impossible to make dipole moment measurements.

The analysis of the spectrum of 2, 1, 3 - benzothiadiazole followed much the same course as that of 2, 1, 3 - benzoxadiazole, The lines were much weaker and the Stark effects correspondingly /

TABLE 4.1

Measured line frequencies for 2,1,3-benzoxadiazole.

	observed (mc/s)	calculated (mc/s)
$6_{25} - 7_{26}$	19583.87	19583.72
$6_{24} - 7_{25}$	21825.50	21825.35
$6_{33} - 7_{34}$	21186.07	21186.16
$6_{42} - 7_{43}$	20589.03	20589.19
$7_{07} - 8_{08}$	20192.31	20192.52
$7_{17} - 8_{18}$	20124.75	20124.84
$7_{26} - 8_{27}$	22162.13	22162.16
$7_{25} - 8_{26}$	24837.33	24837.25
$7_{35} - 8_{36}$	23299.78	23299.67
$7_{44} - 8_{45}$	23517.23	23517.00
$7_{43} - 8_{44}$	23691.83	23691.90
$7_{62} - 8_{63}$	23338.36	23337.60
$7_{61} - 8_{62}$		23337.82
$8_{08} - 9_{09}$	22544.46	22544.44
$8_{18} - 9_{19}$	22510.10	22510.17

Cont'd.

TABLE 4.1 (Cont'd.)

	observed (mc/s)	calculated (mc/s)
$8_{17} - 9_{18}$	25222.44	25222.51
$8_{27} - 9_{28}$	24680.71	24680.65
$8_{36} - 9_{37}$	26099.14	26099.04
$9_{09} - 10_{010}$	24904.97	24904.92
$9_{19} - 10_{110}$	24888.30	24888.15
$(A + C)/2$		2563.36
$(A - C)/2$		1378.01
κ		-0.630151

TABLE 4.2

Measured line frequencies for 2,1,3-benzothiadiazole.

	observed (mc/s)	calculated (mc/s)
$8_{26} - 9_{27}$	20981.63	20981.56
$8_{35} - 8_{36}$	20444.34	20444.32
$8_{45} - 9_{46}$	19943.18	19943.31
$9_{09} - 10_{010}$	19756.11	19756.23
$9_{19} - 10_{110}$	19684.06	19683.86
$9_{18} - 10_{19}$	21936.74	21936.64
$9_{27} - 10_{28}$	23273.14	23273.21
$9_{37} - 10_{38}$	22062.59	22062.87
$9_{46} - 10_{47}$	22195.85	22195.93
$9_{45} - 10_{46}$	22302.51	22302.65
$10_{29} - 11_{210}$	23229.36	23229.51
$10_{28} - 11_{29}$	25487.71	25487.81
$10_{37} - 11_{38}$	25421.61	25421.65
$10_{47} - 11_{48}$	24450.27	24449.99
$10_{46} - 11_{47}$	24653.63	24653.77
$10_{56} - 11_{57}$	24380.01	24379.97

Cont'd.

TABLE 4.2 (Cont'd.)

	observed (mc/s)	calculated (mc/s)
$11_{011} - 12_{012}$	23485.15	23485.19
$11_{111} - 12_{112}$	23458.86	23458.84
$(A + C)/2$		2351.25
$(A - C)/2$		1412.56
κ		-0.779288

correspondingly slower. A list of observed and calculated line frequencies and the least squares rigid rotor constants are given in table 4.2.

(3) Discussion

The moments of inertia of 2, 1, 3 - benzoxadiazole and 2, 1, 3 - benzothiadiazole are shown in the first rows of tables 4.3 and 4.4. The inertial defects are

2,1,3 - benzoxadiazole $\Delta^{\circ} = -0.0269$ a.m.u. Å^2

2,1,3 - benzothiadiazole $\Delta^{\circ} = -0.0401$ a.m.u. Å^2

The small magnitudes of these quantities help to confirm the planar nature of the molecules. Similar inertial defects have been found for 4 - pyrone [11], 4 - thiapyrone [12], and pyran - 4 - thione [13]. In these molecules the major contribution to the inertial defect is due to a low frequency out of plane vibration. An analogous situation could well exist in 2, 1, 3 - benzoxadiazole and 2, 1, 3 - benzothiadiazole.

The angles of the five membered ring in the X - ray structure of 2, 1, 3 - benzoxadiazole are not consistent with the bond lengths and this was rectified by increasing the CCN angle to 102^{o}. The moments of inertia calculated from this structure are shown in the second row of table 4.3. The differences between the observed and calculated moments of inertia are too great to be attributed to changes in molecular geometry occurring on transition from the solid to the vapour phase.

A similar inconsistency between the bond angles and bond lengths occurs in the six membered ring of the X - ray structure of 2, 1, 3 - benzothiadiazole. This was corrected by lengthening the abnormally short $C_4 - C_5$ bond to 1.335Å a value closer to that in ethylene [14] and butadiene [15]. The moments of inertia are shown in the second row of table 4.4 and in this case the agreement with the observed values is more reasonable.

The five membered ring in the X - ray structure

TABLE 4.3

Moments of inertia for 2,1,3-benzoxadiazole.

	Ia ($a.m.u.\AA^2$)	Ib ($a.m.u.\AA^2$)	Ic ($a.m.u.\AA^2$)
observed	128.2628	298.2466	426.4825
X-ray structure	117.34	315.64	432.98
structure fig 4.3	128.26	299.02	427.28
structure fig 4.4	128.26	290.71	418.97

TABLE 4.4

Moments of inertia for 2,1,3-benzothiadiazole.

	Ia ($a.m.u.\AA^2$)	Ib ($a.m.u.\AA^2$)	Ic ($a.m.u.\AA^2$)
observed	134.3136	404.2760	538.5495
X-ray structure	132.64	406.86	539.50
structure fig 4.3	134.31	407.67	541.98
structure fig 4.4	134.31	397.75	532.06

of 2, 1, 3 - benzothiadiazole is very similar to that found in 1, 2, 5 - thiadiazole [16,17]. A calculation was made in which the geometry of the five membered ring of 2, 1, 3 - benzothiadiazole was fixed at that of 1, 2, 5 - thiadiazole (fig. 4.2) and the single and double bonds in the six membered ring were set equal to 1.46 and 1.34 Å respectively. The b co-ordinate of C_4 was fixed from the second moment condition for I_a and the resulting structure and moments of inertia are shown in fig. 4.3 and the third row of table 4.4. The Ib like that calculated from the X - ray structure is nearly one percent higher than the observed value. The calculation was repeated for 2, 1, 3 - benzoxadiazole, the five membered ring being set equal to that of 1, 2, 5 - oxadiazole.[18] The structure and moments of inertia are shown in fig. 4.3 and the third row of table 4.3. The agreement between the observed and calculated Ib is much better than for the X - ray structure.

The bond lengths in the six membered rings were set equal to those in naphthalene[9] and the above calculations repeated.

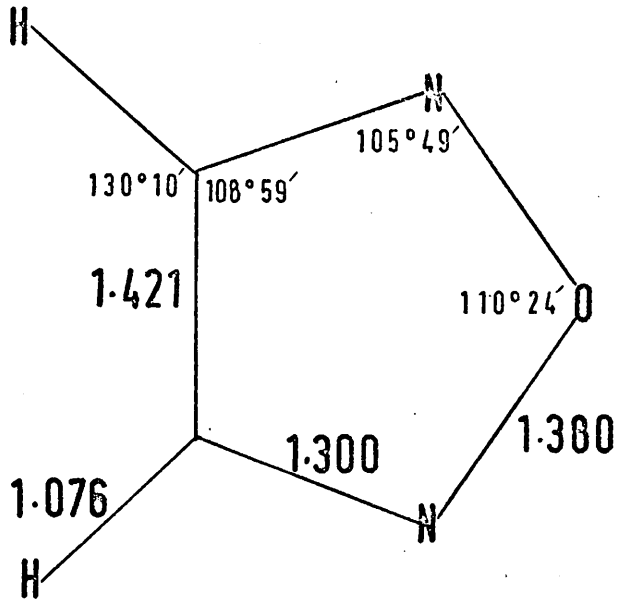

1,2,5-oxadiazole

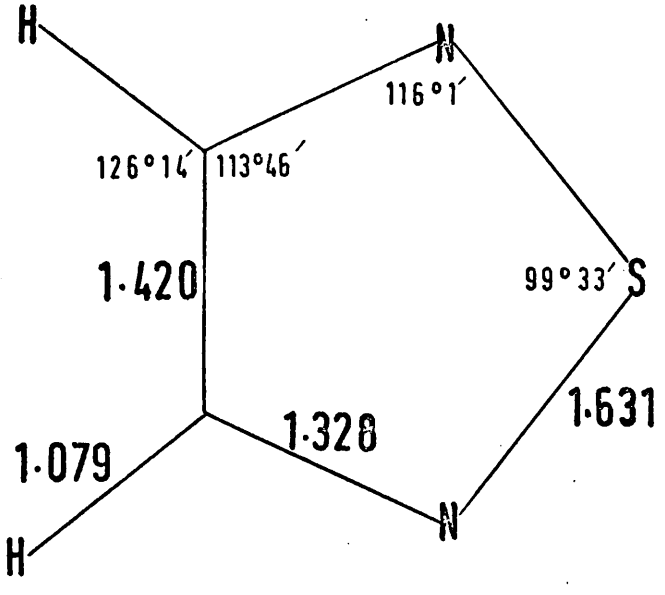

1,2,5-thiadiazole

fig. 4·2

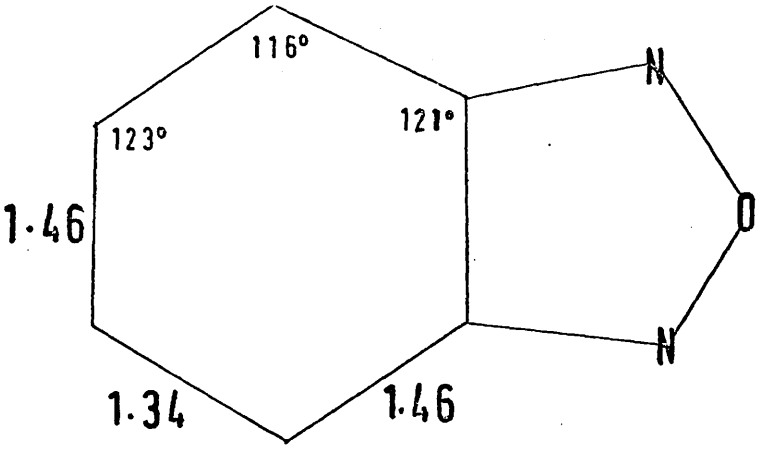

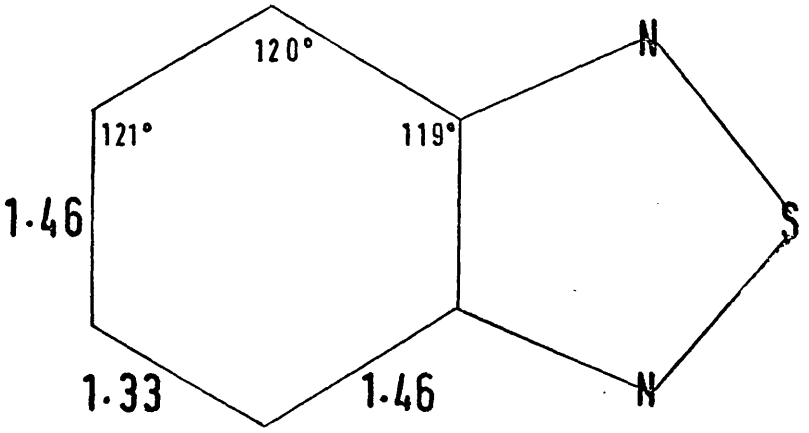

The structures of the five membered rings are shown in fig. 4.2.

fig. 4.3

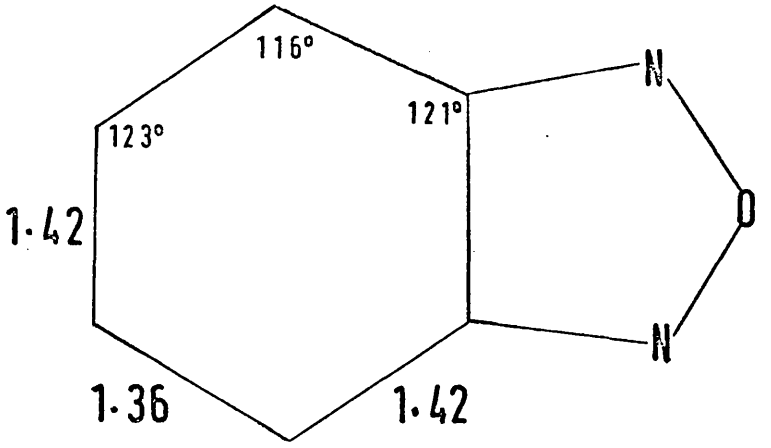

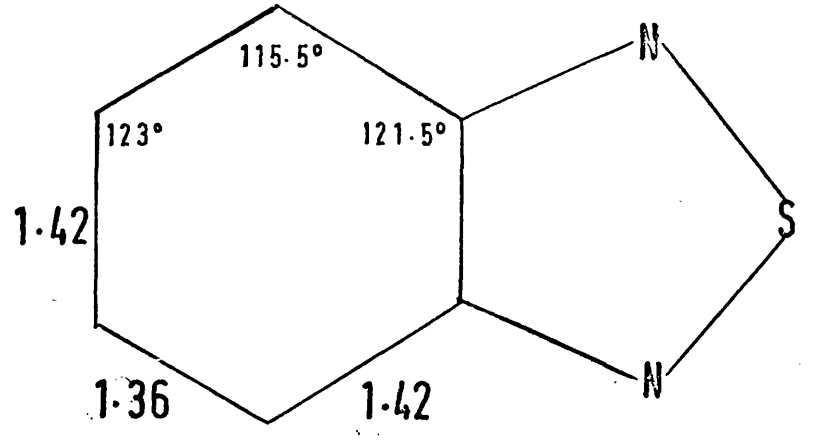

The structures of the five membered rings are shown in fig. 4.2.

fig. 4.4

The resulting structures are shown in fig. 4.4 and the moments of inertia in the fourth rows of tables 4.3 and 4.4. The calculated values of Ib are lower than the observed values and the bond angles at C_4 are rather narrow for sp^2 hybridization. On the basis of these calculations it appears that the degree of double bond fixation in the six membered rings of 2, 1, 3 - benzoxadiazole and 2, 1, 3 - benzothiadiazole is closer to that in butadiene than that in naphthalene. However, the assumption that the five membered rings remain unchanged on annulation is very drastic and before the question of double bond fixation in these molecules can be finally settled more structural information is necessary.

REFERENCES

1. L.S. Efros, Russian Chemical Reviews, 1960, 29, 66

2. W.A. Sherman (editor R.C. Elderfield), "Heterocyclic Compounds", John Wiley and Sons, 1961, 7, 581

3. R.J. Gaughran, J.P. Picard, and J.V.R. Kaufman, J. Amer. Chem. Soc., 1954, 76, 2233

4. D.L. Hammick, W.A.M. Edwards, and E.R. Steiner, J. Chem. Soc., 1931, 3308

5. V. Luzzatti, Acta Cryst., 1951, 4, 193

6. N.M.D. Brown and P. Bladon, Spectrochem. Acta, to be published

7. N.M.D. Brown and G. Doggett, University of Glasgow, unpublished results

8. E.T. Strom and G.A. Russell, J. Amer. Chem. Soc., 1965, 87, 3326

9. D.W.J. Cruickshank, Acta Cryst. 1957, 10, 504

10. R.W. Hill and L.E. Sutton, J. Chem. Phys., 1949, 46, 244

11,12. J.N. Macdonald, University of Glasgow, unpublished results

13. Susan A. Manley, B.Sc. Thesis University of Glasgow, 1968

14. H.C. Allen and E.K. Plyler, J. Amer. Chem. Soc. 1958, 80, 2673

15. A. Almenningen, O. Bastiansen, and M. Traetteberg, Acta Chem. Scand., 1958, 12, 1221

16. V. Dobyns and L. Pierce, J. Amer. Chem. Soc. 1963, 85, 3553

17. F. A. Momary and R. A. Bonham, J. Amer. Chem. Soc. 1964, 86, 162

18. E. Saegebrath and A. P. Cox, J. Chem. Phys., 1965, 43, 166

Chapter 5

The conformation of glycollonitrile

(1) Introduction

Some preliminary conclusions about the structure of glycollonitrile are given in this chapter. The most likely conformations for this kind of molecule are shown in fig. 5.1. The existence of more than one conformer depends on the shape of the potential function describing the internal rotation of the hydroxyl group and the study of molecules with a number of non-equivalent conformations might help to show what kind of effects are responsible for the barriers to internal rotation.

A structure derived by replacing the methyl group of ethyl cyanide[1] with the hydroxyl group of methyl alcohol[2] was used as a model for predicting lines (fig.5.2). Structures for the trans and gauche forms were obtained by making suitable rotations about the C - O bond. All three conformers are prolate slightly asymmetric tops and because of the highly polar cyanide group all

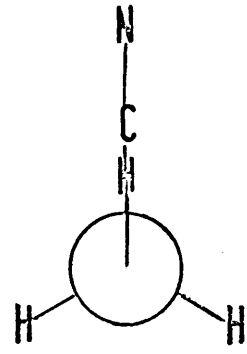

cis

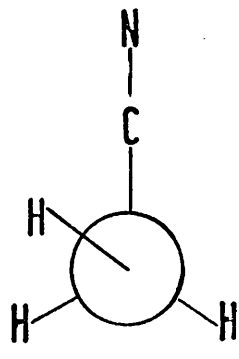

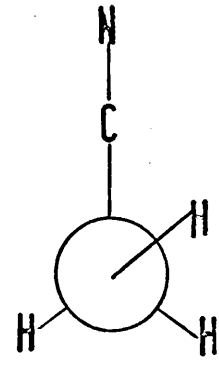

gauche

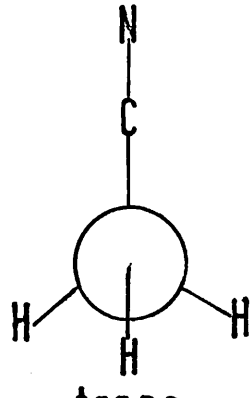

trans

fig. 5·1

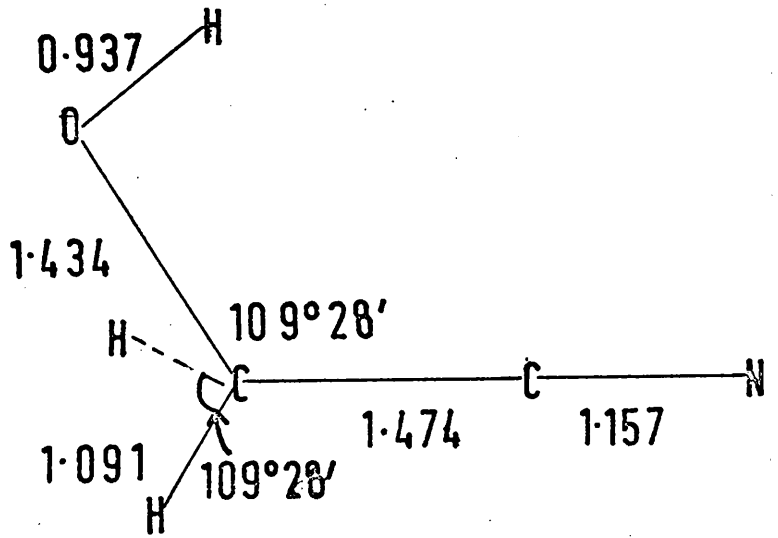

fig.5·2

have appreciable μ_a components of the dipole moment. An initial search for lines was therefore made in the region 36000 - 40000 mc/s where the J = 3 - 4 μ_a R branch lines are predicted.

(2) Analysis of spectra

A very rich spectrum consisting of a large number of low field lines with symmetrical Stark effects was observed. A group of lines near 36800 mc/s with the characteristic Stark effects of the K_{-1} = 0 and K_{-1} = 2,3 μ_a R branch lines of a slightly asymmetric rotor were located. Candidates for the K_{-1} = 1 lines were observed approximately 900 mc/s to high and low frequency of this group of lines. The assignments were confirmed when the J = 1 - 2 and J = 2 - 3 lines were observed at half and three quarters of the frequencies of the J = 3 - 4 lines.

All of the lines so far assigned are accompanied by a very intense vibrational

satellite to low frequency. The relative intensities of the ground state and satellite lines indicate that the first excited vibrational state (V = 1) of glycollonitrile lies less than 50 cm^{-1} above the ground state (V = 0).

The $0_{00} - 1_{01}$ transitions for the V = 0 and V = 1 states were observed at 9217 and 9213 mc/s and both lines showed the expected quadrupole fine structure. For a slightly asymmetric rotor such as glycollonitrile the quadrupole coupling energy of the 1_{01} level may be written

$$W_Q = -\chi_{aa} f(I,J,F)$$

where χ_{aa} is the quadrupole coupling constant along the a inertial axis and $f(I,J,F)$ is Casimir's function. The observed splittings are shown in table 5.1 and the value of $\chi_{aa} = -3.6$ mc/s mc/s may be compared with that in ethyl cyanide[4] ($\chi_{aa} = -3.3$ mc/s).

A search was made for transitions due to the

TABLE 5.1

$^{14}_{N}$ quadrupole fine structure for $0_{00} - 1_{01}$ of $HOCH_2CN$

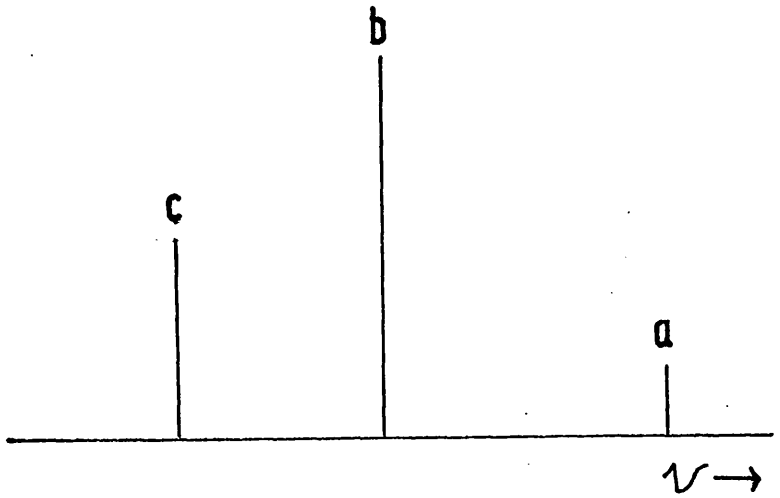

	F - F'		V = 0	V = 1
a	1	0	9219.24	9214.78
b	1	2	9217.57	9213.28
c	1	1	9216.51	9212.23
χ_{aa}			- 3.63	- 3.45

μ_b and μ_c components of the dipole moment. The $J_{0J} - J_{1,\ J-1}$ μ_b Q branch series was located and the first six members have been measured. If rigid rotor theory is obeyed the rotational constants may be derived from the following expressions

$0_{00} - 1_{01}$	B + C
$(1_{10} - 2_{11}) - (1_{11} - 2_{12})$	2(B - C)
$1_{01} - 1_{10}$	A - C

The frequencies of the $0_{00} - 1_{11}$ μ_b and $0_{00} - 1_{10}$ μ_c lines were predicted from a set of rotational constants obtained in this manner. The $0_{00} - 1_{11}$ lines for the V = 0 and V = 1 states were found within 1 mc/s of the predicted frequencies, but an intensive search for the $0_{00} - 1_{10}$ lines was unsuccessful. The measured line frequencies for the normal isotopic species of glycollonitrile are given in table 5.2.

The analysis of the spectrum of $DOCH_2CN$ followed much the same course as that of the normal isotopic

TABLE 5.2

Measured line frequencies for $HOCH_2CN$

	V = 0 (mc/s)	V = 1 (mc/s)
$0_{00} - 1_{01}$	9217.40	9213.10
$0_{00} - 1_{11}$	37998.04	37973.81
$1_{01} - 1_{10}$		
$1_{01} - 2_{02}$	1829.29	18420.78
$1_{11} - 2_{12}$	17974.08	17969.27
$1_{10} - 2_{11}$	18896.92	18887.54
$2_{02} - 2_{11}$	29711.38	29691.49
$2_{02} - 3_{03}$	27629.88	27616.91
$2_{12} - 3_{13}$	26955.79	26948.82
$2_{11} - 3_{12}$	28341.47	28327.81
$3_{03} - 3_{12}$	30422.19	30397.30
$3_{03} - 4_{04}$	36813.93	36796.66
$3_{13} - 4_{14}$	35934.46	35926.85
$3_{12} - 4_{13}$	37781.50	37763.47

TABLE 5.2 (cont'd.)

	V = 0	V = 1
$4_{04} - 4_{13}$	31389.36	31365.15
$5_{05} - 5_{14}$	32628.76	32605.18
$6_{06} - 6_{15}$	34186.44	34160.11
A	33622.54	33601.09
B	4839.41	4830.52
C	4379.99	4382.58

species. The $0_{00} - 1_{11}$, $1_{11} - 2_{12}$ and $1_{10} - 2_{11}$ transitions of this isotopic species have not been observed and the rotational constants have been obtained from the $K_{-1} = 0$ a R branch lines and Q branch plots for the $J_{0J} - J_{1, J-1}$ series of lines. The measured line frequencies are given in table 5.3.

(3) Discussion

The moments of inertia of glycollonitrile are compared with those calculated from the models in table 5.4. The inertial defects are larger than those expected for the cis and trans forms and the substitution co-ordinates of the hydroxyl hydrogen atom (table 5.5) show that glycollonitrile exists in the gauche form. Allyl alcohol [5] and propargyl alcohol[6,7] also have this conformation, while ethyl alcohol[8] has recently been shown to exist in the trans form. In the gauche and trans forms the interactions between the lone pairs of electrons of the oxygen atom and the bonding electron pairs of the $-CH_2X$ group are

TABLE 5.3

Measured line frequencies of $DOCH_2CN$

	V = 0 (mc/s)	V = 1 (mc/s)
$1_{01} - 1_{10}$	26394.44	26389.57
$1_{01} - 2_{02}$	17971.30	17965.05
$2_{02} - 2_{11}$	26867.01	26861.46
$2_{02} - 3_{03}$	26941.62	26932.86
$2_{12} - 3_{13}$	26266.46	26261.98
$2_{11} - 3_{12}$	27662.20	27650.02
$3_{03} - 3_{12}$	27584.38	27575.79
$3_{03} - 4_{04}$	35893.18	35882.08
$3_{13} - 4_{14}$	35014.70	35008.78
$3_{12} - 4_{13}$	36874.52	36859.21
$4_{04} - 4_{13}$	28566.03	28561.34
$5_{05} - 5_{14}$	29823.91	29816.05
$6_{06} - 6_{15}$	31389.02	31383.33
A 30658·50	B 4726·64	C 4262·06

TABLE 5.4

Moments of inertia of glycollonitrile.

		Ia (a.m.u.Å^2)	Ib (a.m.u.Å^2)	Ic (a.m.u.Å^2)	(a.m.u.Å^2)
cis		15.9813	101.1999	113.9814	-2.1398
trans		14.4131	105.9210	1171493	-2.1398
$HOCH_2CN$	V = 0	15.0366	104.4612	115.4710	-4.0268
	V = 1	15.0451	104.6535	115.3501	-4.3485
$DOCH_2CN$	V = 0	16.4891	106.9536	118.6119	-4.8308
	V = 1	—	—	—	—

TABLE 5.5

Co-ordinates of the hydroxyl hydrogen atom

	a (Å)	b (Å)	c (Å)
cis	- 1.022	1.597	0
trans	- 1.763	0.252	0
observed	- 1.442	1.024	0.674

a minimum.

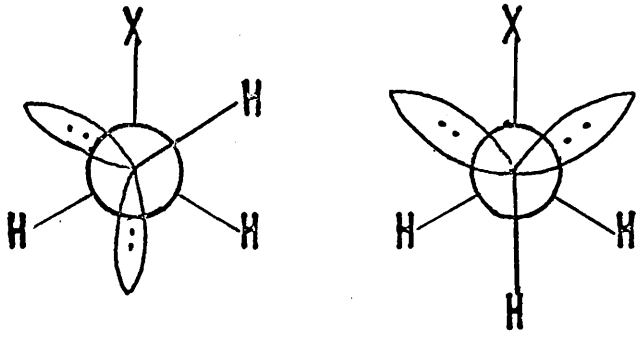

When X is an unsaturated group hydrogen bonding must make the gauche form more stable while in ethyl alcohol repulsions between the hydroxyl hydrogen atom and the methyl group make the trans form more favourable.

Propargyl alcohol also has a very intense satellite to low frequency of the μ_a R branch lines and this has been assigned to the first excited state of the internal rotation. Hirota has studied the internal rotation in this molecule and deduces that this motion effectively takes place in a double minimum potential (fig. 5.3). He explains the absence of the usual μ_c transitions by assuming that

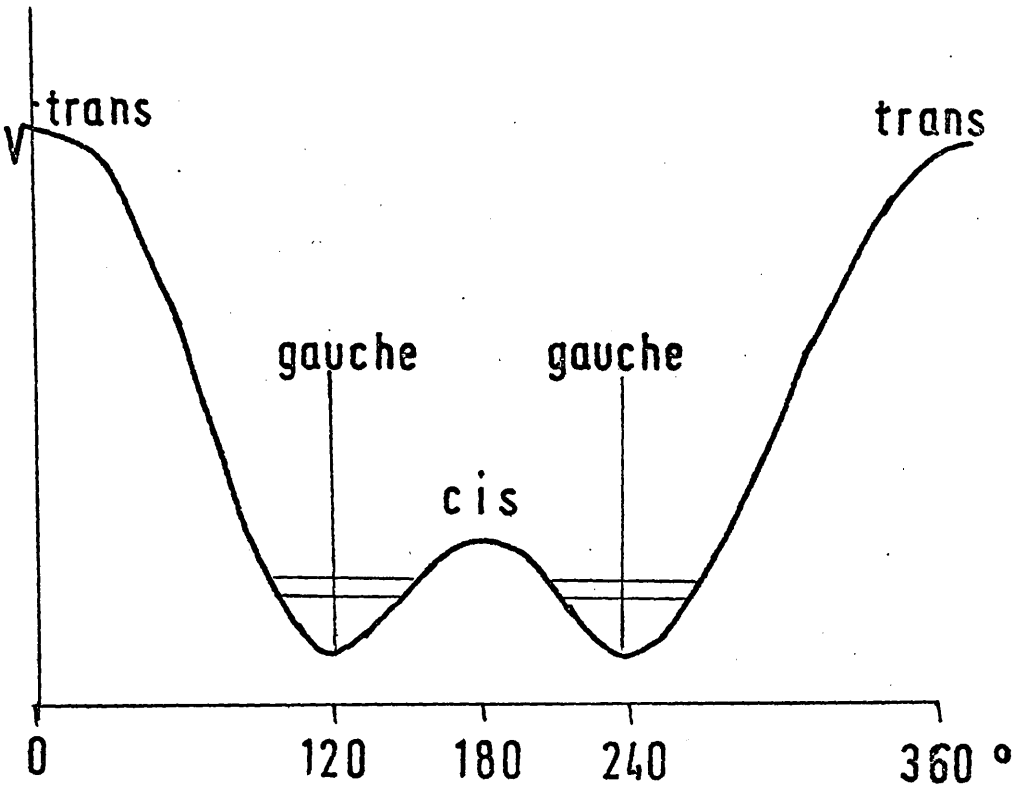

fig.5-3

the V = 0 and V = 1 states are respectively symmetric and antisymmetric with respect to the internal rotation angle and that the μ_c transitions couple these two states. This explanation may also be used to account for the absence of the μ_c transitions in glycollonitrile.

I would like to thank Dr. K. Bolton, Dr. N.L. Owen, Professor J. Sheridan and Professor E. Hirota for allowing me to see their papers on propargyl alcohol prior to publication.

References

1. R. G. Townes and B.P. Dailey, J.Chem.Phys., 1957, 26, 678

2. E. V. Ivash and D. M. Dennison, J.Chem.Phys., 1952, 21, 1804

3. C. H. Townes and A. L. Schawlow, "Microwave Spectroscopy", McGraw-Hill Book Company,1955, Appendix 1, 499

4. V. W. Lauric, J.Chem.Phys., 1959, 31, 1500

5. A.N. Murty and R.F. Curl, J.Chem.Phys., 1967, 46, 4176

6. K. Bolton, N.L. Owen and J. Sheridan, Nature, 1968, 217, 164

7. E. Hirota, J.Mol.Spectroscopy, 1968, 26, 335

8. M. Takano, Y.Sasada and T. Satoh, J.Mol. Spectroscopy, 1968, 26, 157.

CHAPTER 6.

Chemical Preparations

This chapter contains details of a number of chemical preparations carried out by the author.

(1) aniline

(a) aniline - NHD and aniline - ND_2

These isotopic species were prepared by direct exchange with D_2O/H_2O and D_2O. The aniline was extracted into ether and the ether extract dried overnight with anhydrous magnesium sulphate. After filtration the ether was removed under reduced pressure and the aniline was distilled into a sample tube. All of the following preparations required the separation of a mixture of water and aniline and ether extraction was used in each case.

(b) aniline - $2D_1$

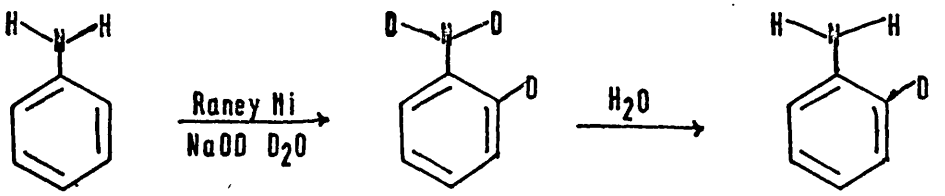

Lauer and Errede have shown that in the presence of base and Raney Nickel the ortho hydrogen atoms of aniline exchange at a much greater rate than the meta and para hydrogen atoms. Aniline (5g), sodium deuteroxide (5g), Raney Nickel (5g) and D_2O (20 ml) were boiled under reflux for twelve hours. The aniline was extracted into ether and the ether removed under reduced pressure. The aniline was washed with normal water (20 ml) and then recovered by the method described above. The infra-red spectrum of the sample had a weak C - D stretching absorption but the relative intensities of the microwave spectra of aniline - $2D_1$ and aniline - H_7 indicated that nearly 50% exchange of the ortho hydrogen atoms had taken place.

(c) aniline - $4D_1$

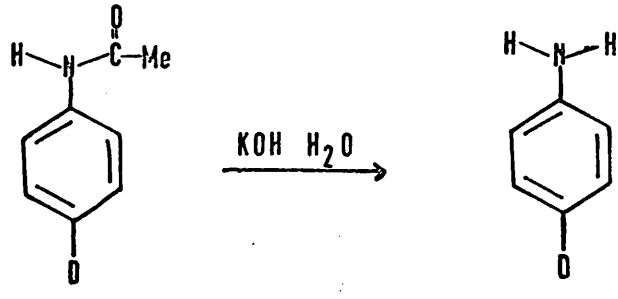

Acetanilide - $4D_1$ (0.50g) was boiled under reflux with a solution of potassium hydroxide (4g) in water (10 ml) for 30 minutes and the aniline was recovered. No trace of aniline - H_7 was found in the microwave spectrum of this sample. However, under conditions of acid hydrolysis[2] it was found that the deuterium was almost completely exchanged.

(d) aniline - 2,4,6 D_3

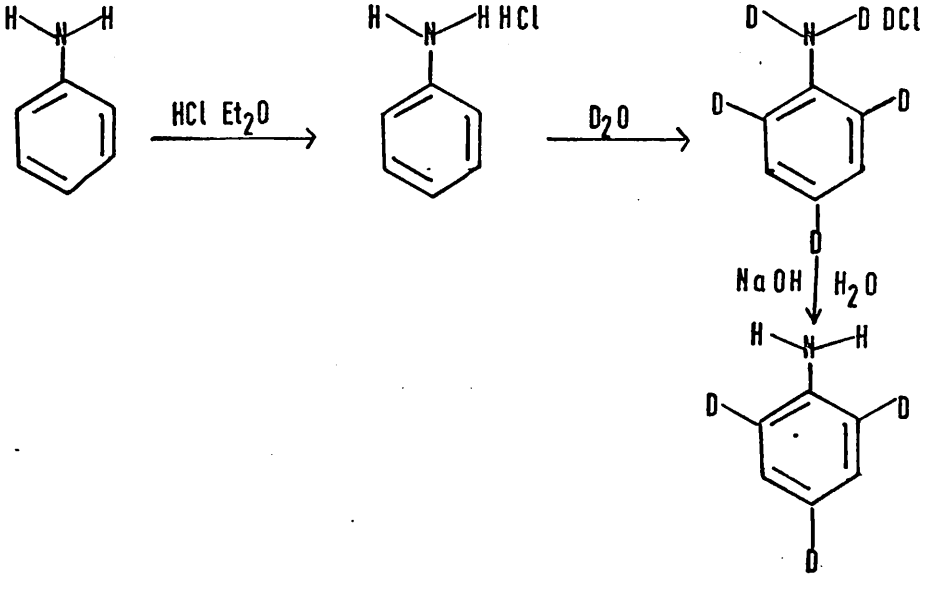

This isotopic species was prepared by essentially the same method as that used by Murray and Williams[3]. Aniline hydrochloride was prepared by passing hydrogen chloride gas into an ethereal solution of freshly distilled aniline. Aniline hydrochloride (1g) was dissolved in D_2O (5 ml) and kept in a sealed flask in an oven at 90°C for five days. The water was removed under reduced pressure and the aniline hydrochloride was dissolved in water (5 ml) and dilute sodium hydroxide (5 ml) was added to the solution. The aniline was recovered in the usual manner.

(e) aniline - D_5 and aniline - 3,5 D_2

Aniline - D_7 (2g) (supplied by Merck, Sharp and Dohme) was washed with methanol to convert N - D to N - H bonds and the methanol was removed under reduced pressure at 50°C using a water bath.

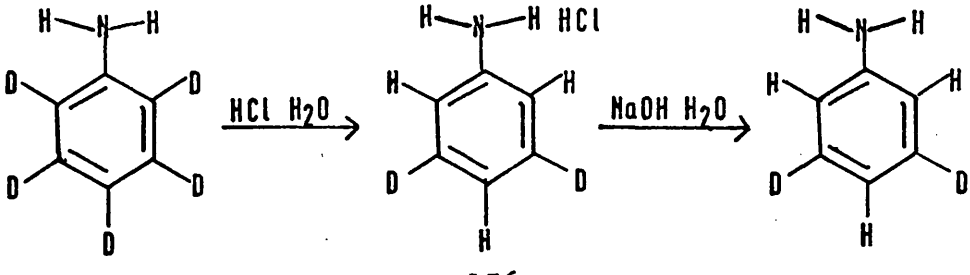

Aniline - D_5 (1g) was dissolved in a solution of concentrated hydrochloric acid (1 ml) in water (5 ml) and the solution was kept at 90°C in a sealed flask for two days. Dilute sodium hydroxide was added to the solution and the aniline was recovered.

(f) preparation of a random mixture of aniline - 13 C_1

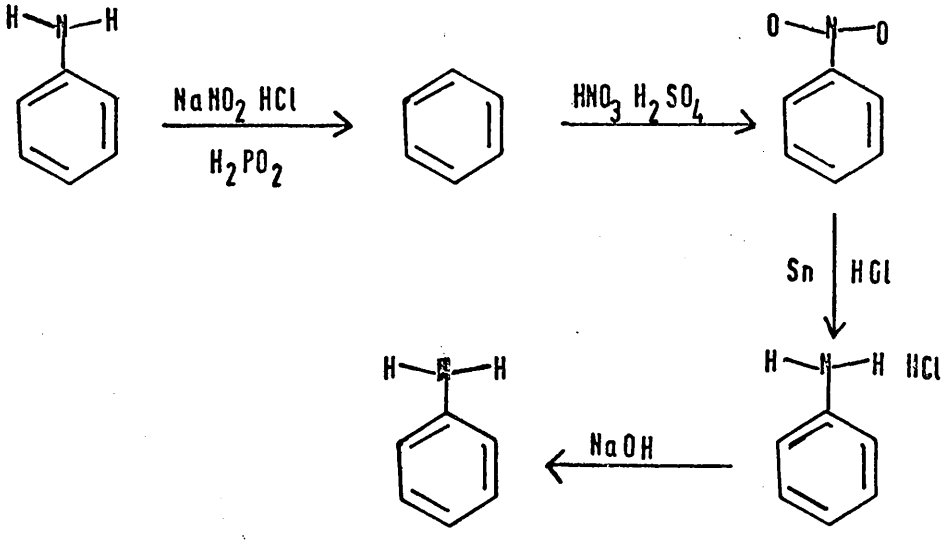

The above reaction scheme was investigated in order to convert the small quantity of aniline - $1^{13}C$

(0.4g supplied by Merck, Sharp and Dohme) to a ramdom mixture of aniline - ^{13}C. The sample of aniline - $^{13}C_1$ was 55% enriched and the product should have the following composition

aniline - H_7	45%
aniline - $1^{13}C$	9%
aniline - $4^{13}C$	
aniline - $2^{13}C$	18%
aniline - $3^{13}C$	

The diazotisation[4], nitration[5] and reduction[6] were essentially modifications of standard preparations. The reaction scheme was tried several times with $\frac{1}{2}$ g samples of normal aniline and good yields were obtained. The first stage of the reaction with the aniline - ^{13}C was accomplished satisfactorily but in the second stage the benzene was converted to meta-dinitrobenzene.

(2) Propiolic acid (DCCCOOH)

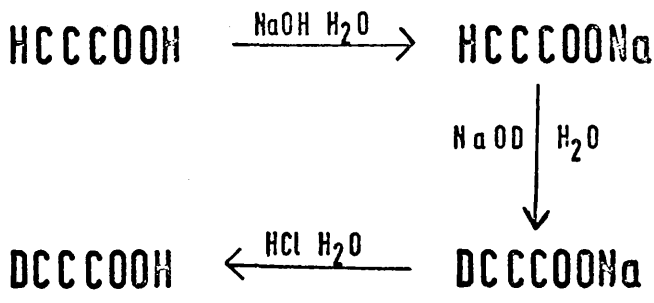

Sodium propiolate was prepared by neutralisation of a 50% aqueous solution of propiolic acid with dilute sodium hydroxide at $0^{\circ}C$. The water was removed under reduced pressure and the salt (1 gm) was dissolved in D_2O (3 ml). The pH of the solution was adjusted to 12 by the addition of a few drops of a solution of sodium deuteroxide in D_2O. The solution was allowed to stand for two days, the water was removed under reduced pressure at room temperature and the residue was dissolved in normal water (3 mls). The solution was cooled to $0^{\circ}C$, a few drops of concentrated hydrochloric acid were added and the propiolic acid was extracted into ether. The ethereal solution was dried

overnight with anhydrous magnesium sulphate, filtered and the ether removed under reduced pressure.

(3) Glycollonitrile.

$$KCN + H_2CO \xrightarrow[KOH]{H_2SO_4} HOCH_2CN$$

This compound was prepared using the method described by Goudry[7]. A solution of potassium cyanide (130 g) in water (250 ml) in a 1 litre three necked flask was cooled to 0°C in a salt bath. The solution was stirred and a solution of commercial 37% formaldehyde (170 ml) in water (130 ml) was added from a dropping funnel at such a rate that the temperature did not rise above 10°C (1 hour). The mixture was allowed to stand (10 minutes) and then ice cold dilute sulphuric acid (57 ml concentrated sulphuric acid in water 173 ml) was added so that the same low temperature was maintained (1 hour).

The pH of the mixture was adjusted to 4 by addition of dilute potassium hydroxide and it was then allowed to

warm up to room temperature. Ether (30 ml) was added and the mixture was filtered at the pump to remove potassium sulphate. The filtrate was extracted with ether 300 ml in a continuous ether extractor (48 hours). The ether extract was dried with anhydrous calcium sulphate (15 g) overnight and filtered. The ether was removed under reduced pressure at 40°C using a water bath.

The crude product was distilled under reduced pressure using a 10 cm. vigreux column lagged with asbestos tape and a nitrogen capillary leak. Three fractions boiling in the range 88 - 95°C at 10 torr were collected. The infra-red spectra of the samples showed traces of water and ethylene glycol as impurities.

The hydroxyl group was deuterated by mixing 2 ml of glycollonitrile with an equal volume of D_2O, allowing the solution to exchange overnight and then extracting with three portions (5 ml) of ether. The glycollonitrile treated in this way

polymerised very rapidly and it was found more convenient to prepare the deuterated species directly in the cell by admitting doses of D_2O and normal glycollonitrile.

REFERENCES

1. W. M. Lauer and L. A. Errede, J. Amer. Chem. Soc., 1954, 76, 5162

2. F. G. Mann and B. C. Saunders, "Practical Organic Chemistry", Longmans, Green and Co. Ltd., 1940, 69

3. A. Murray and D. L. Williams, "Organic Syntheses with Isotopes" part 2, Interscience Publishers Inc., 1958, 1441

4. E. R. Alexander and R. E. Burge, Jr., J. Amer. Chem. Soc., 1950, 72, 3100

5, 6. A. I. Vogel "Practical Organic Chemistry", Longman's Green and Co., 1956, 525, 563

7. R. Gaudry, "Organic Syntheses, Collective Volume 3", John Wiley and Sons Inc., 1955, 437

APPENDIX 1.

The derivation of rotational constants by least squares

The energy levels of a rigid asymmetric rotor may be written in terms of the tabulations of reduced energies as

$$W_{J\tau} = J(J+1)(A+C)/2 + \left(E(\kappa'') + (\kappa - \kappa'')\frac{\partial E(\kappa)}{\partial \kappa}\right)\times (A-C)/2$$

$$\frac{\partial E(\kappa)}{\partial \kappa} = (E(\kappa') - E(\kappa''))\times 1000$$

and κ'' and κ' are respectively the lower and upper entries in the reduced energy tables which κ lies between. A line frequency may be written

$$\nu = \Delta J(J+1)\underline{(A+C)/2} + \Delta\left(E(\kappa'') - \kappa''\frac{\partial E(\kappa)}{\partial \kappa}\right)\underline{(A-C)/2}$$

$$+ (A-C)/2\,\Delta\frac{\partial E(\kappa)}{\partial \kappa}\,\underline{\kappa}$$

where the underlined terms are the parameters to be refined by least squares. The method of least

squares is discussed in the reference.

The coefficients of the underlined terms in equation 1 do not depend very strongly on the parameters to be fitted and the convergence to the least squares minimum is very rapid. Generally the shifts in $(A + C)_{/2}$ and $(A - C)_{/2}$ are found to be less than 0.001 mc/s after two or three cycles.

In the case of propiolic acid where allowance was made for centrifugal distortion equation 1 was used to express the rigid rotor part of the line frequency. The quartic angular momentum terms in equations 3.6 and 3.7 were calculated from the following expressions. These expressions were derived by substituting $X = 1$, $Y = \kappa$, $Z = -1$ into the equations given in the appendix of Watson's paper.

$$\langle P_a^4 \rangle = \langle P_a^2 \rangle^2 + \pi(\kappa+1)/2(1-\kappa)$$

$$\langle P_b^4 \rangle = \langle P_b^2 \rangle^2 - 2\pi/(\kappa+1)(\kappa-1)$$

$$\langle P_c^4 \rangle = \langle P_c^2 \rangle^2 - \pi(1-\kappa)/2(\kappa+1)$$

$$\langle P_a^2 P_b^2 \rangle = \langle P_a^2 \rangle \langle P_b^2 \rangle - \pi/(\kappa-1)$$

$$\langle P_a^2 P_c^2 \rangle = \langle P_a^2 \rangle \langle P_c^2 \rangle + \pi/2$$

$$\langle P_b^2 P_c^2 \rangle = \langle P_b^2 \rangle \langle P_c^2 \rangle - \pi/(\kappa+1)$$

where

$$\pi = 1/3[(1-\kappa)(\langle P_a^2 \rangle \langle P_b^2 \rangle + \langle P_c^2 \rangle)$$

$$+ (\kappa+1)(\langle P_b^2 \rangle \langle P_c^2 \rangle + \langle P_a^2 \rangle)$$

$$-2(\langle P_a^2 \rangle \langle P_c^2 \rangle + \langle P_b^2 \rangle)$$

The expectation values of the quadratic angular momentum terms may be written

$$\langle Pa \rangle = 1/2[J(J+1) + E(\kappa'') - (\kappa''+1)\frac{\partial E(\kappa)}{\partial \kappa}]$$

$$\langle Pb \rangle = \frac{\partial E(\kappa)}{\partial \kappa}$$

$$\langle Pc \rangle = 1/2[J(J+1) - E(\kappa'') + (\kappa''-1)\frac{\partial E(\kappa)}{\partial \kappa}]$$

The coefficients of the quartic angular momentum terms do not depend strongly on and the convergence to the least squares minimum was achieved after two or three cycles.

REFERENCES

1. H. Margenau and G.M. Murphy, "The Mathematics of Physics and Chemistry", D. Van Nostrand Company, Inc., 1964, 517.